PORE PRESSURE DEVELOPMENT IN A BEARING CAPACITY TEST ON AN OVERCONSOLIDATED CLAY MODEL

By

EDWARD JAMES MONAHAN

Bachelor of Science
Newark College of Engineering
Newark, New Jersey
1958

Master of Science
Newark College of Engineering
Newark, New Jersey
1961

Submitted to the Faculty of the
Graduate College of the
Oklahoma State University
in partial fulfillment of
the requirements for
the Degree of
DOCTOR OF PHILOSOPHY
July, 1968

PORE PRESSURE DEVELOPMENT IN A BEARING CAPACITY TEST ON AN OVERCONSOLIDATED CLAY MODEL

Thesis Approved:

J. V. Parcher
Thesis Adviser

[illegible]

[illegible]

[illegible]

D. D. Durham
Dean of the Graduate College

PREFACE

The laboratory research for this study was done *in absentia* over a four year period at Newark College of Engineering. It is largely for this reason that rather exhaustive descriptions of the development of instrumentation, techniques, and procedures are included (Chapter III and IV).

Before acknowledging the many people who have aided this long investigation, I should like to clarify the distinction between two terms used in this dissertation. Because of an unfortunate similarity of more or less standard nomenclature, confusion concerning this work can easily develop without a clear understanding of that distinction. The two terms to which I refer are $k_o = \Delta\bar{\sigma}_3/\Delta\bar{\sigma}_1$ and $K = \Delta\bar{\sigma}_3/\Delta\bar{\sigma}_1$. The lower case letter designates the coefficient of earth pressure *at rest*, i.e., without lateral strain. The capital letter is defined mathematically in an identical manner, i.e., the ratio of the change in minor principal effective stress to the change in the major principal effective stress. The distinction is simply that the latter, by definition, *may* be (and is) *accompanied by lateral strain*. As used in this work, the K-values are associated only with the stresses induced by the loading of the circular footing, as calculated by elastic theory. The k_o-value is associated only with anistropic *preloading*.

Acknowledgments

I have become indebted to many people for their considerable encouragement and aid over the past five years of residency and research. Space precludes a like measure of appreciation, so I will simply extend a simple thank you:

To Dr. Jim Parcher, first and foremost, for his extraordinary help as chairman of the Advisory Committee, extending over a five year period and a two-inch thick folder of correspondence.

To Dr. Hady, Dr. Manke, and Dr. Stone, for their beneficial suggestions as members of the Advisory Committee. A special thanks also to Dr. Hady for his assistance in long-distance registration.

To Professors Robbins and LaLonde, retired chairmen of the Civil Engineering Department at Newark College of Engineering, for their encouragement and help.

To my good friend, Ivan Metzger.

To Dr. Tony Raamot, my Eastern Adviser.

To the National Science Foundation for financial support during my residency as an NSF Faculty Fellow.

To the administration of Newark College of Engineering for their support and use of laboratory facilities.

To the NCE Research Foundation for financial support during periods of the research effort.

To Eldon Hardy for his extra effort in preparing the figures for this work.

To Mrs. Shirley Cunningham for her excellent typing.

TABLE OF CONTENTS

Chapter		Page
I.	INTRODUCTION	1
II.	A STATE OF STRESS ANALYSIS	7
	1. Prior Experimental Work	8
	2. Pore Pressure Analysis.	9
	(a) The A Pore Pressure Parameter.	10
	(b) The K Parameter	16
	(c) The Prediction Equation . . .	16
	3. An Important Limitation of the Predicted Equation.	21
	4. Stress Distribution: $\Delta\sigma_1$	22
III.	INSTRUMENTATION AND PREPARATION OF THE SOIL MODEL.	24
	1. The Pore Pressure Manometry System: Design and Pilot Test	25
	2. The Pore Pressure Probe	34
	(a) Design and Pilot Test of the Probe	34
	(b) Location of the Probes: Stress Distribution.	42
	3. Calibration of All Systems.	50
	4. The Preparation of the Soil Model . . .	62
	5. External Instrumentation.	69
	6. Additional Preliminary Tests.	71
	(a) Slurry Proportions.	71
	(b) Bearing Capacity Estimate . .	74
IV.	TESTING OF THE SOIL MODEL.	76
	1. Planning and Conducting the Test. . . .	76
	(a) Loading	76
	(b) Personnel	77
	(c) Pore Pressure Measurement . .	79
	(d) Settlement and Heave Measurements	80
	2. Compilation of Results.	80

TABLE OF CONTENTS (Continued)

Chapter		Page
	3. General Evaluation.	84
	(a) Loading	84
	(b) Pore Pressure Measurement . .	85
	(c) Settlement and Heave Measurements	89
V.	ANALYSIS OF THE MODEL TEST RESULTS	90
	1. State of Stress Analysis: A Comparison of Predicted and Measured Pore Pressures	90
	(a) A and K for Normally Consolidated Clay.	91
	(b) A and K for Overconsolidated Clay.	97
	(c) Distribution of Pore Pressures	99
	2. Bearing Capacity Analysis	104
VI.	SUMMARY, CONCLUSIONS, AND RECOMMENDATIONS. . . .	116
A SELECTED BIBLIOGRAPHY		119

LIST OF TABLES

Table		Page
I.	Physical Properties of 0.1 Normal Sodium Kaolinite.	7
II.	The K-parameter for Two Typical Soils	20
III.	Major Principal Total Stress Increments at Probes, $\Delta\sigma_1$, in. Hg..	23
IV.	Pilot Tests of the Manometry System	31
V.	Pilot Test of the Porous Probe.	39
VI.	Influence Values for Stresses Beneath a Circular Uniform Load.	44
VII.	Vertical Location of Probes	56
VIII.	System Pressure Tests	58
IX.	Compilation of Model Test Data.	81

LIST OF FIGURES

Figure		Page
1.	Phase Loading of the Soil Model.	11
2.	Relationship Between k_o, $\emptyset'$, and OCR (after Brooker).	12
3.	Relationship Between k_o and OCR for 0.1 N Sodium Kaolinite.	13
4.	Relationship Between A and Stress Level for 0.1 N Sodium Kaolinite	15
5.	Pore Pressure Measurement.	25
6.	Schematic of the Pore Pressure Measuring System. .	27
7.	Photographs of the Manometry Apparatus	33
8.	Pilot Test of the Porous Probe	36
9.	Plan of Probe Arrangement.	43
10.	Mohr Circle of Plane Stress.	46
11.	Cross Section of the Soil Model.	48
12.	Stress Influence Values: Aplha vs. S_{rz} for $R \leq a$. .	51
13.	Stress Influence Values: Alpha vs. S_{rz} for $R \geq a$. .	52
14.	Stress Influence Values: Alpha vs. n_z	53
15.	Stress Influence Values: Alpha vs. n_r	54
16.	Schematic of Tank and Preloading Systems	66
17.	Settlement and Heave Measurements	70
18.	Generalized Failure Mechanisms.	72
19.	Shear Strength of 0.1 N Sodium Kaolinite by Vane Shear Tests.	73
20.	Photographs of the Model Test.	92

LIST OF FIGURES (Continued)

Figure		Page
21.	A-Value Variation for 0.1 N Sodium Kaolinite Clay.	92
22.	A-Value Variation for Boston Blue Clay	93
23.	A-Value Variation for Laurentian Clay.	94
24.	Summary of Functional Instrumentation.	101
25.	Strain Variation Within the Soil Model	102
26.	Failure Mechanisms for General and Local Shear Failure.	106
27.	Mohr Circle Plots of Compression Tests	109
28.	Pore Pressure Distribution for Effective Stress Bearing Capacity Analysis.	115

NOMENCLATURE

A	Skempton's pore pressure parameter
A_f	A, at failure
B	Skempton's pore pressure parameter
B_A	Pore pressure parameter for the case of anisotropic loading
D	Deviator stress in a triaxial test
D_f	Depth of surcharge in Terzaghi Bearing Capacity Theory
C_c	Compressibility of soil structure
C_v	Compressibility of fluid in soil voids
c	Cohesion, the shear strength of a clay soil for ϕ-zero analysis
c'	Cohesion, effective strength parameter
e	Void ratio, V_v/V_s
G_s	Specific gravity of solids
K	Ratio of change in minor principal effective stress to major principal effective stress, $\Delta\bar{\sigma}_3/\Delta\bar{\sigma}_1$, <u>with lateral strain</u>
k_o	Same as above, except <u>no lateral strain</u> (Coefficient of earth pressure at rest)
K_f	K, at failure

NOMENCLATURE (Continued)

k_a	Coefficient of active earth pressure
N_γ, N_c, N_q	Terzaghi's bearing capacity factors for general shear failure
N'_γ, N'_c, N'_q	Same as above except reduced values for local shear failure
n	Porosity, V_v/V
n_r, n_θ, n_z, n_p	Influence unit stresses at a point in a soil mass due to unit uniform pressure on a circular surface load (Jurgensen data; See Fig. 12)
OCR	Overconsolidation ratio, $\bar{p}_c/\bar{p}_o$
$\bar{p}_c$	Maximum vertical effective pressure to which a soil element has ever been subjected
$\bar{p}_o$	Presently existing vertical effective pressure on a soil element
$\bar{p}$	Maximum preload effective pressure = $\bar{p}_c$ for this study
p, q	Contact pressure
Q, P	Total load
Q_i	Load increment
q_f	Ultimate bearing capacity (f for failure)
q_u	Unconfined compression strength
r	Radial coordinate
R	Radius of footing (Terzaghi bearing capacity analysis)
a	Radius of circular loaded area (Jurgensen analysis)
R_M	Radius of Mohr's Circle

NOMENCLATURE (Continued)

S	Maximum shear stress
S_{rz}	Shear stress in radial plane
s	Shear strength of soil
u	Pore pressure
V	Total volume
V_v	Volume of voids
V_s	Volume of solids
V_w	Volume of water
V_c	Volume of soil structure
W_w	Weight of water
W_s	Weight of solids
w	Moisture content, W_w/W_s
w_l	Liquid limit
w_p	Plastic limit
w_n	Natural moisture content
σ	Normal pressure (<u>total</u> stress)
$\bar{\sigma}$	Normal pressure (<u>effective</u> stress)
$\sigma_1, \sigma_2, \sigma_3$	Principal stresses (major, intermediate, minor, respectively)
σ_i	Unit normal stress
γ	Unit weight
γ'	Submerged (effective) unit weight
ϕ	Friction angle of a soil
ϕ'	Friction angle, effective-stress parameter
μ	Micron

NOMENCLATURE (Continued)

α	Angle between vertical centerline of circular loaded area and point in soil beneath the load
β	Angle between the horizontal and the major principal plane

CHAPTER I

INTRODUCTION

The shear strength of soils has been recognized to be greatly dependent upon the development of effective stress. This shear strength is governed by the deceptively simple Coulomb Equation: $s = c' + \bar{\sigma} \tan \phi'$, where s is the shear strength; c', the true cohesion; $\bar{\sigma}$, the effective normal stress; and ϕ', the true angle of internal friction. From Terzaghi's fundamental definition, the effective stress may also be designated as $\bar{\sigma} = (\sigma - u)$, where σ is the total stress, and u, the pore pressure.

In the case of a coarse, granular soil, any pore pressure would be hydrostatic for a condition of submergence, or zero otherwise, since excess pore pressures could not persist in such a porous soil.

However, in the case of pressure increases on relatively impervious clay soils, excess pore pressures will develop, thus affecting the shear strength. In the simple case of an isotropic stress increase on a saturated clay, there is no immediate change in shear strength, since the total stress increase is reflected in an immediate like increase in pore pressure, i.e., $\Delta\sigma = \Delta u$, and the change in effective stress, $\Delta\bar{\sigma}$, is zero. As drainage ensues as a consequence of the ex-

cess pore pressures, the pore pressure diminishes and, correspondingly, the effective stress increases. It is seen that the shear strength of recently loaded (or unloaded) saturated clay soils is time-dependent. When the excess pore pressure is reduced to zero, the effective shear strength of the soil is realized, and the soil is said to be fully consolidated under the stress increment.

Inspection of the Coulomb Equation shows that the shear strength at any instant is governed by the character of the pore pressure. A negative sign designates pore water tension, which results in an internal compression of the soil structure. A common example of the effects of this internal compression is the obvious stability of an unconfined cylindrical test specimen of silt at a sufficiently low moisture content. The effective stress which is responsible for this stability is the pore water tension: $s = c' + (\sigma - u) \tan \phi'$; for silt: $s = o + [o-(-u)] \tan \phi' = \left| u \tan \phi' \right|$.

Recent experimenters (Skempton, et al.) have shown that overconsolidated clays exhibit pore pressure variations under load unlike those of normally consolidated clays. Specifically, it has been demonstrated that the A-coefficient, Skempton's pore pressure parameter, decreases from a value of unity (for normally consolidated clays) as the overconsolidation ratio (OCR) increases. For highly overconsolidated clays, the value of the A-coefficient at failure may be negative, indicating pore water tension.

If a clay soil is formed in an environment conducive to

the development of a honeycombed or flocculent structure, and subsequently heavily loaded, the particle configuration will become more or less dispersed. For purposes of simplicity, these configurations may be thought of as a "card-house" random structure (before loading) and a parallel orientation of the "cards" (after loading).

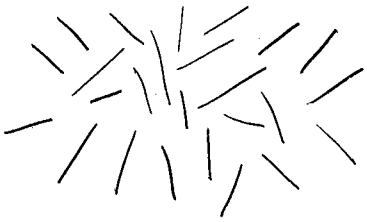

BEFORE LOADING
(NORMALLY CONSOLIDATED)

AFTER LOADING
(HEAVILY OVERCONSOLIDATED)

Intuitively, it would seem that the reactions to subsequent loading of two such soils would be markedly different. The most obvious difference would be the greater shear strength of the preloaded clay. Of import to this study, however, is a more precise consideration of the pore-pressure reaction that might be expected in each case, since these reactions, as already explained, will greatly influence the shear strength. The subsequent loading could be the deviator stress in a triaxial test, the load increment in a consolidation test, or, in the field, the loading by the structure. For purposes of illustration, consider the latter case, spe-

cifically as it is represented by a long footing. On the

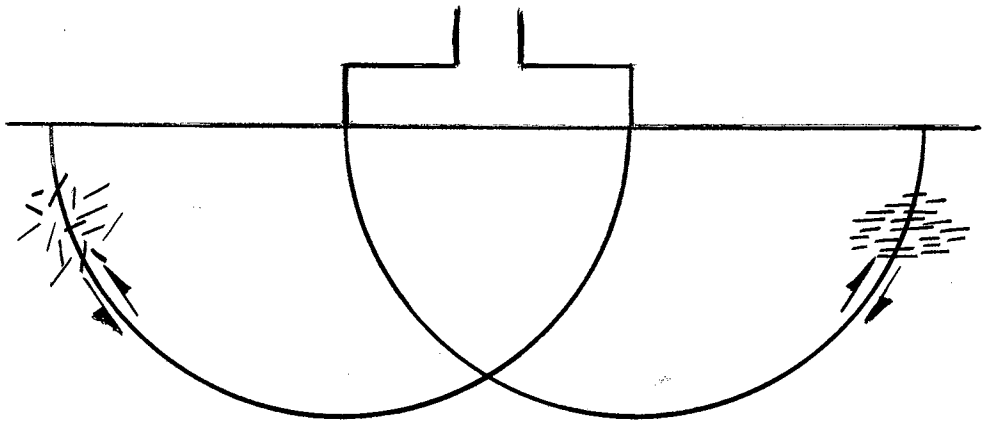

left and right are shown schematically the two extreme conditions of the soil. Also shown are the incipient surfaces of failure (e.g., after Prandtl). Intuition suggests that the dispersed structure of the heavily overconsolidated saturated clay would be conducive to the development of negative pore pressures under loading. Such a soil structure would be resistant to dilatant effects, dilatancy being the tendency of a soil to increase in volume when subjected to shearing stresses. Whatever the extent of overconsolidation, it is apparent that Δu will be influenced in some way, and that $\Delta\bar{\sigma}$ and s must also be affected. A common example of the development of negative pore pressures, and hence higher transient shear strength, is the observed fact that the slopes of an

open cut in a saturated impervious soil are most stable initially (excluding, perhaps, highly fissured clays). As the negative pore pressures dissipate, the clay swells (dilates), and its shear strength is reduced.

The overall purpose of this investigation was to study the development of pore pressures in large soil models, which were prepared from kaolinite clay. The powdered clay was flocculated in a 0.1 Normal Sodium Chloride solution and sedimented in a 4-ft diameter steel tank. After sedimentation, the clay was preloaded as in a consolidation test; the thickness of the clay model thus prepared was somewhat in excess of 24 inches.

Pore pressure instrumentation consisted of fourteen probes and the associated measuring apparatus. An unusual feature of the system was that the probes were installed within the tank before the slurry was placed. In spite of the rather large size of the soil model, it was felt that post-installation of the probes would cause an unacceptable amount of disturbance of the model.

Pore pressures were measured by manometer systems (one for each probe), wherein a head of mercury was used as a back pressure to maintain a no-flow condition at the probe. All lines were saturated and pressure-tested to determine the expansion characteristics of the systems and to check for deaeration. While details and techniques were considerably different, the principles were those usually employed in the measurement of pore pressures in triaxial testing.

Additional instrumentation included provisions for the measurement of settlement of the loading plate, and surface heave outside the loaded area, the load for testing being applied through a concentrically-placed 10-in. diameter bearing plate.

Details of instrumentation, sample preparation, and the conduct of the test, including preliminary pilot tests, are described in subsequent chapters.

The results of the investigation were analyzed on two bases: State of Stress, and Bearing Capacity. The State of Stress analysis was possible because of earlier research work which had been done on samples of Sodium Kaolinite prepared in a like manner. Chapter II includes a summary of the results pertinent to the analysis of the experimental work of this thesis.

CHAPTER II

A STATE OF STRESS ANALYSIS

As mentioned in Chapter I, this work is a continuation of a comprehensive research investigation of the engineering properties of sedimented 0.1 N Sodium Kaolinite. The material (trade name: Hydrite PD-10) was obtained in powdered form from the Georgia Kaolin Company of Dry Branch, Georgia.

Some physical properties of the clay are listed below.

TABLE I

PHYSICAL PROPERTIES OF 0.1 N SODIUM KAOLINITE

Particle Shape		Hexagonal flakes	Grim, p. 108
Particle Size:	Breadth	0.3 to 4μ	
	Thickness	0.05 to 2.0μ	Grim, p. 108
Specific Gravity		2.64_2	Grim, p. 217
Specific Surface Area		15 m^2/g	Grim, p. 311
Liquid Limit		70 percent	---
Plastic Limit		33 percent	---

Prior Experimental Work

The consolidation and shear strength characteristics of the sedimented clay were determined by Ratzburg (1964) and Leitch (1964). All of their samples were prepared by sedimentation and preconsolidation in 2 ft long plastic cylinders, the preconsolidation being effected by a loaded porous piston. The preconsolidation pressure was, in all cases, about 7 psi.

For purposes of consolidation testing, the samples were prepared by direct sedimentation and preconsolidation into a standard consolidation ring ($2\frac{1}{2}$ in. I.D.) which had been fitted to the base of a plastic cylinder of slightly larger inside diameter.

For the shear-testing program, the samples were sedimented similarly, except that the consolidation ring was omitted, and $1\frac{1}{2}$ in. I.D. cylinders were used. After preconsolidation, three-inch long samples were extruded and mounted in a triaxial chamber. Isotropically consolidated undrained triaxial tests with pore pressure measurements were performed on samples with various overconsolidation ratios.

An analysis of the data of the consolidation tests, which was representative of anisotropic loading, and the triaxial tests, representing isotropic consolidation, indicated that for a given average principal stress, the anisotropic condition yielded lower moisture content (French, 1967). Since the induced pore pressures influenced the drainage, i.e., consolidation and hence the resulting mois-

ture content, it was considered necessary to study the pore pressure variations in some detail.

Pore Pressure Analysis

According to Skempton (1954), the pore pressure change in a soil system is given as follows:

$$\Delta u = B[\Delta\sigma_3 + A(\Delta\sigma_1 - \Delta\sigma_3)] \qquad \text{Eq. 1.1}$$

where, Δu = the induced pore pressure

B = a pore pressure parameter, dependent upon the saturation of the system ($B = 1$ for a fully saturated system)

$\Delta\sigma_1$, $\Delta\sigma_3$ = the change in major and minor principal stresses, respectively.

A = a pore pressure parameter.

For isotropic consolidation, $\Delta\sigma_1 = \Delta\sigma_3$, and for a saturated soil $B = 1$. Thus, substituting in the equation:

$$\Delta u = \Delta\sigma_3 = \Delta\sigma_1$$

For anisotropic consolidation with no lateral strain, which is the condition imposed in standard consolidation testing, the ratio of the minor to major principal effective stresses is designated as the coefficient of earth pressure at rest, $k_o = \Delta\bar{\sigma}_3/\Delta\bar{\sigma}_1$. In the experimental work, the preloading of soil model was considered to have produced the k_o condition. Subsequently, the preload was removed so that the only remaining effective stresses were due to the weight of the soil. The model test consisted of the incremental loading of a 10-in. diameter surface footing, which had been placed

concentrically on the 4-ft. diameter soil model.

The procedure may be represented on a typical soil element, as shown in Figure 1. Phases 1, 2, and 3 represent the preloading procedure used to prepare the soil model for the test. The overconsolidation ratio (OCR) is defined as the ratio of the maximum previous vertical effective stress to the presently existing vertical effective stress. Thus, according to the figure, $OCR = \frac{\bar{p}}{\bar{p} - \Delta\bar{p}} = \frac{\bar{p}}{\gamma' Z}$, where $\bar{p}$ is is the maximum preload effective pressure, γ', the effective (submerged) unit weight of the clay, and Z the depth of overburden at a point in question. Brooker (1965) has shown that the coefficient of earth pressure at rest, k_o, increases with the overconsolidation ratio and is a function of the effective angle of internal friction ϕ' (See Figure 2). Utilizing Brooker's general relationships of Fig. 2, it was possible to construct the k_o-OCR relationship (Figure 3) for the Sodium Kaolinite. This plot is based upon Leitch's determination of $c' = 1.3$ psi and $\phi' = 25.9^\circ$ for the effective-stress, shear-strength parameters of the clay.

The A Pore Pressure Parameter

It has been reported by many investigators that the A-value is not a constant soil property. Lambe (1962) presents a summary of factors affecting A, among which are the stress history, including overconsolidation and anisotropy; strain, and strain rate. Wu (1966) points out that the A-value also depends upon the stress level. Values of A at failure are consistently reported to be lower in overconsol-

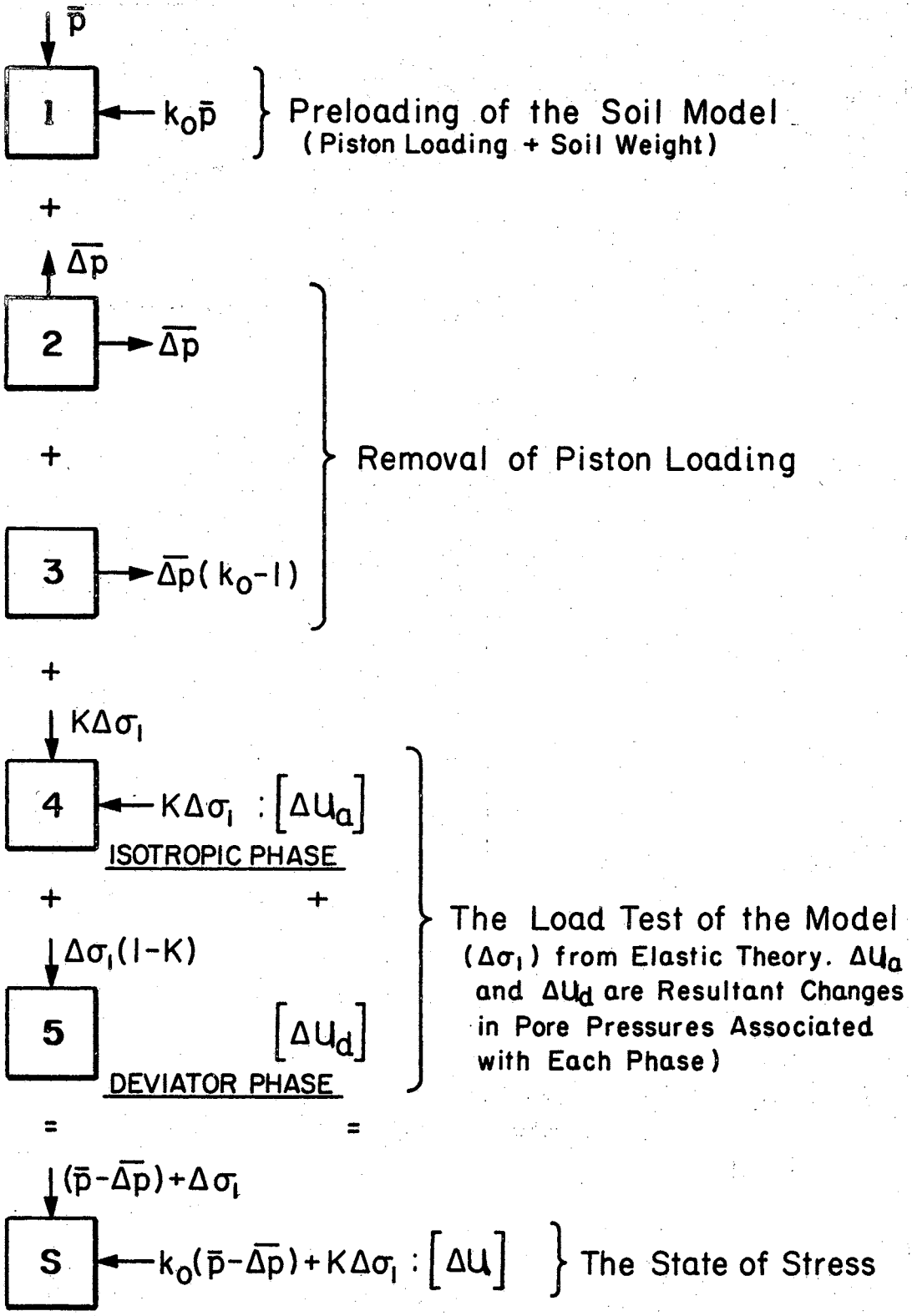

Figure 1. Phase Loading of the Soil Model

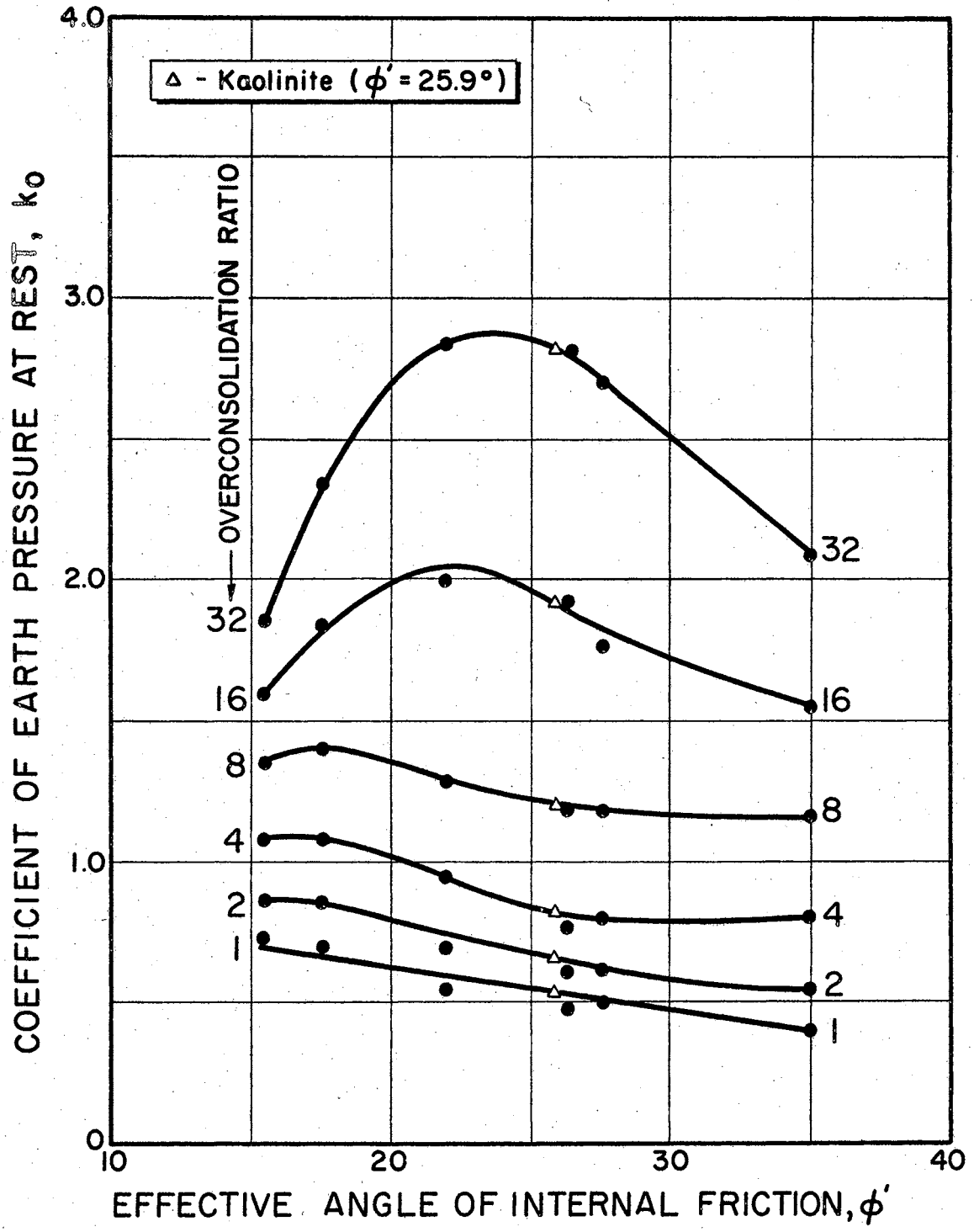

Figure 2. Relationship Between k_o, Ø', and OCR. (after Brooker)

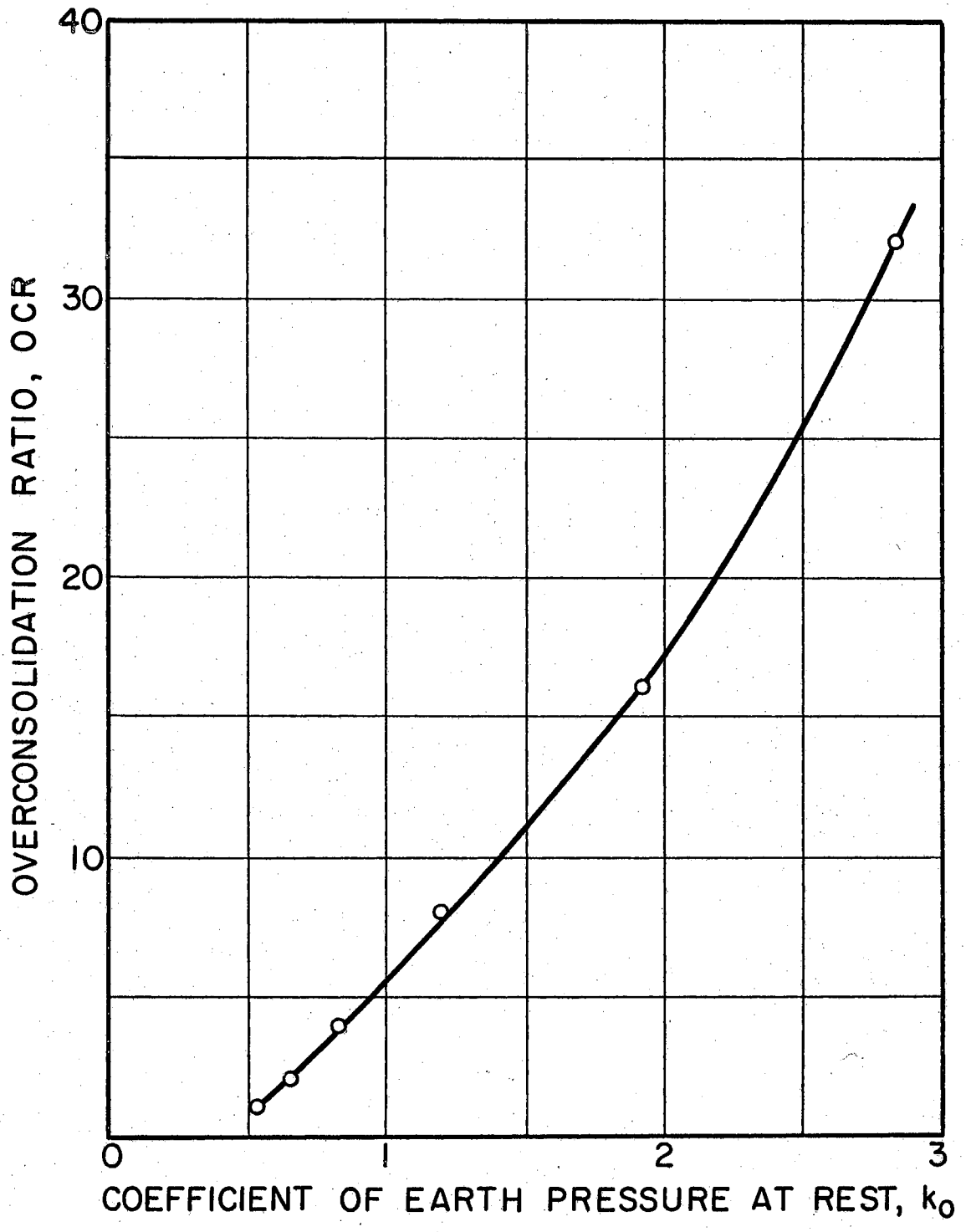

Figure 3. Relationship Between k_o and OCR for 0.1 N Sodium Kaolinite

idated test specimens.

In order to predict pore pressure changes prior to failure for a state-of-stress analysis, it is necessary to determine A-values for the stress levels and OCR-values of interest. Such A-values may be determined by running consolidated-undrained triaxial shear tests, with pore pressures measure during the application of the deviator stresses. Thus, comparing Eq. 1.1 and phase 5 of Figure 1, $A = \Delta u_d/(\Delta\sigma_1-\Delta\sigma_3)$, where $(\Delta\sigma_1-\Delta\sigma_3)$ is the deviator stress, and Δu_d is the pore pressure induced by application of the deviator stress.

Figure 4 is a plot of such data obtained by Leitch (1964) on Sodium Kaolinite which was identical to the clay used in the model test. As noted, the data are for overconsolidation ratios of 8 and 12. After initial preparation by sedimentation, the samples were mounted in a triaxial chamber, and consolidated isotropically in 10 psi increments to a predetermined effective stress. To produce a specified OCR, the samples were then unloaded (cell pressure reduced) in 10 psi increments to a final cell pressure of 10 psi. Thus, for example, the sample with OCR = 12 was fully consolidated at a maximum cell pressure of 120 psi, with subsequent unloading to 10 psi. Swelling was allowed under the reduced pressure, whereupon the deviator stress was applied at a rate of 0.60 inches per hour. Pore pressure and deviator stress readings were recorded at pre-selected strain intervals until 20% strain was reached.

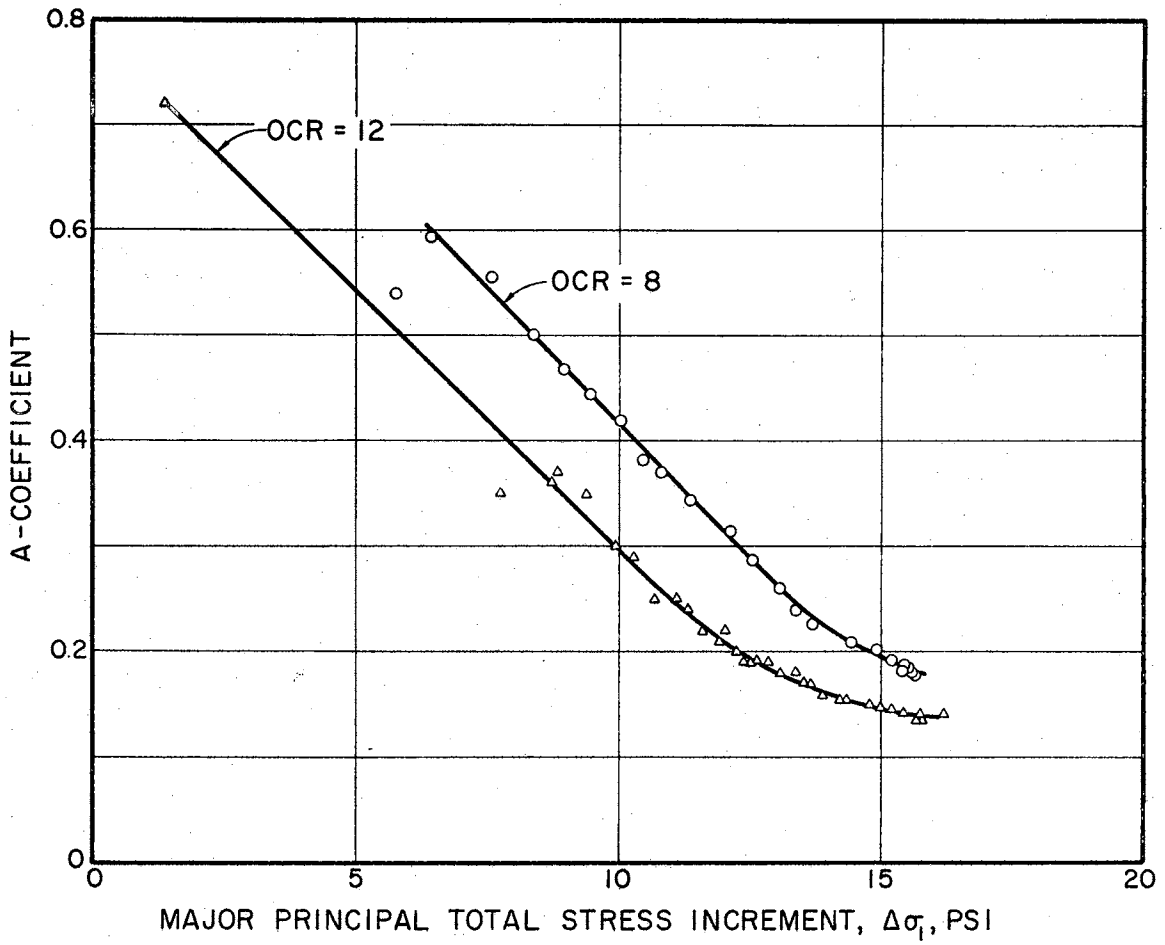

Figure 4. Relationship Between A and Stress Level for 0.1 N Sodium Kaolinite

The K Parameter

As is suggested by phases 4 and 5 of Figure 1, the pore pressures developed during the load test will depend upon the K parameter, which is defined as the ratio between the effective stress change in a lateral direction and the effective stress change (applied load) in the vertical direction, i.e. $K_o = \frac{\Delta\bar{\sigma}_3}{\Delta\bar{\sigma}_1}$ (Bishop, 1954). For convenience of presentation, it will be temporarily assumed that these directions correspond to those of the minor and major principal stresses, respectively.

In the extreme condition of a soft soil, i.e., a fluid, $\Delta\bar{\sigma}_3 = \Delta\bar{\sigma}_1$ and $K = 1$. As the consistency increases, K decreases, and attains a meaningful value at $K = k_o$ which is the coefficient of earth pressure at rest. As the consistency is further increased, K will continue to diminish, and probably assumes its minimum value at failure of k_a, the coefficient of active earth pressure which, as Bishop (1954) points out, corresponds to the stress ratio at failure in the triaxial test. It may be noted that the development of lateral pressure changes is known to be dependent upon strain, so that the introduction of the K-parameter will reflect the effects of strain in addition to those of consistency, though certainly these parameters are themselves related.

The Prediction Equation

Reference to Figure 1 indicates that phases 4 and 5 may be analyzed separately for pore pressure changes, Δu_a and

Δu_d, respectively, and the results added to yield the pore pressure change, Δu (after Skempton, 1954).

Phase 4: The Isotropic Phase

The increases in effective stresses, from Terzaghi's fundamental relationship for total stresses, effective stresses and pore pressures, are:

$$\Delta\bar{\sigma}_1 = \Delta\bar{\sigma}_2 = \Delta\bar{\sigma}_3 = K\Delta\sigma_1 - \Delta u_a.$$

With C_c = the compressibility of the soil structure, the change in volume of the soil structure is

$$\Delta V_c = -C_c\, V(K\Delta\sigma_1 - \Delta u_a)$$

where V = initial volume.

With C_v = the compressibility of the fluid in the voids

$$\Delta V_v = C_v n V \Delta u_a$$

where n is the porosity,

and ΔV_v is the change in volume of the voids.

Equating volume changes leads to

$$\frac{\Delta u_a}{K\Delta\sigma_1} = \frac{1}{1 + \frac{C_v n}{C_c}} = B_A$$

where B_A is a pore pressure parameter for the anisotropic case (directly analogous to Skempton's B-parameter). For full saturation, the compressibility of the voids is negligible as compared to that of the soil structure, and $B_A = 1$.

Thus,

$$\Delta u_a = K\Delta\sigma_1$$

Phase 5: The Deviator Phase

The increases in effective stresses are

$$\Delta\bar{\sigma}_1 = [\Delta\sigma_1 (1-K) - \Delta u_d]$$

$$\Delta\sigma_2 = \Delta\sigma_3 = [0 - \Delta u_d]$$

For an elastic material, the change in volume of the structure

$$\Delta V_c = -C_c V \, 1/3[\Delta\sigma_1(1-K) - \Delta u_d + 2 (-\Delta u_d)]$$

where the bracketed quantities are the changes in the 3 principal stresses. For the void space, the change in volume

$$\Delta V_v = -C_v n V \Delta u_d$$

Equating volumes leads to

$$\Delta u_d = \frac{1}{1 + \frac{C_v n}{C_c}} \cdot \frac{1}{3} \Delta\sigma_1(1-K)$$

or, $$\Delta u_d = B_A \cdot \frac{1}{3} \Delta\sigma_1(1-K)$$

As Skempton points out, the behavior of soils is not elastic, so the equation must be written empirically as

$$\Delta u_d = A \, \Delta\sigma_1(1-k)$$

with $B_A = 1$, as before.

Combining for both phases

$$\Delta u = \Delta u_a + \Delta u_d$$

$$\Delta u = K\Delta\sigma_1 + A\Delta\sigma_1 (1-K)$$

$$\Delta u = \Delta\sigma_1 [K + A - AK)]$$

$$\Delta u = \Delta\sigma_1 [K(1-A) + A] \qquad \text{Eq. 2.2}$$

Equation 2.2 is considered to be the prediction equation. Inserting some typical values of A, at failure (Skemp-

ton, 1954) and suggested compatible values of K, affords a general analysis of the equation.

(1) For a normally consolidated clay; A = 1, any K value

$$\underline{\Delta u} = \underline{\Delta \sigma_1}$$

(2) For lightly overconsolidated clays; A = $\frac{1}{2}$, K = 0.2

$$\underline{\Delta u} = \Delta \sigma_1 [0.2(1-\tfrac{1}{2}) + \tfrac{1}{2}] = \underline{0.6\ \Delta u}$$

(3) For overconsolidated clays; A = o, K = 0.4

$$\underline{\Delta u} = \Delta \sigma_1 [0.4(1-0) + o] = \underline{0.4\ \Delta u}$$

(4) For heavily overconsolidated clays; A = $-\frac{1}{2}$, K = 0.2

$$\underline{\Delta u} = \Delta \sigma_1 [0.2(1-[-\tfrac{1}{2}]) - \tfrac{1}{2}] = \underline{-0.2\ \Delta u}$$

It may be noted that for a heavily overconsolidated clay (A = $-\frac{1}{2}$), a K-value of less than 1/3 is required for the development of negative pressures.

The suggested K-values are arrived at on the basis that these values are dependent on both consistency and strain. Since the K-values would be inversely related to both consistency and strain, it is felt that either very high consistency or very high strains would result in lower values of K. For soils of intermediate consistencies and corresponding strains, the K-values would be somewhat higher.

Bishop (1954) presents some data indicating that the K-value does diminish in the manner described (See Table II). The soils listed were compacted earth fills for the embankment of a dam and thus were not saturated (B = 0.8 for both soils). It may be noted that the clay-gravel, having a lower A-value, is the more heavily overconsolidated of the two

TABLE II

THE K-PARAMETER FOR TWO TYPICAL SOILS

Soil	K_o	K_f	A
Sandy clay	0.5	0.3	0.5
Clay-gravel	0.4	0.25	0

soils. Of import to this study is the fact that its K_f value, the K value at failure, is also lower.

It may be noted that the Eq. 2.2 suggests that the induced pore pressures will diminish at higher load levels, since these load levels will produce greater strains, thus reducing K, and hence, Δu. This behavior would be more pronounced for soft soils, since the strain increase would be greater than for stiffer soils. A further consideration of the effects of strain variation suggests that the tendency for the development of negative pore pressures in heavily overconsolidated soils is most pronounced at shallow depths outside of the loaded area. This observation is based upon two facts: First, in such areas the planes of principal stresses are rotated such that the minor induced principal stresses are almost vertical. Secondly, the only effective stress which resists vertical heave is the weight of the soil. At shallow depths, then, the strain will be great, K will be near minimum, and for a given negative A-value for a

heavily overconsolidated soil, the "negative coefficient" of $\Delta\sigma_1$ in the prediction equation will be a maximum. An example of what would probably be the most extreme case would be K = 0.15 and A = -0.5. Whence $\Delta u = -0.275\ \Delta\sigma_1$. It should be noted, however, that $\Delta\sigma_1$ would be quite small in relation to the contact pressure at the footing.

An Important Limitation of the Prediction Equation

The preceding sections imply that the prediction equation is applicable to all soils. While there appears to be no theoretical justification for excluding certain soils, it seems intuitive that clay soils of low consistency, i.e., soft clays, should not be analyzed for pore pressure development by the use of the prediction equation, at least not without modification.

Perhaps a distinction should also be made between a clay with a high overconsolidation ratio and a firm, stiff, or hard clay; the two are not necessarily synonymous. That is to say, a clay with a very high overconsolidation ratio may be quite soft, even though a high OCR is generally suggestive of higher consistency. The seeming anomaly is explained on the basis of the definition of $OCR = \bar{p}_c/\bar{p}_o$. As in the model tested in this study, $\bar{p}_c$ may be quite low, at least with respect to effecting a consolidation to the higher ratings of consistency or shear strength. With $\bar{p}_c$ almost totally removed, the remaining effective pressure may be minute. The result would be a soft clay with a high over-

consolidation ratio. It is further thought that the undispersed structure of such a soft clay would not tend to favor the development of negative pore pressures, which are usually associated with stiffer clays of dispersed structure.

Thus, it is suggested that the prediction equation be limited to the analysis of clays of relatively high consistency. It is likely that softer clays would react essentially like a normally consolidated clay, irrespective of the magnitude of overconsolidation ratio.

Stress Distribution: $\Delta\sigma_1$

The stresses induced in the soil model by the loading of the 10-in. diameter loading block were calculated for eleven probe locations within the soil model, using stress distribution theory and the published data of Jurgensen (1934). The vertical positioning of the probes was largely based upon this analysis. The theoretical details, including the preparation of special graphs, are included in Chapter III: Instrumentation and Preparation of the Soil Model. The results are shown in Table III.

TABLE III

MAJOR PRINCIPAL TOTAL STRESS INCREMENTS AT PROBES, $\Delta\sigma_1$, IN. HG.

Influence value $\Delta\sigma_i$			.0103	.0299	.0427	.2005	.1687	.1245	.6715	.2780	.1423	.0835	.0695
Load Increment	Contact Pressure, p		PROBES										
			A1	A2	A3	B1	B2	B3	C2	C4	C5	C6	D1
	(psi)	(in. Hg.)	$\Delta\sigma_1$, inches of mercury										
1	1.76	3.61	.04	.11	.15	.72	.61	.45	2.4	1.00	.51	.30	.25
2	4.45	9.13	.09	.27	.39	1.83	1.54	1.14	6.1	2.54	1.30	.76	.63
3	6.45	13.2	.14	.40	.56	2.65	2.23	1.65	8.9	3.67	1.80	1.10	.92
4	8.45	17.3	.18	.52	.74	3.47	2.92	2.16	11.6	4.81	2.46	1.44	1.20
5	10.4	21.3	.22	.64	.91	4.27	3.60	2.65	14.3	5.92	3.03	1.78	1.48
6	12.4	25.4	.26	.76	1.08	5.10	4.30	3.17	17.1	7.06	3.62	2.12	1.76
7	14.5	29.8	.31	.89	1.27	5.98	5.03	3.72	20.0	8.29	4.25	2.49	2.07
8	16.5	33.8	.35	1.01	1.44	6.77	5.70	4.21	22.7	9.40	4.82	2.83	2.35
9	18.5	37.9	.39	1.13	1.62	7.60	6.40	4.72	25.4	10.5	5.40	3.17	2.63

($\Delta\sigma_1 = p \times \Delta\sigma_i$), where p is the contact pressure, $\Delta\sigma_i$ is the influence value from stress distribution theory (after Jurgensen).

CHAPTER III

INSTRUMENTATION AND PREPARATION OF THE SOIL MODEL

Since the measurement of pore pressure was to be the most important aspect of the experimental work, it was particularly necessary to design a probe and the associated instrumentation which would respond accurately to pore pressures developed within the soil model. Because of the large size of the model and the extensive instrumentation, it was considered prudent to test all critical equipment on a small-scale, pilot basis before proceeding with the construction of the model.

As with most laboratory pore pressure measurements, e.g., in triaxial testing, it was required that some type of no-flow system be employed in order to minimize time lag and pressure drop across the probe. Since the probes were to be pre-installed, with subsequent sedimentation and pre-consolidation of the clay, a very critical and practical requirement was that the probes would function as intended. Thus, the possibility of clogging had to be investigated.

The Pore Pressure Manometry System: Design and Pilot Test

The basic requirements of a pore pressure measuring system may be best illustrated by a simple schematic (Figure 5).

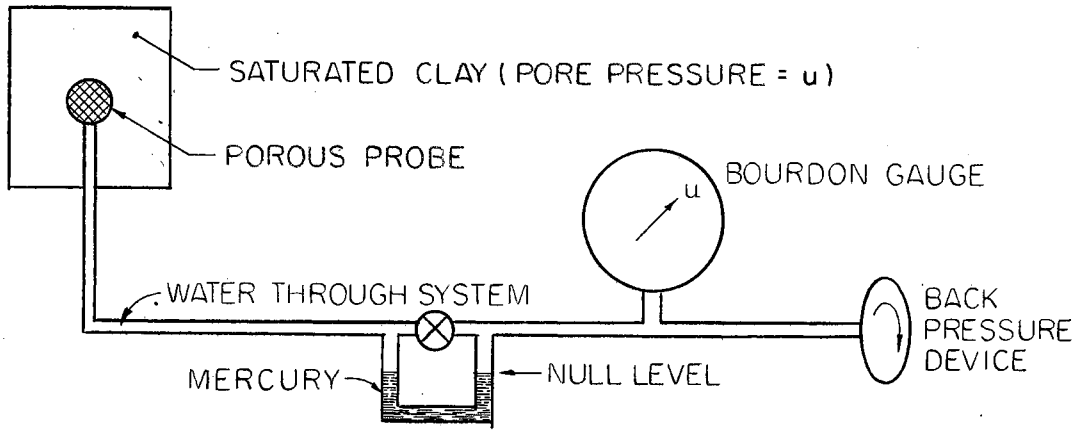

Figure 5. Pore Pressure Measurement

If a load increment is applied to the saturated clay, e.g., the deviator stress in a triaxial test, and the entire system shown is filled with deaired water, then the response in the mercury-filled U-tube would be reflected in a rise of the mercury above the null level. If a back pressure is applied to maintain null, i.e., to prevent volume change or maintain a no-flow condition, then the reading of the pore pressure can be taken at the Bourdon gauge.

While simple in principle, the problems attendant to the development of such a system were manifold and complex.

Principal among these problems were (a) the preparation and introduction of deaired water throughout the system, (b) the selection of fittings and valves to insure the reliability of the system under the range of anticipated pressures, (c) the determination of the expansion characteristics of the system under these pressures, (d) the design of a probe which would function properly, and (e) the precise method of measurement (Bourdon gauge?) and method of supplying back pressure to maintain null.

Consideration of all of these problems led to the development, after considerable revision, of the system shown schematically in Figure 6. The system is composed of the following lines and components:

OM - $\frac{1}{4}$ in. O.D. copper tubing. The water in the high head tank is brought to a vigorous boil to drive off all gases. The top of the tank is equipped with a loosely-fitting cap to contain saturated steam above the boiling water, thus effectively preventing reabsorption of gases into the water. After approximately one hour of boiling, a connection is made with a flexible plastic tube between points M and H, the valve in the OM line is opened, and flushing of the entire system commences.

HL - $\frac{1}{4}$ in. O.D. copper tubing, with a high-duty valve at K.

LF - $\frac{1}{4}$ in. O.C. rigid plastic tubing with a serrated plastic tee-connection at F. To insure the rigid-

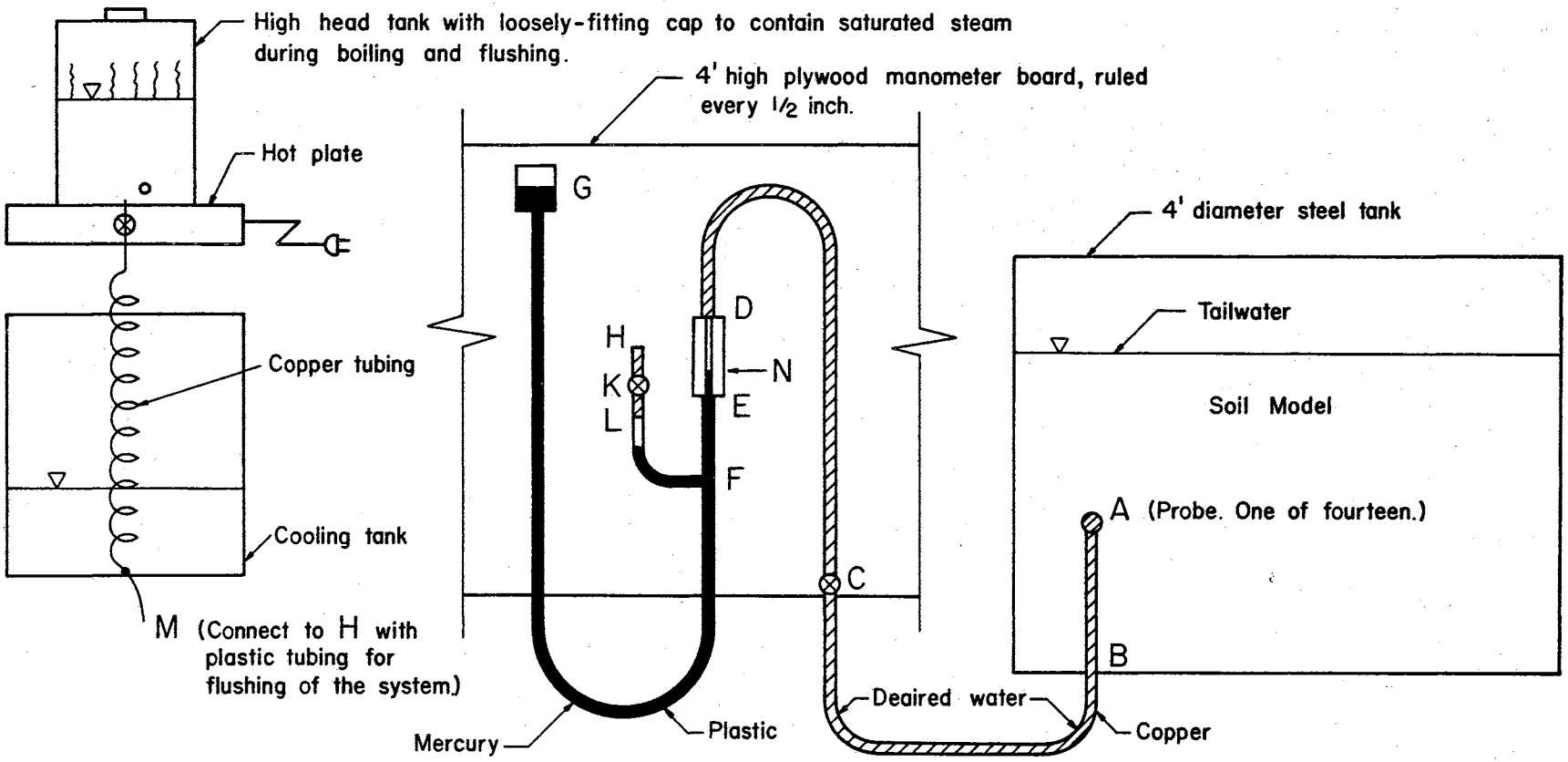

Figure 6. Schematic of the Pore Pressure Measuring System

ity of this connection, the splices were reinforced by an epoxy bond. This section was curved upward and partially filled with mercury in order to provide a seal against hydraulic instability at the tee-connection.

G - Mercury pot, the back pressure source. The height of the pot was adjustable via a pulley arrangement.

GE - ¼ in. O.D. flexible plastic tubing.

ED - The null section, a 3/4 in. O.D., 1/16 in. I.D. rigid plastic cylinder; length, approximately 6 in.

DC - 1/8 in. O.D. copper tubing.

C - High-duty valve.

CB - ¼ in. O.D. copper tubing, with a compression nut straight-through connection at B, the bottom of the tank.

A - The pore pressure probe, one of fourteen.

After initial flushing had filled the entire system with deaired water, mercury was inserted into the pot, with valves K and C closed. The mercury was stirred gently to insure separation of any entrapped water, whereupon Valve K was cracked to allow the mercury to flow into line GF to a point somewhat below the tee-connection at F. Flushing was then resumed. During this phase of the flushing, the inverted-U section of the manometry system, i.e., F to C, was temporarily removed from the board, and all trouble spots were manipulated to effect the dislodging of air bubbles. Trouble spots were, in general, all valves and connections, and the

high spot of the inverted U, where any air tended to accumulate. The most troublesome points were the threaded plastic connections of the null section (at D and E). Since these points were readily visible, it was a simple matter to continue the manipulation until all bubbles were dislodged and flushed out of the lines. When all visible air had been excluded, the apparatus was remounted on the board as shown in Figure 6, and additional flushing was allowed; Valves K and C were alternately opened and closed to clear any remanent air. Valves K and C were then closed. The mercury pot was adjusted to what would later become the static level, that is, a level such that the subsequent opening of Valve C would bring the mercury level to some point within the null section, designated as N on the figure. To attain this condition, Valve K was cracked to allow the mercury to flow into the branch section, FL. Valve K was closed and valve C was then opened to allow the mercury to flow up to the null level, N. When the mercury had thus stabilized at this point, valve C was closed. The system was then ready for pressure testing.

The pressure test of the system was accomplished as follows: The mercury pot was raised to its maximum level, corresponding to about 11 psi, with valve C closed. The expansion of the system, and the extent to which the water in the system had been deaired, was reflected in the rise of the mercury at the null level. No movement indicated a "perfect" system. If the change of the null level proved to be

relatively small, calibration data could be obtained for later use for the testing of the model.

The results of two such pilot tests of the system are shown in Table IV. Explanatory comments are as follows:

System A1L

(1) Reading no. 1 is the static condition, as described previously.

(2) Reading no. 2 reflects the response of the system to the raising of the mercury pot to its maximum height of 47 inches; this corresponds to a line pressure of about 11 psi (47-25.2 = 21.8 in. Hg). Note that the immediate response of the null level was only 0.2 in. (24.25-24.05). This small volume change of approximately 0.0006 cu. in. was considered to be due largely to the expansion of the system under pressure.

(3) The subsequent stability of the null level, with only relatively minor fluctuations (Readings 3-18), indicated that the system was tight, with no leaks at valves or connections, and that the flushing techniques employed had been effective in saturating the system with deaired water.

(4) Subsequent testing (data not included) involved the incremental unloading of the system to 8, 5, and 0 psi, respectively, with a set of null readings being taken for each reduced pressure. The entire loading and re-loading cycle was then repeated for purposes of checking replication performance. The entire test extended over a period of about

TABLE IV

PILOT TESTS OF THE MANOMETRY SYSTEM

Reading No.	Time	Null Reading, In.	Pot Setting, In.
		System A1L	
1	1424:30	24.05	25.2 (Static condition)
2	1425	24.25	47
3	1427	24.2	"
4	1428	24.15	"
5	1430	24.1	"
6	1435	24.05	"
7	1440	24.0	"
8	1445	24.0	"
9	1455	24.0	"
10	1500	24.0	"
11	1515	24.0	"
12	1530	23.95(+)	"
13	1545	23.95	"
14	1600	23.95	"
15	1615	23.95	"
16	1630	23.95	"
17	1645	23.95	"
18	1700	23.95	"
		System B1L	
19	1520	22.95	24.15 (Static condition)
20		25.3	35
NO GOOD - Repeat flushing and manipulation.			
21	1553	22.25	23.5 (Static condition)
22	1555	22.8	47.2
23	1600	22.9	"
24	1606	22.9	"
25	1610	"	"
26	1620	"	"
27	1630	"	"
28	1640	"	"
29	1650	"	"
30	1700	"	"
31	1720	"	"
32	1740	22.9(+)	"
33	1800	22.95	"
34	1920	22.95	"
35	2205	23.15	"
36	2207	22.8	23.5 (Static condition)

two days. The results were quite satisfactory.

System B1L

(1) Readings 19 and 20 represent what may be termed a false start. As the pot was raised from the static condition, it was noted that the mercury climbed rapidly in the null section from 22.95 to 25.3; this occurred with a pot setting of 35. It was concluded that the line still contained appreciable amounts of entrapped air, assuming there were no leaks. Thus, as noted in the interruption of the data, the system was re-flushed, and the pressure-test resumed (Reading no. 21).

(2) As can be seen by subsequent readings, the second flushing was effective. Although the immediate response at the null (Readings 21 and 22) was in excess of that for System A1L (0.55 in. as compared to 0.2 in.), the fact that the system stabilized was considered most significant to the test.

It was concluded from the results of these final pilot tests that the pore pressure measurement system, as shown in its final design in Figure 6, would be acceptable for its intended purpose. The design and procedures for flushing and pressure testing were duplicated for all systems. Pressure-test data for the systems are shown in a succeeding section of this chapter: Calibration of All Systems. Photographs of the apparatus are shown in Figure 7.

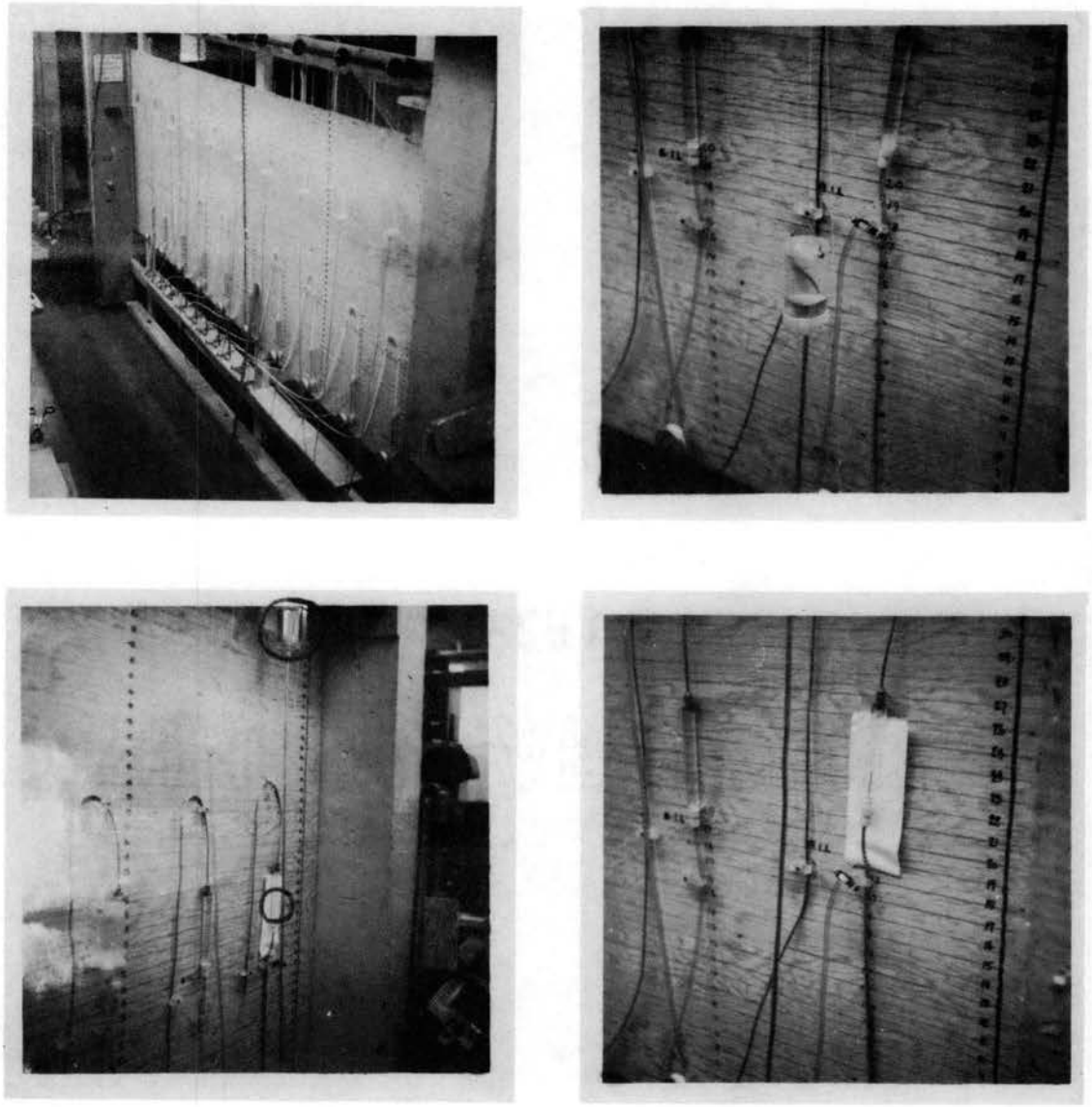

Upper left: General view of the left manometer board.
Upper right: Flushing procedure. (Mercury is below tee-connection).
Lower left: Pressure test. Null level and mercury pot are circled.
Lower right: Close-up of null level during pressure test.

Figure 7. Photographs of the Manometry Apparatus.

The Pore Pressure Probe

Of parallel importance to the investigation was the development of a reliable probe for the measurement of pore pressure. Since the probes were to be pre-installed, it was considered necessary to design and test a probe on a small-scale, pilot basis to insure, (1) that the sedimentation of the clay would not clog the probe, and (2) that the response of the entire measuring system would be acceptable.

Design and Pilot Test of the Probe

A search of the literature revealed that there did not seem to be any rational basis upon which to choose a probe for a given application, nor could any experimental data be found which might be of some aid to such a choice.

Various types of probes were considered and rejected for one reason or another. It had been hoped, for example, to use ceramic probes, since it has been reported, most notably in Bureau of Reclamation publications, that these types of probes were generally superior to porous-stone types, particularly in their response to negative pore pressures. With this in mind, ceramic probes of four different porosities were obtained for the purpose of pilot-testing. However, before any testing was done, it was decided that their use would not be feasible. The commercially available probes were larger than was considered desirable. The principal reason for their rejection, however, was that they were rather fragile and could not readily be connected firmly to the copper lines of the system. In view of these deficien-

cies, it was decided to fabricate a smaller, more substantial probe and test it on a pilot basis in conjunction with the proven manometry system.

The probe finally adopted consisted of 1/8-in. O.D. brass tube, 1½ in. long, with 3/4 in. longitudinal slots cut on both sides. Inserted in the tube was tightly-rolled #325 stainless steel mesh (wire cloth). The portion of the exposed mesh at the slots served as the porous element of the probe. It was found by trial that a 3/4 in. wide, 1 in. long piece of mesh could be rolled into a tight cylinder which would fit snugly into the brass tube sleeve. One end of the tube was then closed by silver soldering; the other end was silver soldered to the end of the ¼ in. copper tube at the predetermined location within the steel tank (See Figure 6, point A).

The method used to test the probe was identical in all respects to that planned for the final model test, with the exception that the soil was prepared in a 6 in. diameter plastic tube. The system is shown in Figure 8. The significant steps in the test were as follows:

(1) All lines, including the probe, were installed and connected to the manometer system, as shown on the schematic.

(2) The plastic tube was mounted and firmly bolted to the plastic base, the tube was filled with tap water, and the periphery at the bottom checked for leaks.

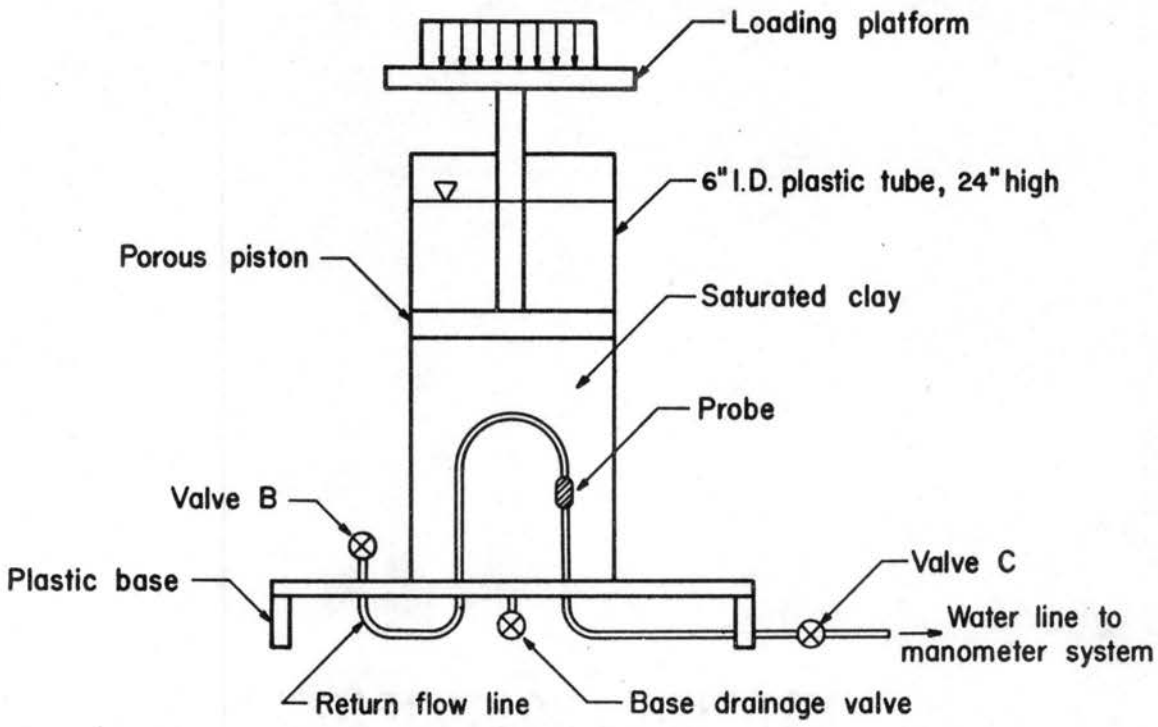

Figure 8. Pilot Test of the Porous Probe

(3) The entire system was flushed with deaired water, Valves B and C open. (Valve C is identical to that shown in Fig. 6.)

(4) Valves B and C were closed, and the system was pressure-tested between Valve C and the null section; steps 3 and 4 were repeated until the pressure test indicated successful deaeration. Data for this test are shown in Table V.

(5) Water was removed from the tube to a level somewhat above the probe; sufficient NaCl was added to attain a 0.1 N salt concentration.

(6) The tube was filled with a clay slurry consisting of 0.1 N salt solution and sufficient clay solids to yield a final height of consolidated clay above the level of the probe and the associated tubing, as shown in the schematic. The moisture content of the slurry was 409%.

(7) Sedimentation was allowed, with base drainage, for approximately one week, whereupon a graded sand filter was added by sedimentation. The purpose of this sand filter was two-fold. First, it provided a very light pressure to initiate the consolidation of the sedimented slurry, which was of a very soft consistency. Secondly, the filter acted subsequently as a fairly effective means of preventing excessive extrusion of the clay between the piston and the walls of the tube. The initial loading of

the sedimented slurry was, in general, a very delicate operation. In fact, in the very early research work on this clay, one investigator had the frustrating experience of observing the loading piston sink virtually to the bottom of the container, as the clay was squeezed upward around the piston. For this test, the piston was introduced to the tube by means of a counter-weighted pulley arrangement, wherein the counter-weights were successively removed periodically so as to give adequate control of extrusion during the initial consolidation. Once the piston was seated successfully it was found that loading could safely continue by adding five-pound weights (about 1/6 psi on the 30 sq. in. area) and then doubling subsequent loads, with sufficient time intervals for at least partial consolidation under the given increment. In this manner, the clay was loaded to approximately 3 psi.

(8) The pilot test results are given in Table V. The first set of data (Readings 1-7, incl.) represents a successful pressure test of the system under a pressure of approximately 7 psi (37.4-23.0 = 14.4 in. Hg), as indicated by the stability of the null section. At 1431 (Reading 7), the pot was lowered to 23.7, and slurry was added, as noted. Subsequently, the clay was sedimented and consolidated

TABLE V

PILOT TEST OF THE POROUS PROBE

Reading	Time	Pot Setting, in.	Null	Comments	
	2/18/67	23.0	24.4	Static condition	
1	1315	37.4	24.5		Pressure
2	1316	"	24.35		test
3	1320	"	24.35		of
4	1330	"	24.3		system
5	1400	"	24.3		
6	1430	"24.3			
7	1431	23.7	24.3	Slurry added	
Sedimentation and consolidation to 3 psi, Valve A closed					
	3/1/67				
8	1600	23.6	23.8		Settlement, in.
9	1620-1625	25-28	23.8	3 psi added at 1620 hours; Valve A opened.	
10	1633	28.6	23.8		
11	1959	28.5	23.8		4/32
12	1900	27.8	23.8		11/32
13	2100	26.8	23.8		17/32
	3/2/67				
14	1000	22.7	23.8		31/32
	1135	22.7	23.8		21/32(+)

under a pressure of 3 psi. Reading 8 was taken after settlement readings indicated that consolidation was virtually complete; the 0.6 in. Hg pressure (23.6-23.0) being a slight residual pore pressure caused by the 3 psi loading. At this point, the test of the probe was initiated. At 1620 (Reading 9), a load representing an increment of 3 psi was added. The response of the system, particularly as represented by the data of Reading 9, is explained as follows: In the time interval, 1620-1625, the pot had to be slowly and continuously adjusted upward (25-28) to maintain the null level at 23.8. This reaction was apparently caused by the effects of side friction in the tube, particuarly the friction developed between the piston and the walls of the tube through the mixture of slurry and sand which had been unavoidably extruded during the initial loading. Thus, the test-load increment of 3 psi (approximately 6" of Hg) was, initially, partially resisted by wall friction rather than the pore water in the saturated clay. Immediately after loading, during the time interval 1620-1625, the friction dissipated, with the pressure being transferred to the saturated clay. This type of reaction was anticipated. That is to say, if the system was frictionless, one would expect an immediate reading of 29.6 for the pot set-

ting (23.6 + 6.0) to balance null. Since some unknown amount of side friction would, in fact, be developed, it follows that the immediate reaction should indicate some pore pressure less than 6" of Hg. Also, the subsequent maximum reading, as represented by Reading 10, should be somewhat less than 29.6, since some consolidation would already have occurred, and there would still exist some lesser amount of side friction. In summary, it was anticipated that no precise, quantitative check of the performance of the probe would be possible with the equipment employed. However, the qualitative or semi-quantitative results were interpreted as being quite favorable. Of considerable importance is the fact that side friction in the final model would not be an inhibiting factor in the proper quantitative interpretation of the results, since the loading would be concentrically applied via a 10 in. diameter block on a 4 ft. diameter soil model.

One of the most significant aspects of this pilot test was the fact that no flushing was employed after preconsolidation of the sample. On the basis of this determination, the decision was made to eliminate the return flow lines in the final test model. If the response in the pilot test had been unfavorable, the probe would have

been flushed using the return flow line, and then re-tested with another load increment. Had flushing been required, the undesirable effects of the use of return flow lines would have included, (a) twice as many copper lines in the soil model, and (b) the possible serious disturbance by flushing of the very quantity to be subsequently measured, the pore pressure.

Location of the Probes: Stress Distribution

The arrangement of the probes in plan was decided on the basis of attaining symmetry of the overall design. Since the tank is circular in cross section, it was logical to employ a circular footing for loading purposes and to arrange the probes in a similar manner. Figure 9 illustrates the plan.

The vertical location of the probes was based upon a stress distribution analysis employing the published data of Jurgensen (1934). These data are reproduced as Table VI. The data shown are influence values for stresses beneath a circular loaded area, and are interpreted as indicated in the sketch of Figure 12. The data may be used for a three-dimensional stress analysis. However, as is pointed out by Jurgensen, the maximum shear stress acts in a radial plane. Thus, for purposes of simplicity, the analysis was treated as a planar (z, r) problem.

The Mohr Circle of plane stress is as shown in Figure 10. Additional nomenclature, other than Jurgensen's data,

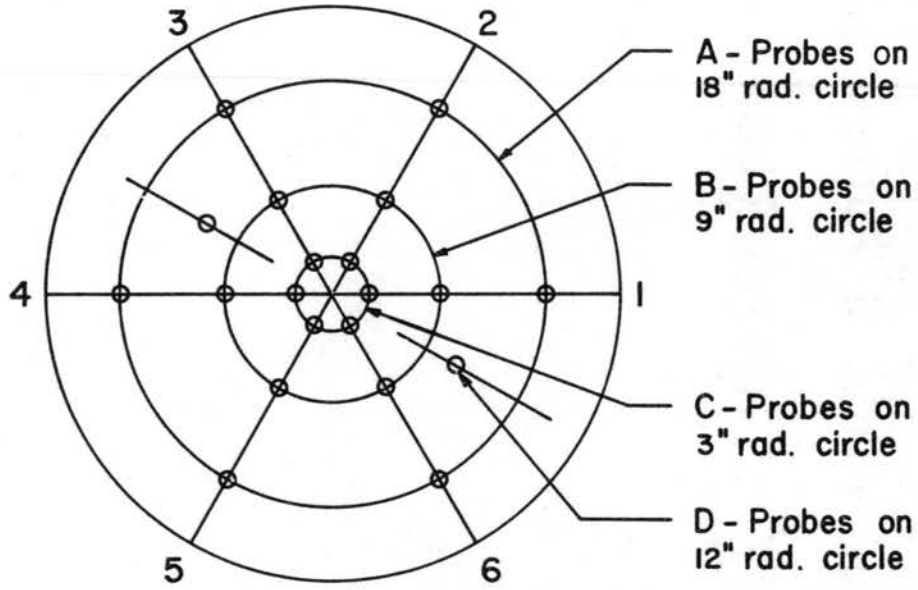

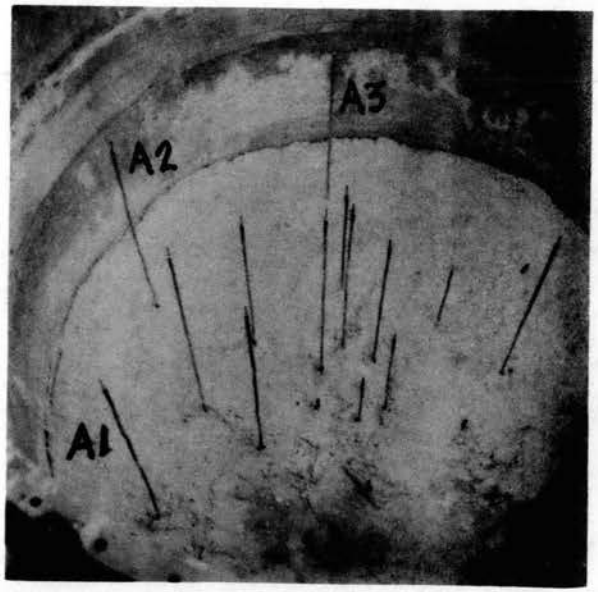

Figure 9. Plan of Probe Arrangement

TABLE VI

INFLUENCE VALUES FOR STRESSES BENEATH A CIRCULAR UNIFORM LOAD (AFTER JURGENSEN AND CAROTHERS)

α	n_r	n_e	n_z	S_{rz}	S
R=0	-.9500	-.9500	-1.0000	0	
R=2/3a					
0°	-.2310	-.2310	-.7904	0	-.280
30	-.2548	-.2625	-.8376	-.0637	-.298
45	-.3344	-.3243	-.8585	-.0529	-.267
60	-.4129	-.4252	-.9062	-.0500	-.252
80	-.6910	-.7213	-.9910	-.0270	-.152
85	-.8134	-.8324	-.9991	-.0071	-.093
90	-.9500	-.9500	-1.0000	0	-.025
R=a					
0	-.1016	-.1016	-.6466	0	-.273
30	-.1406	-.1121	-.6283	-.1364	-.280
45	-.1903	-.1409	-.6064	-.1980	-.287
60	-.2607	-.1879	-.5769	-.2533	-.287
75	-.3516	-.2676	-.5406	-.2996	-.314
80	-.3852	-.3201	-.5272	-.3075	-.316
85	-.4194	-.3935	-.5127	-.3136	-.317
90	-.4500	-.5000	-.5000	-.3162	-.317
R=$\sqrt{2}$a					
0	-.0265	-.0265	-.4810	0	-.227
30	-.0944	-.0430	-.3979	-.1306	-.200
45	-.1337	-.0470	-.3442	-.1599	-.192
60	-.2144	-.0533	-.2117	-.1906	-.191
75	-.2138	-.0498	-.0694	-.1112	-.133
80	-.1564	-.0435	-.0384	-.0579	-.083
85	-.0732	-.0348	-.0164	-.0160	-.033
90	+.0250	-.0250	0	0	-.013
R=2a					
0	-.0119	-.0113	-.2825	0	-.135
30	-.0538	-.0118	-.2234	-.1015	-.132
45	-.0904	-.0128	-.1583	-.1200	-.125
75	-.0932	-.0133	-.0200	-.0373	-.052
80	-.0660	-.0129	-.0037	-.0181	-.035
85	-.0257	-.0186	-.0013	-.0047	-.012
90	+.0125	-.0125	0	0	-.006

TABLE VI (Continued)

R=3a					
0°	-.0013	-.0013	-.1463	0	-.073
30	-.0273	-.0013	-.1052	-.0534	-.066
45	-.0482	-.0024	-.0643	-.0560	-.057
60	-.0575	-.0031	-.0256	-.0388	-.043
75	-.0361	-.0044	-.0038	-.0128	-.022
80	-.0241	-.0046	-.0018	-.0065	-.012
85	-.0090	-.0051	0	-.0015	-.005
90	+.0055	-.0055	0	0	-.003
R=4a					
0	-.0008	0	-.0863	0	-.043
30	-.0160	-.0002	-.0603	-.0325	-.040
45	-.0317	-.0005	-.0313	-.0324	-.032
60	-.0327	-.0011	-.0192	-.0202	-.021
75	-.0203	-.0020	-.0017	-.0067	-.011
80	-.0136	-.0023	-.0002	-.0031	-.007
85	-.0052	-.0027	-.0001	-.0008	-.003
90	+.0031	-.0031	0	0	-.002

Note: The signs shown herein were taken from the original paper, cited by Jurgensen: Carothers, S. D., Elastic Equivalence of Statically Equipollent Loads, Proceedings of the International Mathematical Congress, Vol. 11, Toronto University Press, p. 518. (The negative signs indicate compression.)

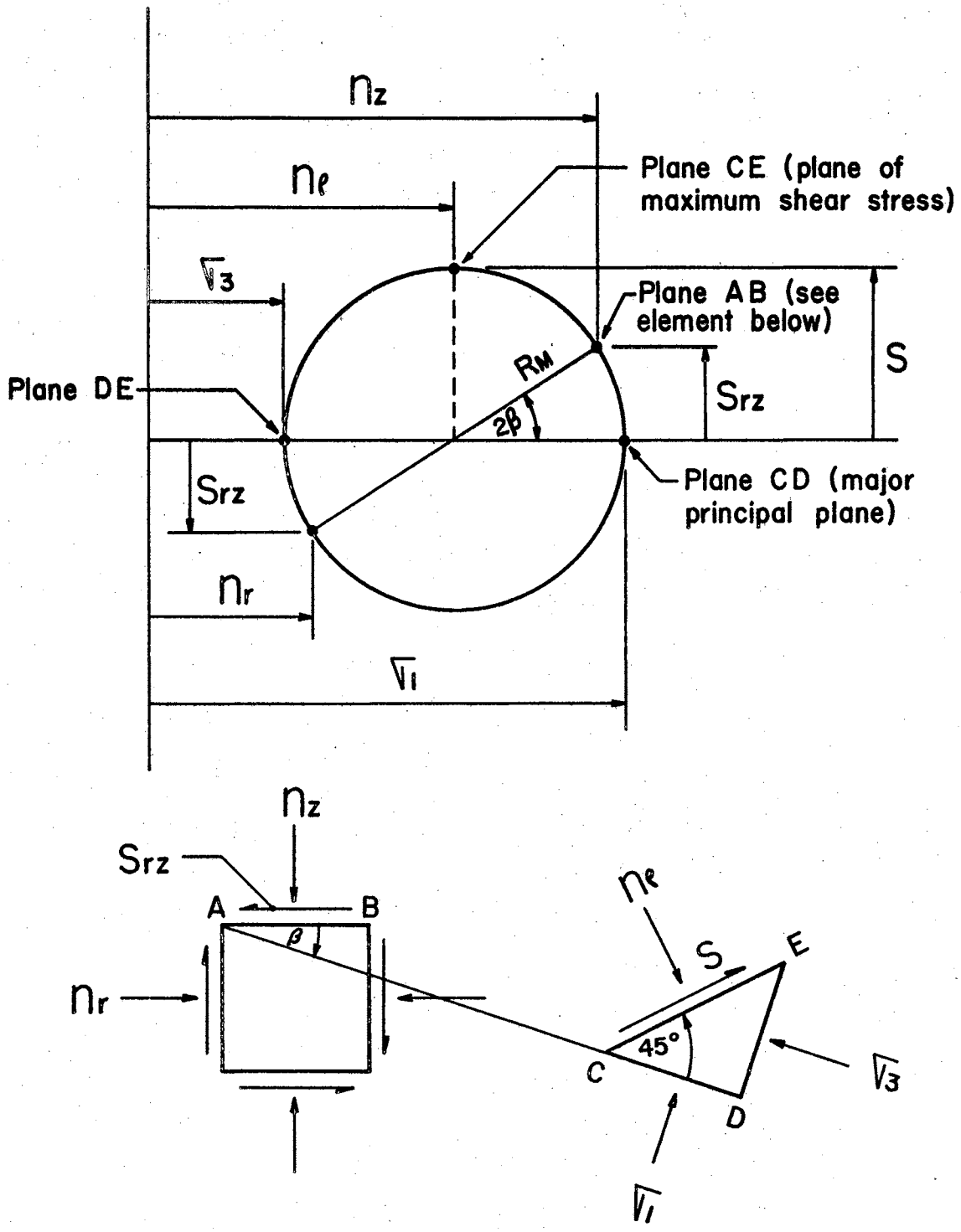

Figure 10. Mohr Circle of Plane Stress

is as follows:

σ_1, the major principal stress

σ_3, the minor principal stress

S, the maximum shear stress

n_ρ, the normal stress on the plane of maximum shear stress

β, the angle between the horizontal and the major principal plane

R_M, the radius of Mohr's Circle

From the geometry of the circle,

$$\text{Tan } 2\beta = \frac{2\, S_{rz}}{n_z - n_r} \qquad \text{Eq. 3.1}$$

$$R_M = \frac{S_{rz}}{\text{Sin } 2\beta} \qquad \text{Eq. 3.2}$$

$$\sigma_1 = \frac{n_z + n_r}{2} + R_M \qquad \text{Eq. 3.3}$$

$$\sigma_3 = \frac{n_z + n_r}{2} - R_M \qquad \text{Eq. 3.4}$$

The application of the foregoing analysis can best be explained by reference to a cross section of the soil model, Figure 11. Shown on the figure, which is drawn to scale, is the lower 3 foot section of the tank containing the soil model. Elevation zero is taken as the top of the tank. As can be seen, the plan was to prepare a soil model 27 inches thick (after sedimentation and preconsolidation) with the top of the model at elevation -9; shown also at this level is the 10 inch diameter footing. Within the cross section of the soil are plotted semi-circles of radii which are func-

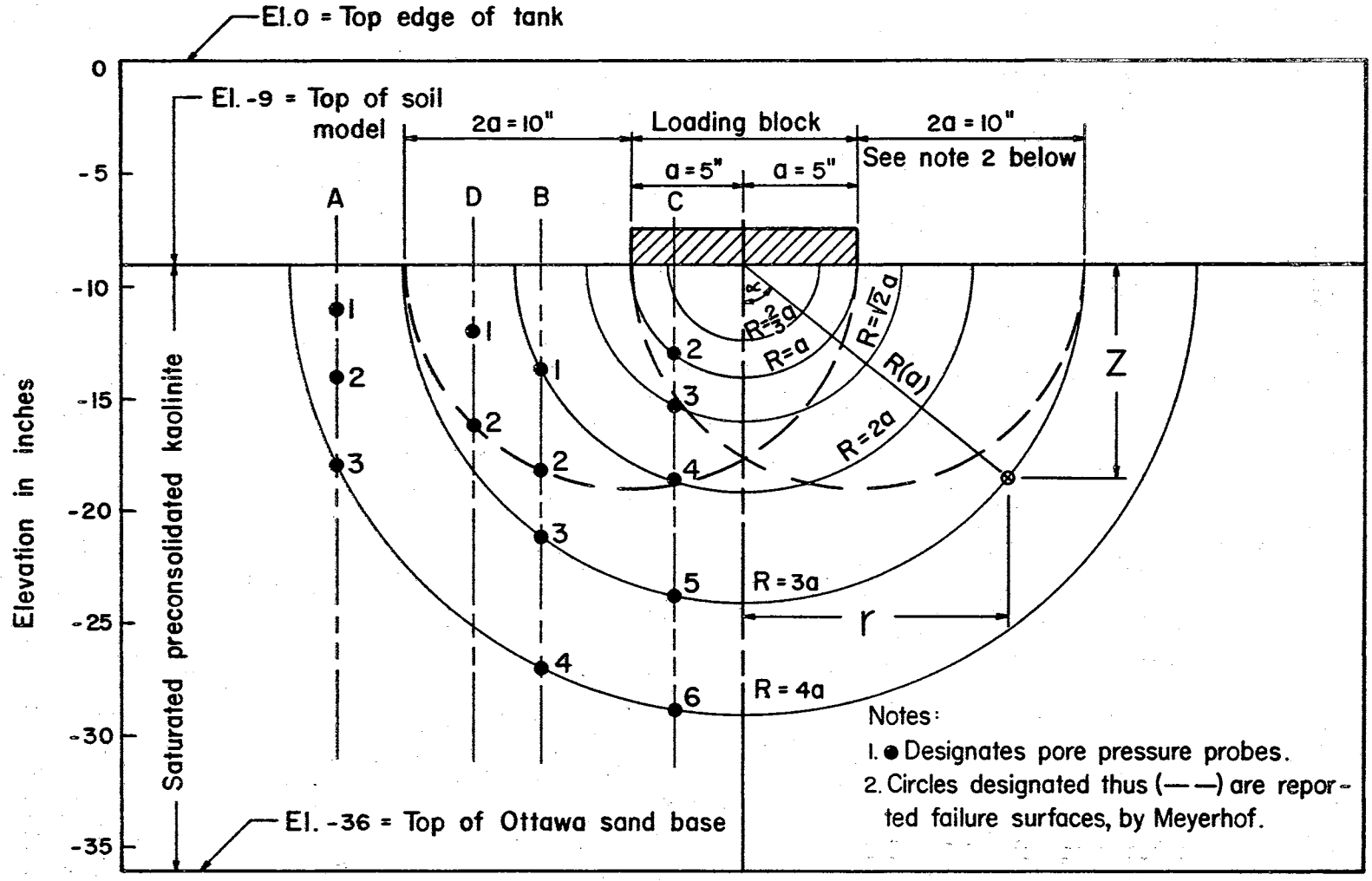

Figure 11. Cross Section of the Soil Model

tions of the radius of the loaded area (R = 2/3 a, a, . . . 4a). The eccentric semi-circles emanating from the right and left edges of the footing (shown dotted) designate the approximate failure surface of such a footing, as reported by Meyerhof (1950-51).

The vertical locations of the probes were decided on the basis of these criteria. A comparison of the figure with Jurgensen's data (Table VI) illustrates the reasoning behind the plotting of the series of concentric semi-circles. This procedure enabled some of the probes to be located at points which would eliminate interpolation of the tabulated data, e.g., the locations of Probes C2 to C6. C1 was eliminated as being too close to the bottom of the footing. Other probes were eliminated on the basis of their being so far removed from the location of the footing that the stresses imposed would be negligible. Jurgensen's data indicate that all stresses of any significant magnitude occur within a radius of R = 4a. Thus, with additional reference to Figure 9, Probes A4, A5, A6, B5, and B6 were eliminated. With C1 also eliminated, the number of probes remaining in the design was fourteen. Of these, some were plotted along the Meyerhof semi-circle, notably D2, B2, and C4, as shown.

Since it was not possible to position all probes at points corresponding to Jurgensen's tabulated data, and since the precise elevation of the top of the soil model could probably not be attained, it was recognized that some interpolation of the data would be necessary. The error involved

in linear interpolation was investigated cursorily by plotting some of the data. The conclusion was that the amount of error could be considerable, depending upon the specific area of interpolation. Thus, a full plot was made of the data. Inspection of Equation 3.1 through 3.4, and the soil cross section, Figure 11, indicated that the most useful plots would be α versus, respectively, the three stress influence values, S_{rz}, n_z, and n_r. To achieve this, it was necessary to construct intermediate plots of R(a) versus the influence values directly from Jurgensen's data. With these graphs it was then possible to construct the more useful sets of curves, presented as Figures 12, 13, 14, and 15. From these curves and Equations 3.1 through 3.4, the complete state of total stress could then be determined in a straightforward manner for any point. That is, summarizing, the angle α could be determined from the actual position of any probe (See Figure 11), the stress influence values could then be read from the curves, and, finally, the complete state of stress could be calculated by the use of Equations 3.1 through 3.4.

Calibration of All Systems

After the successful completion of the pilot tests on both the manometry system and the response of the pore pressure probe, the other systems were constructed and pressure tested. The first step in this sequence of operations was to cut the $\frac{1}{4}$ in. copper tubes within the tank to elevations

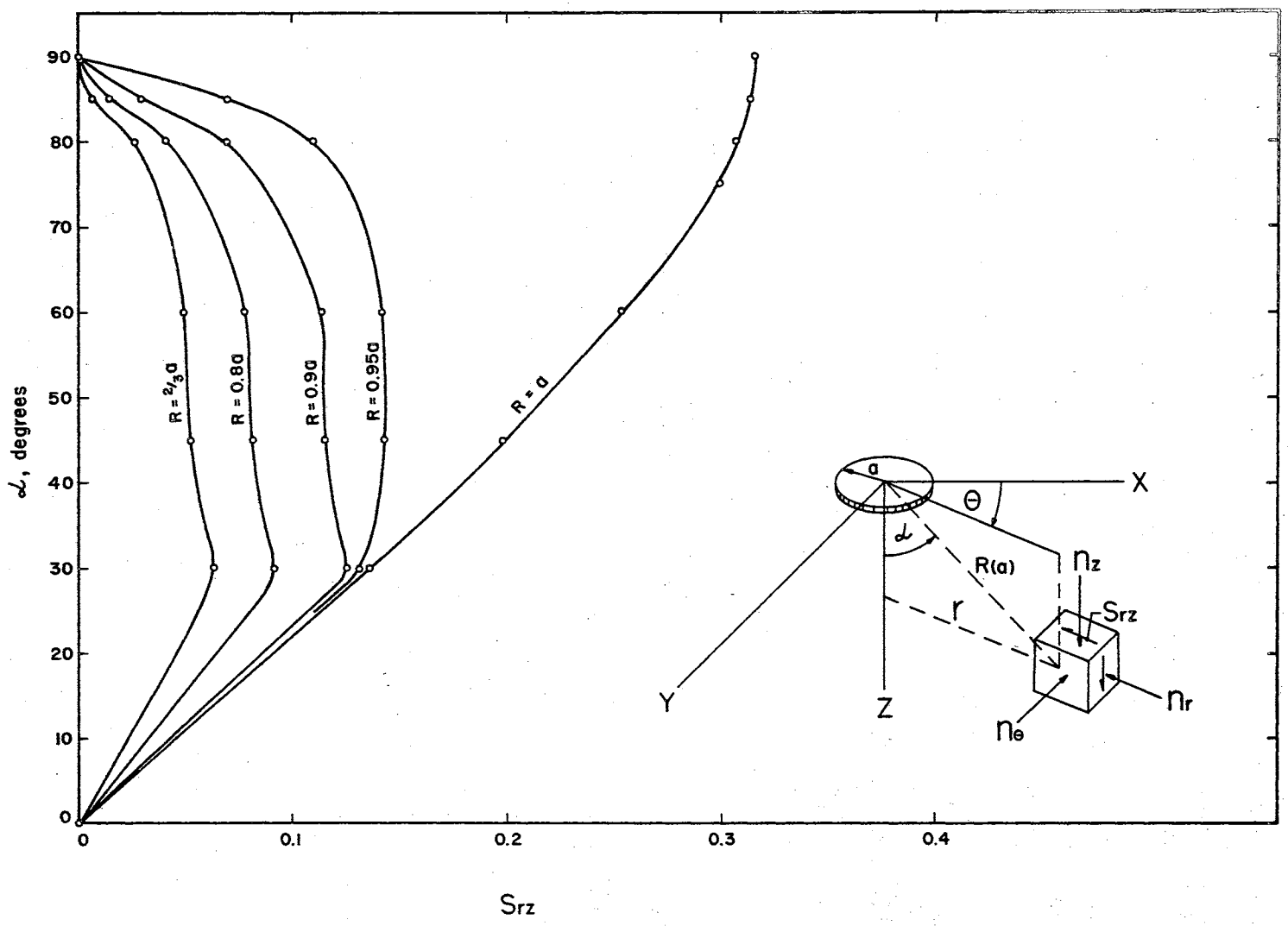

Figure 12. Stress Influence Values: Alpha vs. S_{r_z} for R ≤ a

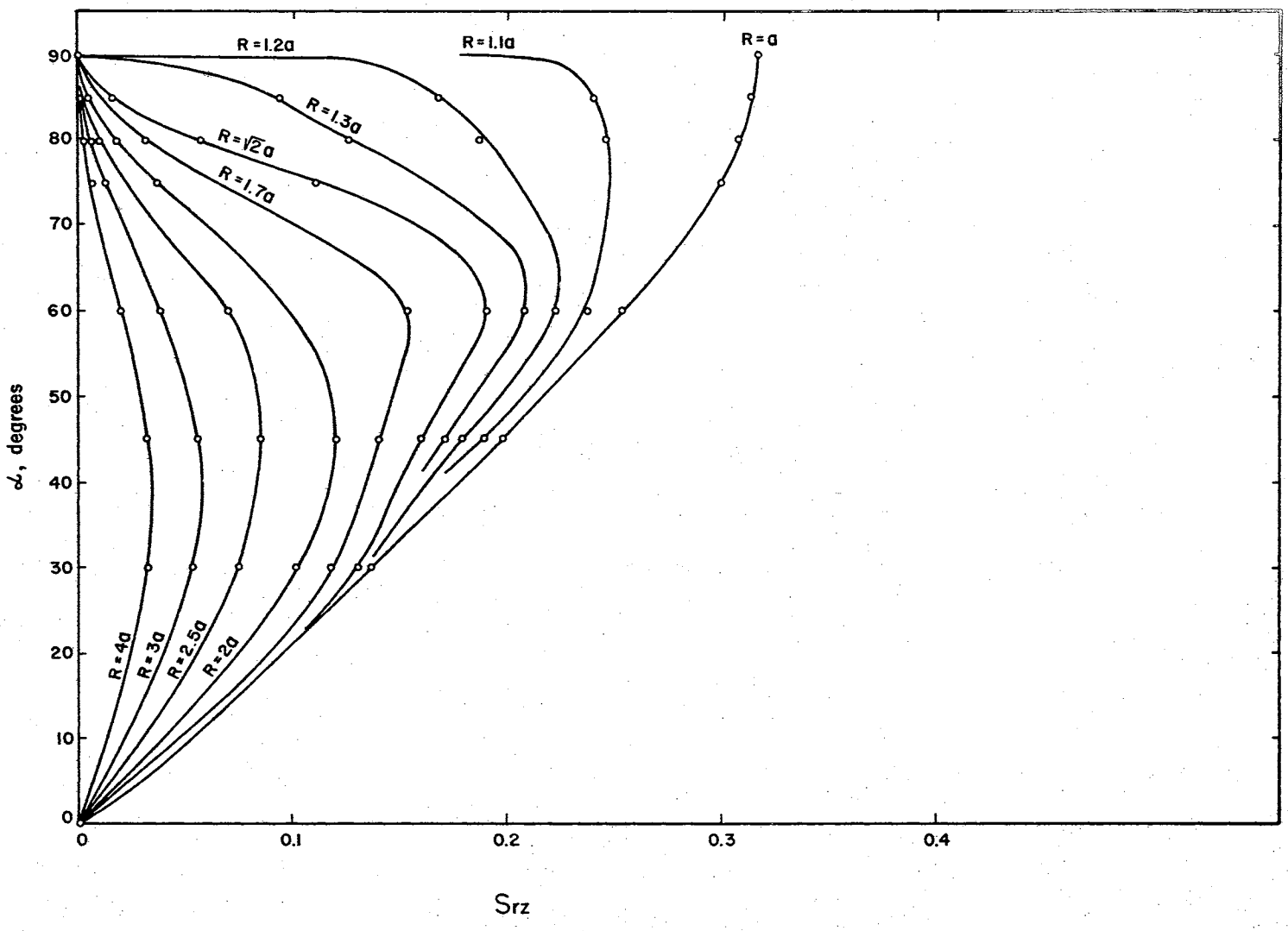

Figure 13. Stress Influence Values: Alpha vs. S_{r_z} for $R \geq a$

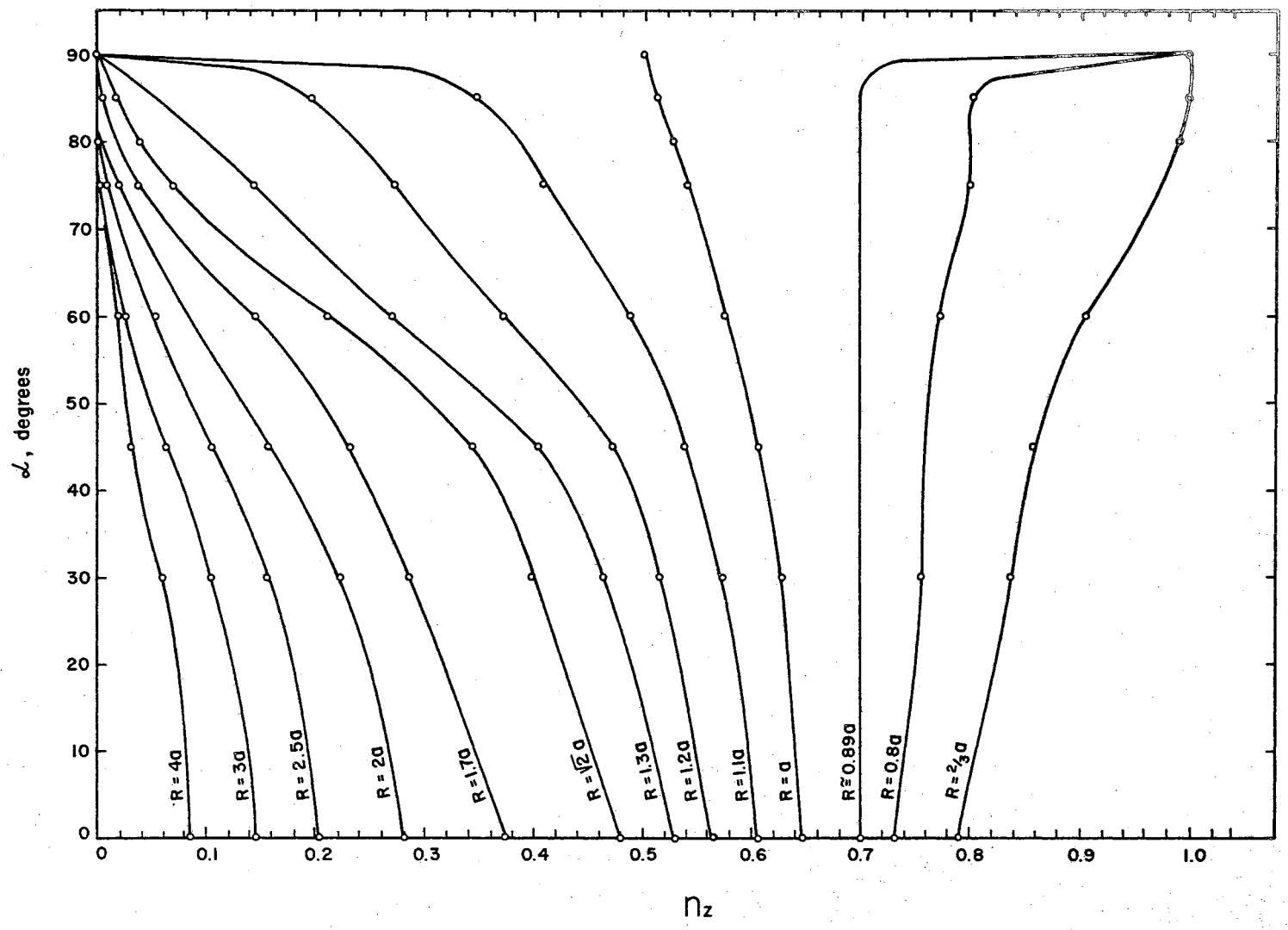

Figure 14. Stress Influence Values: Alpha vs. n_z

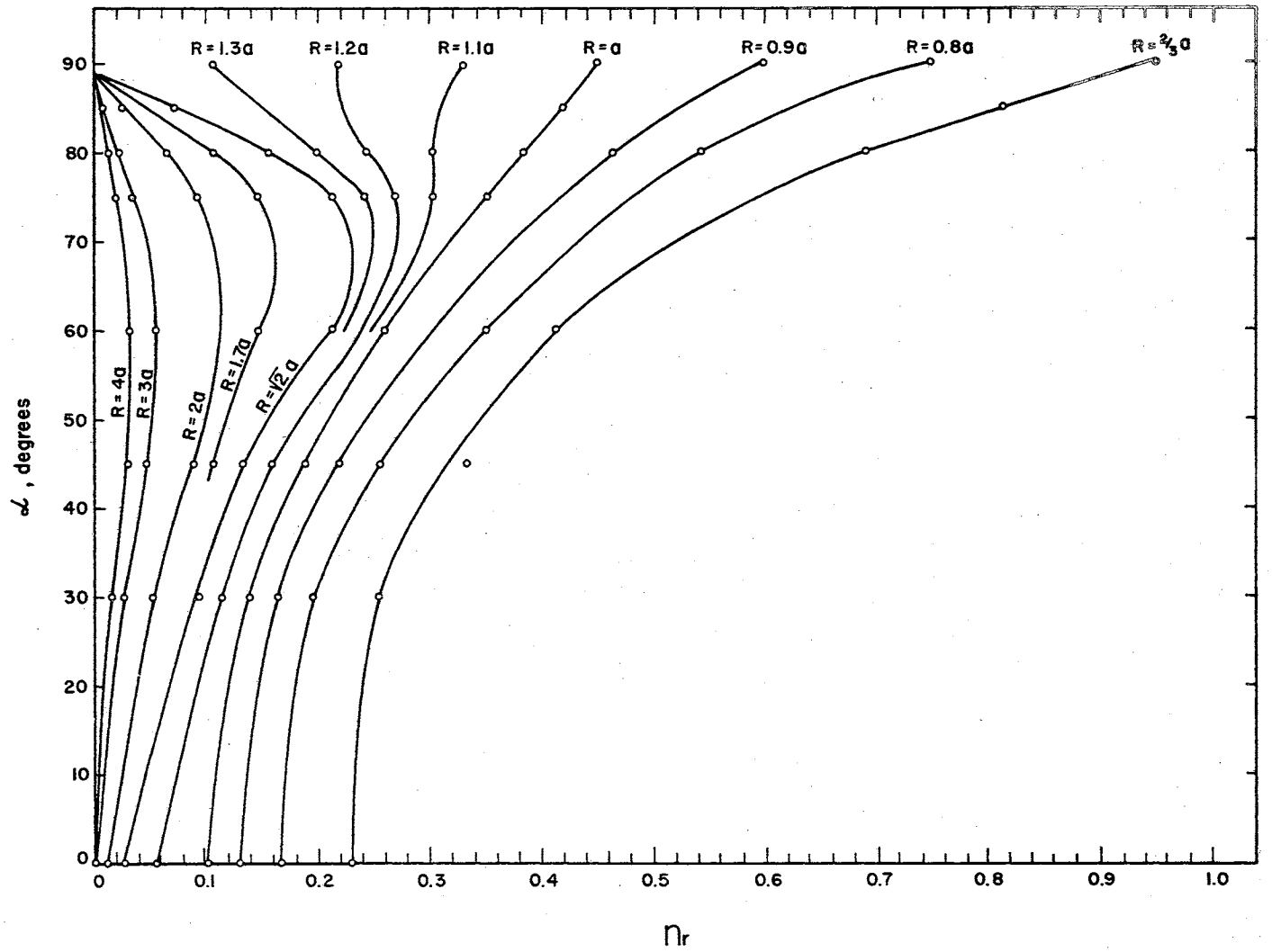

Figure 15. Stress Influence Values: Alpha vs. n_r

such that the center of the subsequently mounted probes would be properly located, as in Figure 11. These locations are summarized in Table VII. After this was done, the probes were mounted and soldered in place. All lines were then flushed to insure that the soldering operations had not sealed the line, either by a complete blockage or by fusing the mesh within the probe. This precaution proved to be important as three of the probes had been completely blocked by the flowing solder. These were removed and replaced successfully. Finally, all lines within the tank were carefully plumbed into the horizontal positions shown in Figure 9.

A 0.1 N NaCl solution was then introduced into the tank to Elevation -9, the planned surface of the soil model. This solution and all subsequent slurry solutions were mixed in a 55 gal. drum and fed into the tank by gravity flow. Thus, all probes were submerged beneath a tailwater elevation which would exist at the conclusion of the preparation of the soil model.

The next major step was the flushing and pressure-testing of all systems preparatory to the construction of the soil model itself. Before proceeding with final calibration tests, all systems were investigated as follows: The lines were quickly flushed with tap water, with no particular attention being paid to complete deaeration. All systems were then pressure-tested for the purpose of discovering leaks at the various connections between Valves K and C (See Figure 6). Many problems were encountered during this phase: loose

TABLE VII

VERTICAL LOCATION OF PROBES

Probe	Elevation of Probe Center, as scaled from Figure 11. (in.)	Cut-off of Copper Tubing (approx. 7/8" below El. of Probe Center).
A1	-11.0	-11.88
A2	-14.0	-14.88
A3	-17.6	-18.88
D1	-12.0	-12.88
D2	-16.0	-16.88
B1	-13.2	-14.08
B2	-18.0	-18.88
B3	-21.0	-21.88
B4	-27.0	-27.88
C2	-13.0	-13.88
C3	-15.4	-16.38
C4	-18.5	-19.38
C5	-23.7	-24.58
C6	-28.8	-29.68

Note: Elevation 0 is taken as the top of the lower 3 ft tank section, see Figure 11.

connections; a few bad valves; small cracks in the ends of the plastic null section which caused leaking under pressure; partial clogging of several lines, apparently caused by cosmoline packing grease in the valves; etc. The problems were all eventually corrected before proceeding with careful deaeration and pressure-testing.

The flushing and testing procedures were described in detail in a preceding section and will not be repeated except for the description of two modifications which proved to be very effective. First, the high-head tank for boiling water was installed in the room above (See Figure 6). A small hole in the floor permitted the flushing to be accomplished through a plastic line (M to H, Figure 6). The second modification was the provision of an ice bath in the cooling tank. It was realized that cold water would be theoretically more effective in the dissolution of any air in the water and also in dislodging any small bubbles that might be trapped in the threads of the various connections. The results of the pressure tests subsequent to the provision of this ice bath confirmed the efficacy of the procedure. These results are shown in Table VIII. The first two readings for each system are an indication of the success of the deaeration. For example, in System C2L (the L refers simply to the left manometer board), the Readings 23.8 and 23.4(-) refer, as noted, to the pot setting and corresponding null level, respectively, for the static condition with Valve C open. When the null level had apparently stabilized, Valve

TABLE VIII

SYSTEM PRESSURE TESTS

System	Time	Pot(in.)	Null(in.)	Comments
C2L	4/1/67			
		23.8	23.4(-)	Static condition, Valve C open (1)
	1425	47	23.75	Valve C closed (2)
	1450	47	23.65	"
	1452	35	23.45	"
	1520	35	23.35	"
	1522	23.9	23.15	Valve C closed
	1522	23.9	23.45	Valve C opened (3)
	1522	23.9	23.45	Valve C closed
B2L	4/4/67			
		23.5	23.0	(1)
	1058	47	23.0	(2) No change
	1147	47	22.85	"
	1147	34.8	22.85	"
	1220	34.8	22.85(-)	"
	1221	23.6	22.85(-)	"
	1221	23.6	23.1	(3)
	1221	23.6	23.1	(2)
A1L	4/4/67			
		23.6	23.15	(1)
	1207	47	23.15	(2) No change
	1245	47	23.0	"
	1246	23.6	23.0(-)	(3)
	1246	23.6	23.25	(3)
	1246	23.6	23.25	(2)
B1L	4/4/67			
		23.65	23.25	(1)
	1332	47	23.4(+)	(2)
	1350	47	23.25	"
	1353	23.65	23.0	"
	1353	23.65	23.4	(3)
	1353	23.65	23.4	(2)
D45L	4/4/67			
		23.95	23.65	(1)
	1552	47	23.65	(2) No change
	1703	47	23.4(+)	"
	1703	23.95	23.4(+)	"
	1703	23.95	23.7	(3)
	1703	23.95	23.7	(2)

TABLE VIII (Continued)

A2L	4/5/67				
		23.75	23.35	(1)	
	1141	47	23.35	(2)	No change
	1225	47	23.25	"	
	1226	23.85	23.25	"	
	1226	23.85	23.50	(3)	
	1226	23.85	23.50	(2)	
B3L	4/5/67				
		23.5	23.0	(1)	
	1729	47	23.5	(2)	Maximum change
	1815	47	23.4	"	
	1816	23.5	22.9	"	
	1816	23.5	23.0	(3)	
	1816	23.5	23.0	(2)	
C3L	4/6/67				
		22.75(+)	22.3	(1)	
	1202	47	22.4(-)	(2)	
	1214	47	22.3	"	
	1215	22.8	22.2	"	
	1215	22.8	22.4(+)	(3)	
	1215	22.8	22.4(+)	(2)	
B4R	4/6/67				
		23.0	22.5	(1)	
	1753	47	22.8	(2)	
	1812	47	22.75(-)	"	
	1813	23.0	22.4(-)	"	
	1813	23.0	22.55	(3)	
	1813	23.0	22.55	(2)	
D23R	4/7/67				
		22.8	22.4	(1)	
	1245	47.6	22.7	(2)	
	1315	47.6	22.7(-)	"	
	1316	23.0	22.4	"	
	1316	23.0	22.5	(3)	
	1316	23.0	22.5	(2)	
C4R	4/8/67				
		23.0	22.55	(1)	
	1158	47	22.8	(2)	
	1217	47	22.4	"	
	1218	23.0(+)	22.15	"	
	1218	23.0(+)	22.6	(3)	
	1218	23.0(+)	22.6(+)	(2)	

TABLE VIII (Continued)

C6R	4/8/67				
		23.0	22.6(+)	(1)	
	1558	47	22.65	(2)	No change
	1605	47	22.6(+)	"	
	1606	23.0(+)	22.65	"	
	1606	23.0(+)	22.65	(3)	
	1606	23.0(+)	22.65	(2)	
A3L	4/8/67				
		23.2	22.75	(1)	
	1302	47	22.75	(2)	No change
	1400	47	22.2	"	
	1401	23.25	22.15	"	
	1401	23.25	22.8(+)	(3)	
	1401	23.25	22.8(+)	(2)	
C5R	4/8/67				
		22.8	22.4(-)	(1)	
	1532	47	22.4	(2)	No change
	1546	47	22.35	"	
	1550	22.8	22.3	"	
	1550	22.8	22.5	(3)	
	1550	22.8	22.5	(2)	

C was closed and the pot was raised to its maximum level of 47 inches, thus creating a pressure in the closed system of about 11.5 psi. The immediate rise of the null level was, for this sytem, about 0.35 in., which represents a volume change of about 0.0011 cu. in. (0.015 cc, or about 0.005 cc per 1/10 th inch). It is seen that the next reading listed reflects a 0.1 inch depression of the null level. This behavior was found to be typical of all systems, and its occurrence led to two conclusions: (a) the systems were tight, and (b) there was some slight hydraulic instability in the Hg columns. The explanation of the latter conclusion is that the small amounts of water that had been unavoidably trapped in the Hg columns within the null section slowly moved upward and eventually created additional pressure above the null level, thus depressing the mercury. This upward movement of water was observable in many cases and in fact, the accompanying vertical drag forces split the mercury column on several occasions. The last three sets of readings for each system tend to verify these observations. These readings were taken with the pot returned to the static level. When the C-Valve was opened (2nd from the last reading of any system), the null level immediately returned upward an amount equal to the original depression. The additional pressure caused by the unstable action had been relieved by flow through the probe.

A general inspection of the data of Table VIII illus-

trates the success of the flushing for deaeration. As noted in the comments, seven of the fourteen systems were completely deaired, and the maximum null change was 0.5 inches. It should be noted that the use of the ice bath in the cooling tank appeared to make a substantial difference. Before its adoption, extensive flushing and manipulation procedures did not produce results as consistently good as were finally attained. In fact, it had appeared that movements at null level of up to one inch might have to be accepted.

The Preparation of the Soil Model

As in the pilot test of the probe and in other preliminary tests, the preparation of the soil model was accomplished in two phases, sedimentation and preconsolidation. Of course the scale of operations and the quantities involved were considerably larger. The total amount of slurry necessary to yield a sedimented, preconsolidated specimen approximately 27 inches thick had been estimated from the pilot tests. Simple weight-volume relationships were used in conjunction with the pilot test data for the determination of the quantities for preparation of the slurry. Details of these estimates are not included, but a brief listing of some of the results serves to illustrate the magnitude of the operations.

(1) Total volume of slurry, at a moisture content of 400%: 149.4 ft^3.

(2) Total weight of clay solids: 2130 lbs.

(3) Total weight of salt (for 0.1 N solution): 50 lbs.

(4) Total volume of tank with extensions (h = 7.5 ft.): 94.3 ft^3.

As can be seen by items (1) and (4), it was necessary to sediment the clay in stages. That is, the tank was first filled with slurry and sedimentation was allowed until the surface of the clay was such as to allow decanting (by siphoning) of some of the excess water. The removal of this water allowed additional slurry to be added. Four slurry additions were employed to fill the tank. To accelerate the sedimentation rate between decanting operations, the drainage hose at the bottom of the tank was connected to a large glass bottle which, in turn, was connected to a vacuum pump. This arrangement provided additional drainage pressure to effect a greater sedimentation rate. It was recognized that this procedure would tend to cause non-uniform consolidation, in that the drainage pressure would vary linearly with depth. However, it was felt that this effect would be largely negated by the subsequent much heavier preconsolidation which was planned. Also, as a practical matter, it was evident that simple sedimentation, i.e., without base drainage, would have required a very long waiting period of perhaps many months. A definite additional advantage accruing from this procedure was a lessening of the subsequent problem of the very delicate initial loading for preconsolidation, as described previously for pilot testing. The sedimentation phase was accomplished in about three months.

The initial preloading was done by gravity loading which could be readily controlled so as to minimize the danger of extrusion. The piston used to transmit the load was made entirely of 3/4 in. plywood so that initially it would float in the water above the clay. The clay surface at this stage was at about El. +15 in. as a result of sedimentation with drainage pressure.. The lower platform of the piston was perforated with drill holes and encased, by stapling, with a cotton cloth to allow egress of water during the loading of the clay. The upper and lower platforms were separated by six 6 in. X 3/4 in. plywood joists, arranged symmetrically in 60° segments. No permanent connections were used in the fabrication of the piston. The joists were attached to the bottom platform by the use of wood cleats, one on each side of the joists, so that the joists could later be pulled out of the slots thus formed. The top platform rested on top of the 3/4 in. joists, with no connection whatever. Thus, it would later be possible to remove all or any part of the piston without significant disturbance to the clay.

The initial loading of the piston was accomplished with some difficulty. The extrusion was kept within tolerable limits, but because of some unavoidable load eccentricity, the piston started to tip. However, with some judicious shifting of the loading weights, the piston was righted to an approximately level and stable orientation. Increments of load were on the order of 0.2 psi or less and the total load added was about 1500 lbs. or approximately 0.8 psi.

This initial preloading resulted in a settlement of about nine inches to El. +6 in. The next phase was a continuation of the preloading, but with conversion to a jacking system for load application. The jacking scheme was as shown in Figure 16. In order to provide for a more rigid piston for the heavier loads and also to allow clearance for the jacks, the joists of the piston were removed, and the exterior joist system of steel plates and I-beams installed as shown in the figure. The 8 W 28 reaction-beam and its bolted connections were designed to allow about 18 tons total jacking load, corresponding to about 20 psi maximum on the 4 ft. diameter area.

The soil model for the test was preloaded to a pressure of 15 psi (13.6 tons total load on the 4 ft. diameter area). Because of many problems which developed, including extrusion of soil and binding of the piston, this preloading operation took approximately four months to complete. To insure reasonably uniform preconsolidation, the last preload increment was made as small as was considered reasonable, 0.8 tons, and it was repeated fifteen times for approximately one-hour durations. It should be noted that the principal disadvantage of using hydraulic jacks was that load levels could not be maintained to very small fluctuations without the use of some type of servomechanical device. As a new load increment was applied, it would immediately diminish as consolidation ensued. Thus, as a reasonable compromise, the last increment employed in the loading schedule was regulated

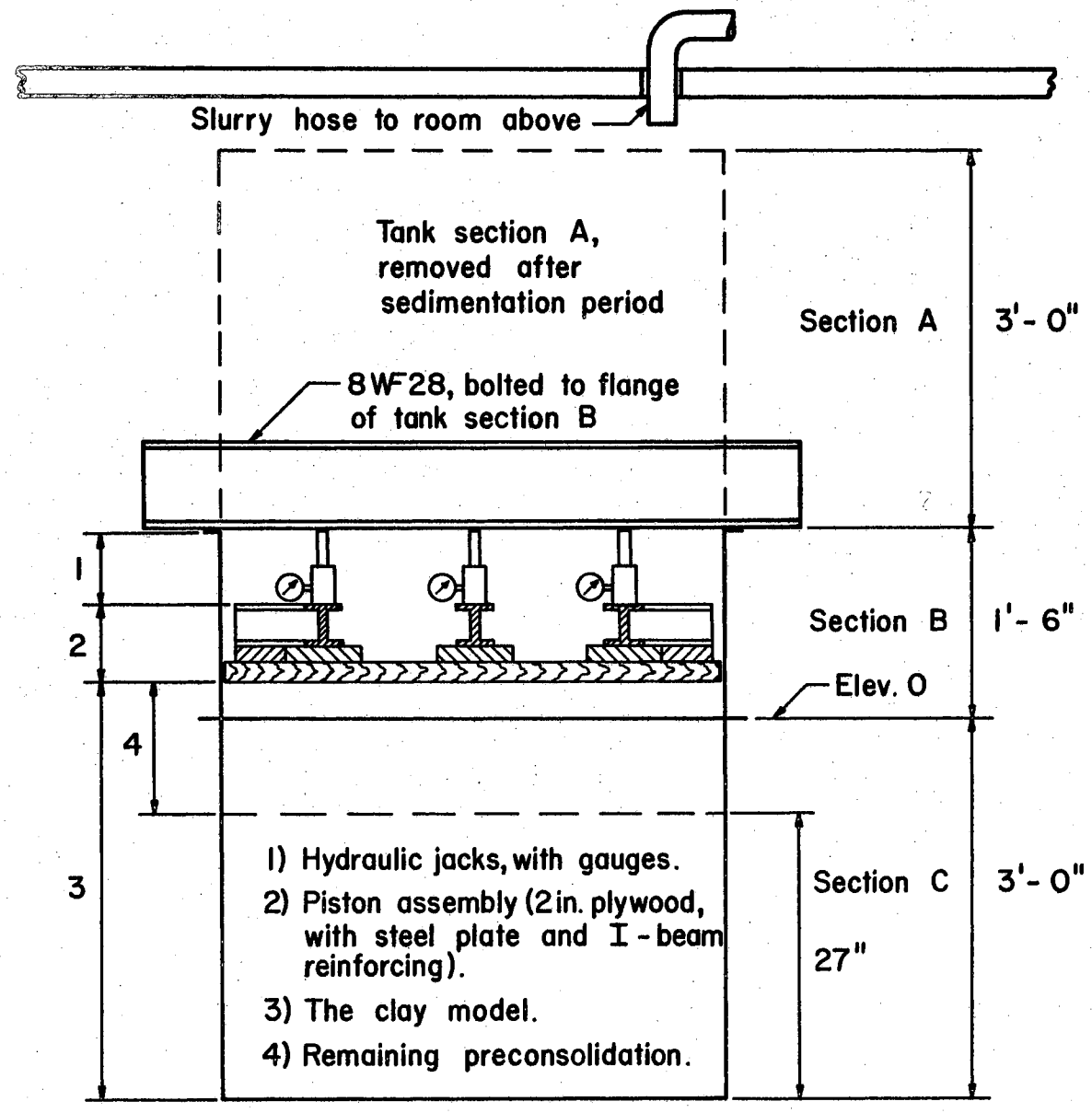

Figure 16. Schematic of Tank and Preloading Systems

by hand from about 13.5 to 14.3 tons (average value = 13.9 T, as planned). As noted this fluctuation occurred within about one hour, whereupon the load was adjusted upward to the higher value. With fifteen repetitions of this loading process completed, it was assumed that the model was finally and uniformly preconsolidated to an average pressure of 15 psi. The time for 90 percent consolidation had been estimated to be approximately 12 hours. As a consequence of the preloading operation, the model attained a grade level of El. -9 inches, as planned, indicating that the preliminary pilot-test data, as they pertained to preparation of the model, were quite reliable.

During the period of soil model preparation, an unexpected problem developed with respect to the stability of the null level. As noted previously, all systems had been flushed and successfully pressure-tested prior to the placement of the clay slurry. In succeeding weeks, it was observed that all null levels were slowly rising and gave no appearance of stabilizing. At first it was thought that differential temperature expansion was the cause, but this was ruled out as a major factor because of the randomness of the amount of rise among the essentially identical fourteen systems. In fact, one system (C3L) had a null rise much greater than any of the others. Eventually the mercury in this system had climbed out of the 1/16 in. bore of the null section and into the threaded section of the top connection, a distance of about 5 inches. The only plausible explanation was

evaporation of water from the (ostensibly) closed system.

Since this system would have been useless if left untouched, it was decided to investigate the effect of the evaporation on the deaeration of the system by rerunning the pressure test. In order to do this, the static null level was re-established by opening the valve leading to the probe within the tank. At this stage of model preparation, the level of the clay was at about El. +15 in. This excess tailwater, as compared to that corresponding to the static null level, caused a backflow through the probe and depressed the mercury column. With the static null level regained, the pressure test was repeated. This test was apparently unsuccessful in that the mercury column rose steadily under pressure. Upon close inspection, however, it was found that a very small crack, indiscernable to the eye, had somehow developed in the top of the plastic null section. Water was slowly leaking through this crack under the induced pressure of the test. Because this system had exhibited no such leak in the earlier pressure test, i.e., before the start of the model preparation, it was concluded that some internal forces must have developed to cause the crack. A rational explanation is that, (a) the evaporation of water created a vacuum, thus effectively placing the plastic null section in compression, and (b) the copper connection at the top of the null section expanded relative to the plastic as a consequence of a general increase in the ambient temperature (April to July), resulting in outward radial forces at the top of the

null section. The effect of these opposing forces was the development of the crack in the plastic null section, resulting in the observed fluid leak in the July pressure test.

Because of the fact that the pressure test on this system was inconclusive with respect to evaporation effects on deaeration, it was decided to check all other systems in an identical manner. The results were positive in that all pressure tests were successful. No other disqualifying leaks were found and it was shown that the probes had not become clogged. The effect of disturbance of the clay around the probes caused by the induced flow in re-establishing null levels was not considered significant because the clay had to be compressed another two feet before the final load test.

In an attempt to prevent the same behavior from reoccurring, all connections were wrapped with absorbent strips of cloth and saturated twice per day. The null levels continued to rise in spite of this effort.

Because the evaporation could not be prevented, it was decided to make a mathematical correction for the creep which would develop during the remaining period of the preloading phase. To prevent physical damage to the null section apparatuses, all mercury pots could be raised to create a small positive pressure in the lines.

External Instrumentation

Instrumentation for settlement and surface heave measurements was as shown in Figure 17. As is typical for field

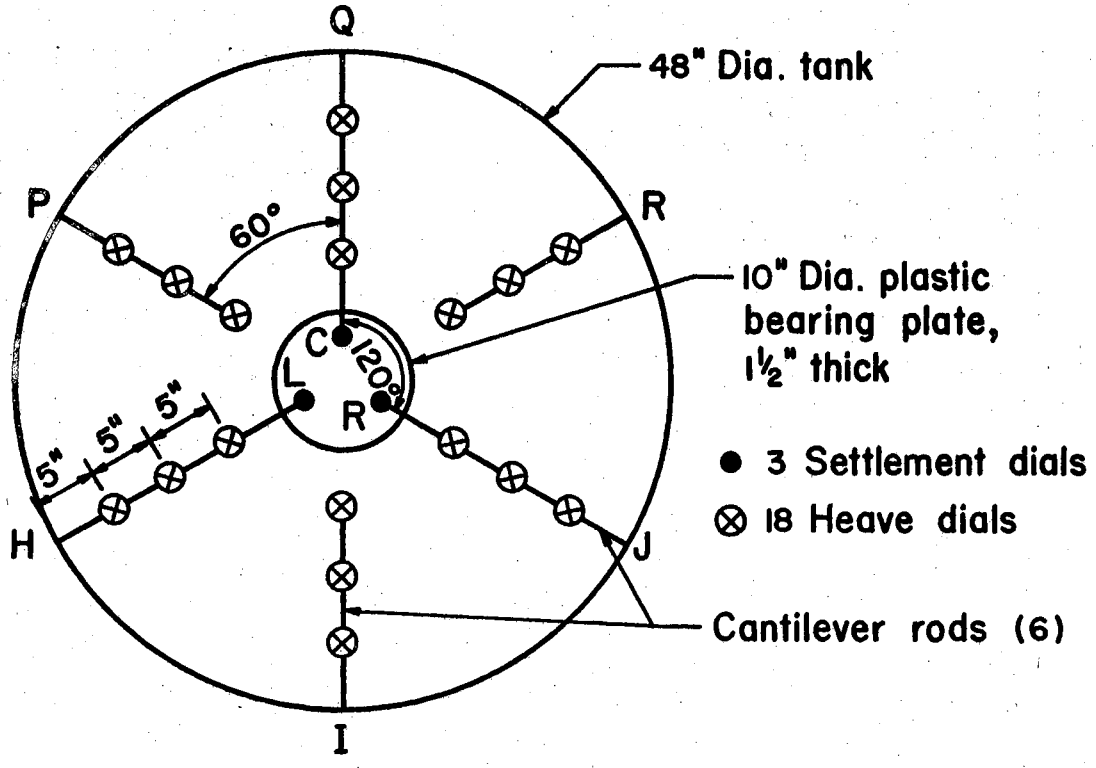

(a) SCHEMATIC PLAN

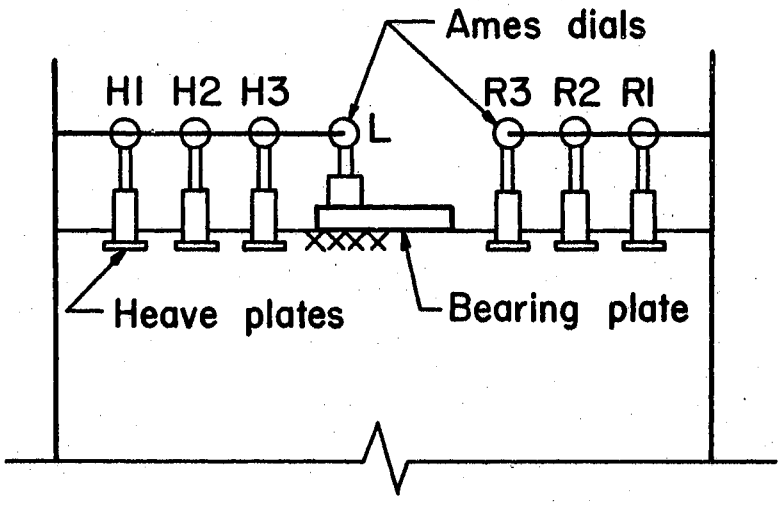

(b) SCHEMATIC SECTION (HLR)

Figure 17. Settlement and Heave Measurements

plate bearing tests, settlement was measured at the 3rd points of the circular footing.

The major purpose of the heave measurements was to determine, indirectly and in a general way, the configuration of the failure mechanisms. It was thought that a local shear failure (soft clays) would result in a concave-upward radial profile, and that a general shear failure (firm or stiff clays) would produce a more-or-less concave-down profile, with the maximum heave value corresponding approximately to the terminus of the failure surface, i.e., the "Meyerhof Circle" in Figure 11. Figure 18 illustrates the generalized profiles described and the corresponding settlement curves.

Additional Preliminary Tests

The shear strength of the clay, as governed by its cohesion values, was determined by a series of vane shear tests. The results are shown in Figure 19. This graph was used as a basis for estimating the proportions for the slurry preparation and, subsequently, for an estimate of the ultimate bearing capacity of the circular footing.

Slurry Proportions

Since it was decided to preload the first model to a pressure of the order of 15-20 psi, a representative moisture content, w, of about 45%, was chosen. On this basis the total volume of sample, 27" preloaded thickness was:

$$v = 0.785 \times 4^2 \times 2.25 = 28.3 \text{ ft}^3$$

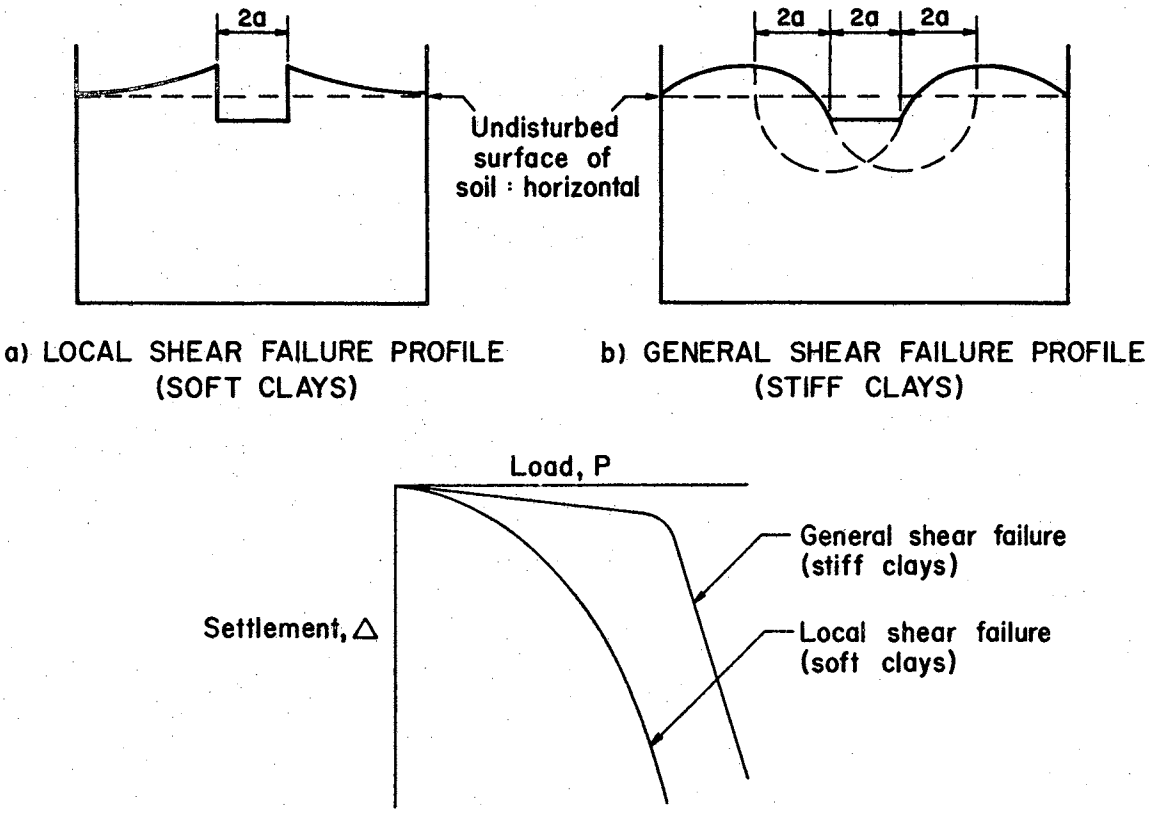

Figure 18. Generalized Failure Mechanisms

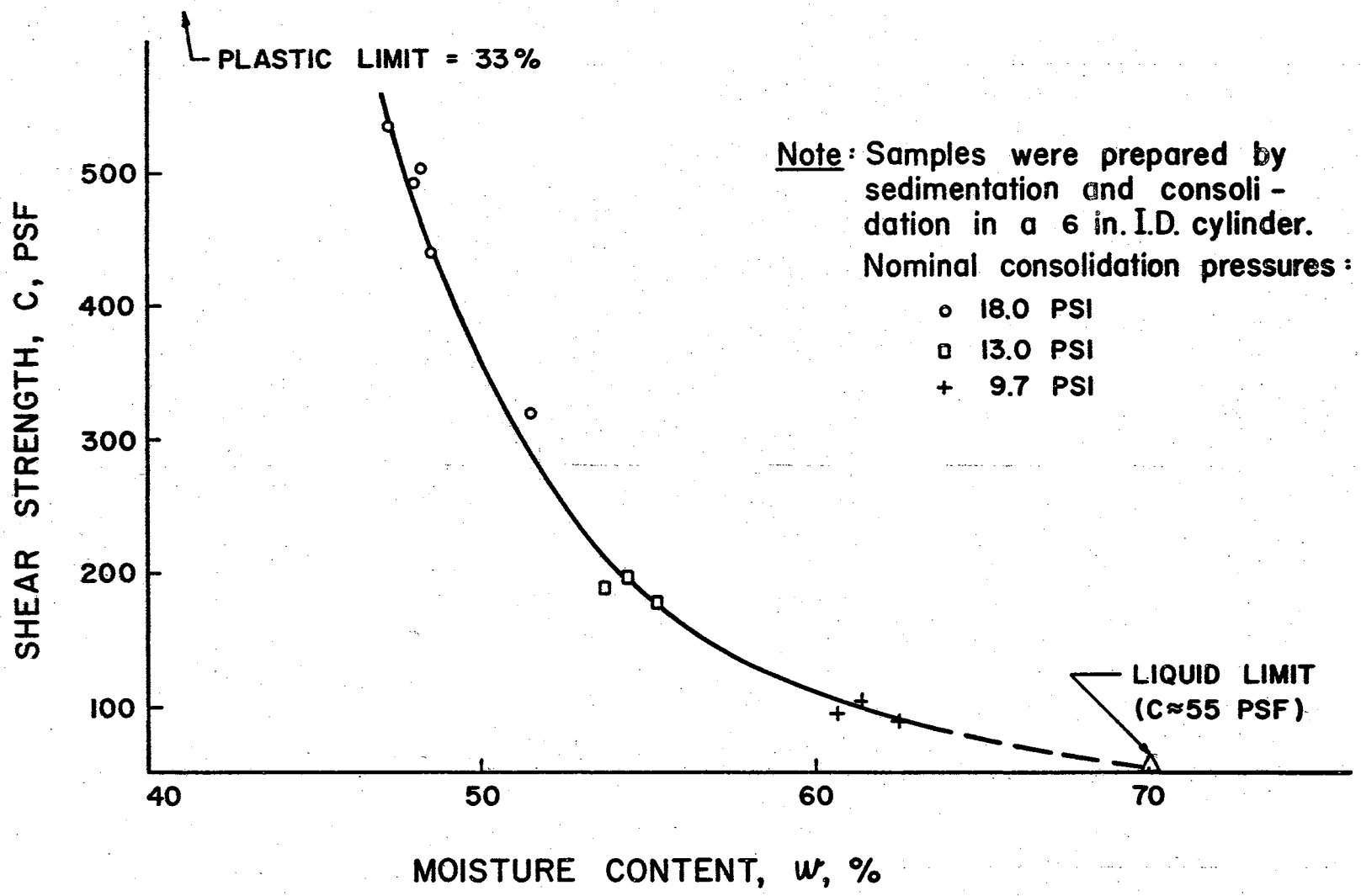

Figure 19. Shear Strength of 0.1 N Sodium Kaolinite by Vane Shear Tests

For a fully saturated sample, the void ratio,

$$e = wG_s = 0.45 \text{ X } 2.64 = 1.187 = V_v/V_s$$

The total volume,

$$V = V_v + V_s; \qquad \text{and} \qquad V_v = V - V_s$$

Thus,

$$\frac{V - V_s}{V_s} = 1.187 = \frac{V}{V_s} - 1; \quad V = 2.187\ V_s$$

$$V_s = \frac{28.3}{2.187} = 12.93 \text{ ft}^3$$

The total weight of solids was:

$$W_s = V_s G_s \gamma_w = 12.93 \text{ X } 2.64 \text{ X } 62.4 = 2130 \text{ lb.}$$

Adopting a slurry moisture content of 400%, the weight of water,

$$W_w = 4 \text{ X } 2130 = 8520 \text{ lb.}$$

Volume of water,

$$V_w = 8520/62.4 = 136.5 \text{ ft}^3$$

Volume of solids,

$$V_s = \frac{W_s}{G_s \gamma_w} = \frac{2130}{2.64 \text{ X } 62.4} = 12.9 \text{ ft}^3$$

Thus the total volume of slurry to produce the model was estimated to be 149.4 ft^3. Using a standard 55 gal drum (V = 7.38 ft^3), the number of barrels required was 149.4/7.38 = 20.3. Similar weight-volume relationships produced the following proportions for one barrel of slurry: 105 lb. clay; 50.3 gal. water; 2.46 lb. salt.

Bearing Capacity Estimate

Using Terzaghi's bearing capacity formula for a circu-

lar footing, for the ϕ-zero condition, the ultimate bearing capacity,

$$q_f = 7.4c$$

From Fig. 19, at a preload pressure of 15 psi,

$$c \doteq 350 \text{ psf}$$

$$q_f \doteq 7.4(350) \doteq 2590 \text{ psf.}$$

For a 10-in. diameter footing, the ultimate load,

$$P \doteq (2590)(.785)\left(\frac{10}{12}\right)^2 \doteq 1410 \text{ lb.}$$

CHAPTER IV

TESTING OF THE SOIL MODEL

The preload pressure of 15 psi produced a grade level of -9.0 inches, corresponding to a model thickness of 27 inches, which was as planned. The preload apparatus was dismantled, the piston was removed, and the 10-inch diameter loading plate was centered and leveled.

Planning and Conducting the Test

Loading

The method of loading was chosen on the basis of the estimated ultimate bearing capacity of Q = 1410 lbs. Static loading was considered to be preferable to the use of hydraulic jacks, since the former method would be more representative of construction conditions. Load increments were selected as one-ninth of the ultimate load, in order that the addition of the third increment would result in a load level approximately that of a typical allowable bearing pressure, i.e., with a safety factor of 3. The pore pressures developed at this level would be considered as most pertinent to the state-of-stress analysis. Thus, Q_i = 1410/9 = 157 lb.

The rate of loading was to be as fast as possible, consistent with obtaining what would appear to be reliable pore

pressure readings at all probes, and at each load level. The rapid loading rate was considered necessary to minimize the effects of consolidation.

In order to prevent significant initial load eccentricity, the loading was to be started simply by adding water to a 2-ft. diameter barrel, which had been carefully placed concentrically on a stack of 6-in diameter steel plates. The plates were necessary to allow clearance for the settlement dials at the 3rd points of the bearing plate and to provide a platform for the barrel. Successive increments were to be placed with additional water, sand, and steel weights, in that order. During the test loading, the barrel was to be restrained from tipping by a steel tripod-hoop device. The legs of the tripod were bolted to the flange of the tank. The initial clearance between the barrel and the hoop was about one inch. Figure 20 shows photographs taken during and shortly after the test.

Personnel

Twenty-two people were involved with the final loading test: twelve staff members of the Department of Civil Engineering, nine undergraduate students, and one graduate student, all of the Newark College of Engineering. The rather high personnel requirements was occasioned largely by the decision to balance continuously all null pressure devices (for pore pressure measurements) throughout the test. Job assignments were made as follows: seven two-man teams for pore pressure measurements, two men for settlement measure-

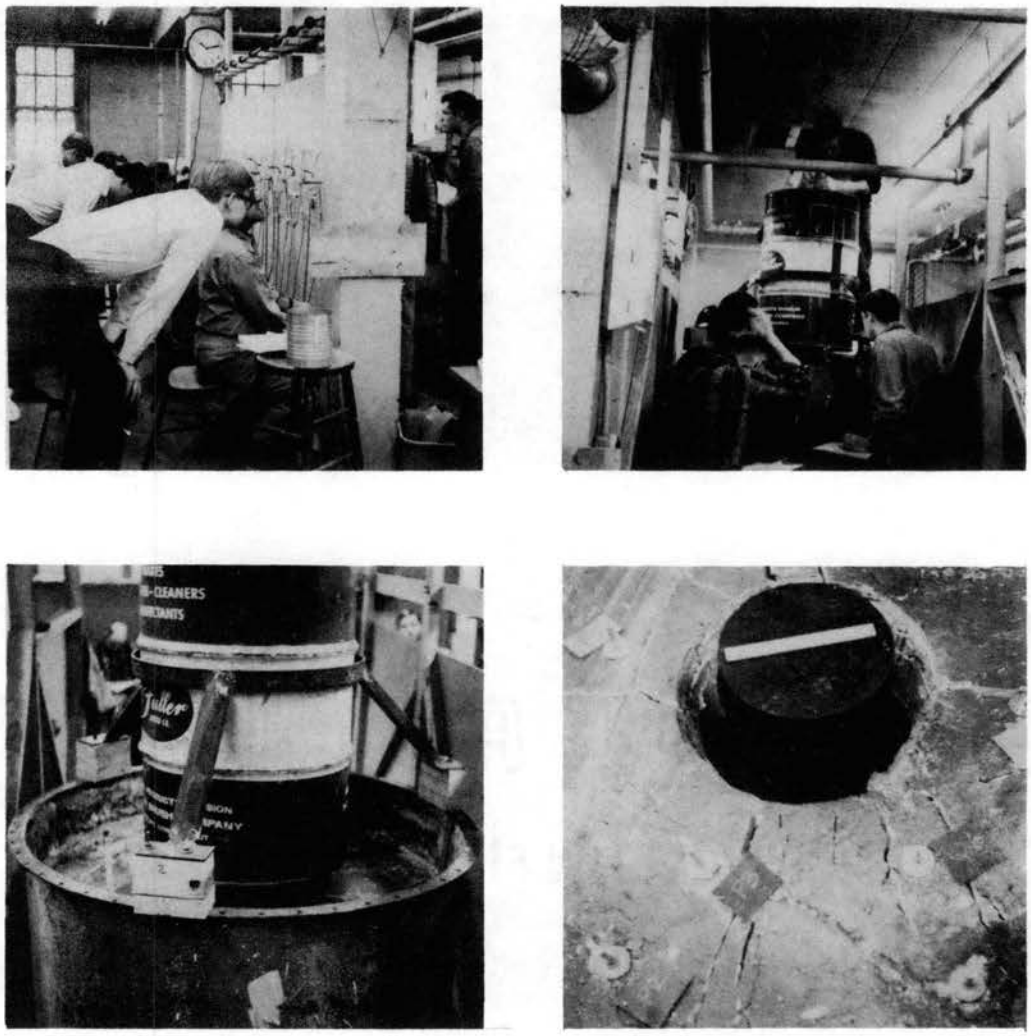

Upper left: Pore pressure measurement during test.
Upper right: Loading operation. Settlement and heave observations.
Lower left: General view of loading barrel and restraint.
Lower right: General view of loaded area after test.

Figure 20. Photographs of the Model Test.

surements, two men for heave measurements, three men for loading (and stand-by), and one man (the writer) for control of operations.

Pore Pressure Measurement

Each team was assigned to one, or, in some cases, two manometry systems. The teams consisted of an operator and a recorder. The operator's job was to balance null continuously by adjusting the pot (or two pots) to whatever level was necessary to accomplish the balancing. The recorder's function was to read the pot setting at frequent intervals, at the command of the operator. All teams were requested to take readings as often as comfortably possible.

In addition to the randomly-spaced readings of each team, it was decided to acquire simultaneous sets of readings periodically. These readings were to be accomplished by the announcement to everyone: "Get ready to read all pots" -- (long pause to allow all operators to balance null) -- "Read." A simple numbering system was adopted for these readings; Smn, where S was to designate a simultaneous reading, m the load increment number, and n the number of the reading during that particular load increment.

Because of the extreme importance of obtaining reliable pore pressure readings, all reasonable precautions were taken to insure this end. First, the most experienced people were chosen as operators. (Two of the operators had had considerable experience with pore pressure measurement in triaxial shear testing of soils.) Secondly, all operators and record-

ers were individually instructed on the procedures, including "hands-on" experience. This precaution was considered important enough to use one of the actual systems for this purpose. Thus, each of the fourteen people to be involved in the pore pressure measurements was given the opportunity to balance null at a no-load condition so as to develop some feel for the operation prior to the test. The recorders were also instructed on the pot-balancing (operator) job so that relief would be possible from the tedium of continuous balancing.

Settlement and Heave Measurements

The instrumentation for settlement and heave (Chapter III) is indicative of the manner in which data were taken. Two men were assigned to the settlement readings, one to read the three dials and the other to record. Two men were assigned to read the eighteen heave dials. The basic purpose of the heave measurements was to obtain some idea of the failure mechanism of the clay (See Fig. 18, Chapter III). Thus, it was deemed necessary only to determine where and when the heave developed, and where the maximum heave developed subsequently. Also, it was anticipated that the magnitude of the heave would not be appreciable at the lower load levels. All of these factors suggested that two men could reasonably handle the heave readings.

Compilation of Results

Table IX is a summary of all data taken during the load

TABLE IX

COMPILATION OF MODEL TEST DATA

LOAD INCREMENT	READING NO.	TIME (MIN.)	CONTACT PRESSURE	SETTLEMENT (IN.)	MAX. HEAVE (IN.) AMOUNT	MAX. HEAVE (IN.) LOCATION	STRESSES AND PORE PRESSURES AT DESIGNATED PROBES																													
							A1			A3			B1			B2			B3			C2			C4			C5			C6			D1		
							$\Delta\sigma_1$	Δu		$\Delta\sigma_1$	Δu		$\Delta\sigma_1$	Δu		$\Delta\sigma_1$	Δu		$\Delta\sigma_1$	Δu		$\Delta\sigma_1$	Δu		$\Delta\sigma_1$	Δu		$\Delta\sigma_1$	Δu		$\Delta\sigma_1$	Δu		$\Delta\sigma_1$	Δu	
								OBS.	PRE.		OBS.	PRE.		OBS.	PRE.		OBS.	PRE.		OBS.	PRE.		OBS.	PRE.		OBS.	PRE.		OBS.	PRE.		OBS.	PRE.		OBS.	PRE.
1	1-1	1008	3.61	.023	0		.04	0	.02	.15	0.9	.09	.72	0	0.4	.61	-0.2	0.4	.45	-0.2	0.3	2.4	0.9	1.4	1.00	0.3	0.6	.51	-0.7	0.4	.30	0.2	0.2	.25	-1.3	0.2
	1-2	10		.028				0.3			1.0			0			-0.1			-0.1			0.6			-0.1			-0.6			0.3			-1.0	
2	2-1	16	9.13	.081			.09	-0.7	.05	.39	1.0	0.2	1.83	0	1.1	1.54	0.5	0.9	1.14	0.4	0.7	6.1	1.9	3.6	2.54	0.3	1.5	1.30	0.6	0.8	.76	0.3	0.5	.63	-1.2	0.4
	2-2	17		.082	.084	Q3		-0.6			0.6			0			0.5			0.6			1.4			0.5			0.7			0.3			-1.2	
	2-3	18		--				-0.1			0.6			0			0.5			0.6			1.4			0.3			0.9			0.3			-1.0	
3	3-1	21	13.2	—			.14	—	.08	.56	0.6	0.3	2.65	—	1.6	2.23	0.8	1.3	1.65	1.0	1.0	8.9	2.5	5.3	3.67	0.2	2.2	1.88	0.5	1.1	1.10	1.6	0.7	.92	-0.7	0.4
	2	23		.48				-0.5			1.0			—			0.8			1.1			2.5			0.3			0.5			1.6			-1.5	
	3	26		.54	.040	Q2		-0.1			1.0			—			0.6			1.3			2.5			0.4			∓			1.6			-1.0	
	4	28		.55	.077	Q3		0.1			0.4		C	0.4			0.6			1.0			1.8			0.4			0.5			1.9			-0.9	
	5	29		.56	.087	P3		0.2			0.4		C	0.3			0.6			1.0			1.8			0.3			0.3			1.1			-1.0	
	6	30		—				-0.1			1.0			—			0.6			1.0			2.4			0.3			0.4			1.2			-1.0	
	7	31		—				—		C	1.6		C	-0.2			0.6			1.0			2.4			0.3			0.4			1.1			-1.3	
	8	33		.57				—			1.0			—			0.6			1.0			2.4			0.1			0.3			1.1			-1.0	
4a	4-1	38	16.0	—			.16	0	.10	.68	1.0	0.3	3.20	-0.5	1.6	2.70	—	1.4	2.00	1.9	1.0	10.7	4.0	5.4	4.45	-0.3	2.2	2.08	0.6	1.0	1.34	1.3	0.7	1.11	-2.8	0.6
	3	40		—				—			1.0		C	-0.4			-0.4			1.5			7.3			-0.2			0.4			—			-2.1	
	6	43		—			D	-0.5			1.0			-0.5			-0.2			1.2			6.2			0.3			0.4			1.6			-2.4	
	9	46		—				-0.5			0.3			-0.8			-0.2			1.0			3.0			0.3			0.4			2.3			-2.3	
	12	50		—				0.5			1.2			—		A+	-0.2			0.8			4.2			0.3			0.2			1.9			-2.1	
	15	56		2.2				-0.5			0.3			—		A+	-0.2			1.0			4.3			0.3			0.4			1.9			-2.1	
	19	1104						-0.9			0.9			-1.2		A+	-0.2			0.6			3.2			-0.1			0.5			1.2			-2.1	
4b	4-20	1107	17.3	2.98			.18	-1.0	.09	.74	0.9	0.4	3.47	-1.2	1.7	2.92	—	1.5	2.16	1.0	1.1	11.6	3.2	5.8	4.81	0.2	2.4	2.46	0.5	1.2	1.44	2.2	0.7	1.20	-2.2	0.6
	25	12		3.69				-1.5	-.04		0.4	-0.2		—	-0.9		-0.7	-0.7		1.0	-0.5	Ⓔ	—	-2.9		0.3	-1.2		0.3	-0.6		1.6	-0.4		-2.5	-0.3
	30	17		4.69				-2.0			-0.1			-1.5			-0.6			0		Ⓢ	-3.2			0.2			0.3			1.9			-2.5	
	35	19.5		5.16	0.90	P3		-2.0			0.2			-1.5			-0.5			-0.2			-3.2			∓			0.6			2.3			-2.8	
	40	22		5.55	1.15	Q3		-2.0			0			-0.9			-0.3			0			-3.2						0.9			2.3			-2.5	
	45	24.5		5.77	1.20	P3		-1.5			0			-1.5			-0.1			0.4			-2.7						0.8			2.9			-2.9	
	50	27		5.95				-2.0			0			-1.5			-0.1			0.5			-2.0						1.3			2.3			-2.3	
	55	29.5		—				-1.5			0			-1.5			-0.1			0.6		Ⓔ	-1.7						1.5			2.6			-2.9	
	58	32		—				-2.5			-0.6			-1.5			-0.1			0.6		Ⓢ	-2.7					C	1.4			2.5			-2.7	
	61	33.5		—				-1.5			-0.7			-1.5			-0.1			0.6			-2.2						2.2			2.6			-2.9	
	64	35		—				-2.0			-0.6			-1.5			-0.1			1.0			-1.7						2.4			2.6			-3.0	
								OK			OK			*			OK			OK			OK			*			*			OK			*	

test, including representative values of induced pore pressures at eleven probe locations, settlement readings of the loading plate, and significant heave readings and their approximate locations.

Since the data presented is a digest of a rather complex operation, some general explanation of the entries and notations in Table IX is in order. The subsequent section of this chapter deals with a qualitative analysis of each aspect of the test. Chapter V contains a more detailed, quantitative analysis of the data.

Five load increments were found to produce failure. Increment 4a represents approximately two-thirds of the planned load increment. Thus, Load Increment 4a = 107#, and Increment 4b = 50#. As can be seen in Table IX, the settlement increased rapidly at this failure point.

The listed readings were all simultaneous readings, as previously described. Since approximately one thousand pore pressure readings were taken during the test, including intermediate readings by individual operators, it was not considered necessary to include all readings in the compilation. Thus, as the numbers of the readings indicate at load levels 4a and 4b, some readings were omitted.

The total time for the test was about one and one-half hours, from 1008 to 1135.

The contact pressures listed are in inches of mercury.

Settlement values are the average of 3rd point readings, as taken from Ames Dials during the first three load levels.

The settlement values during the failure stage (4a and 4b) are single-reading values, as determined by the use of an engineer's level.

Heave data are indicated only where relatively high values were noted. Locations are designated by a letter-number system. The letter designates one of six radial lines (H, I, J, P, Q, R - see Fig. 17, Chapter III). Numbers designate the location of an Ames dial along the radial line, with the numbers (1, 2, 3) increasing toward the central loading plate.

Stresses and pore pressures are designated at ten probe locations. Units are in inches of mercury head. The three columns under each probe location list $\Delta\sigma_1$, the total principal stress increment caused by the contact pressure, the observed pore pressure, and the predicted pore pressure. Certain symbol designations were adopted to facilitate the presentation of the pore pressure data, and their meanings are as follows. The designation (*) under a column of observed pore pressures means that all readings in that column are questionable. This notation was made on those systems where a vacuum collapse was observed at the null level before the start of the test, this collapse indicating the possibility of the existence of a disqualifying leak in the system. The character ($\neq$) indicates that a visible leak was observed at the threaded connection between the copper line and the plastic null section. The designation (OK) means that the vacuum held steady before the start of the test,

indicating that the system was pressure-tight when the test began.

Letter designations, which are placed in the $\Delta\sigma_1$ column for convenience, are self-imposed "grades" on the adjacent observed pore pressure; the operators had been asked to do this so as to provide some additional reliance on later interpretation of the data. The grades A, B, C, D have the usual connotation of decreasing reliability. All un-marked data were rated either A or B. The E and S notations (circled, System C2) mean "erratic fluctuation," and "steady." The underlined predicted pore pressure values (all negative) which are listed for Load Increment 4b, are based upon an alternate interpretation of the prediction equation. Details are explained in Chapter V, Analysis of the Model Test Results.

General Evaluation

Loading

As is suggested by the fact that nine loading increments were planned, and somewhat more than three were required to induce a bearing failure, the ultimate bearing capacity was not estimated accurately. First, the use of Terzaghi's bearing capacity formula ($q = 7.4c$, Chapter III) should have been modified for the more probable eventuality of a local shear failure. Terzaghi (1943) recommends for such a case $c' = 2/3\ c$. An additional factor which contributed to the over-estimation of the undrained shear strength was the choice of $c = 350$ psf (Fig. 19, Chapter III). This value

was chosen from the curve on the basis of the nominal preload of 15 psi. It is probable that the actual preload pressure was somewhat less because of wall friction. Moisture content data, taken after the test, tends to substantiate this supposition. An average moisture content of about 52%(nine values) gives a c-value from the curve of about 275 psf. Thus, the ultimate bearing capacity, with the modifications for local shear and wall friction, computes as $q_f = \frac{2}{3}(275)(7.4) = 1360$ psf. For the 10-in footing, $Q = (1360)(.785)(\frac{10}{12})^2 = 740$ lb, which is comparable to the observed failure load of about 630 lb. (As noted in Chapter III, the original estimate was 1410 lb.)

The method of loading was adequate, but barely so. Much of the difficulty stemmed simply from physical restrictions such as space limitations and handling of the sand loads.

Pore Pressure Measurement

Because of the over-estimation of the bearing capacity, there are not sufficient data to enable a thorough analysis of pore pressure build-up, i.e., through nine load levels. However, the limited data do appear to be in reasonable accord with the theory developed in Chapter II.

The prediction equation, $\Delta u = \Delta\sigma_1 [K(1-A) + A]$, as applied to the relatively low stress levels of this test, yielded an approximation of predicted pore pressures before failure of $\Delta u \doteq 0.6\ \Delta\sigma_1$, with K and A being estimated as 0.3 and 0.4, respectively. For failure conditions, values of K = 0.15 and A = 0.4 were chosen as representative, yielding

predicted failure pore pressures $\Delta u_f \doteq 0.5\ \Delta\sigma_1$. An alternate interpretation of failure conditions (K = 0.15 and A = -0.5) resulted in negative values of predicted pore pressures, as cited in Table IX, Load Level 4b. The reasoning employed in estimating A and K values has been described in Chapter II. Specific details and data supporting the choice of the numerical values of the parameters are described in Chapter V. For this general qualitative analysis, it may just be noted that the pore pressures almost consistently diminished upon the application of Load Increment 4. In fact, most of the systems indicated the development of negative pore pressures during failure. This behavior is contrary to what was expected for such a soft clay, which suggests that the important limitation described in Chapter II is not correct, and hence the prediction equation may be applicable to all soils on the basis of the overconsolidation ratio, irrespective of consistency.

One of the important problems concerning the pore pressure instrumentation and consequent behavior was associated with the collapse of the vacuum in five of twelve systems. Four of these systems (B1, C4, C5, and D1) are listed in Table IX. The fifth system, A2, leaked badly from the start of the test, so that system could not be used. Any attempt to raise the pot to balance null resulted in an immediate leak at the top connection, which in turn resulted in the mercury rising in the null section to replace the escaping water. Though seemingly implausible, it is a matter

of record that the five systems exhibited this vacuum collapse almost simultaneously just before the start of the test, and before anything had been touched. Valve C (Fig. 6, Chapter III) had not yet been opened, which was to have been the first step in the testing procedure. It should be emphasized that the vacuums had been developing and had persisted over a period of nine months. The probability that five systems would collapse simultaneously just prior to testing, as a matter of chance, is remote. The only causative agent that can be surmised is differential expansion at the null section connection (brass to plastic) as a result of an increase in ambient temperature. The only source of a relatively sudden temperature rise at the precise moment of the simultaneous collapse of the vacuums in the systems was the body heat of the twenty-two people surrounding the apparatus. It is believed that possibly daily and seasonal temperature fluctuations may have weakened the connection (of dissimilar materials) by cyclic stressing, so that the sudden temperature increase on the morning of the test, though probably small, caused the final damage to the systems. It should be added that there was specific evidence of structural damage. Two of the plastic null sections developed myriads of cracks throughout their length, the cracks having developed slowly during the nine-month period between calibration and the model test.

The technique of having operators appraise their own readings by a grading system was quite beneficial, especially

in that one of the operators devised an excellent method of balancing pore pressures, and graded accordingly. It will be noted that Readings 4-12, 15, and 19, System B2, are graded "A+". This was partially facetious braggadocio on the part of the operator, but when queried about the high grade, the explanation was that the balance point had been determined by a "trapping" method, which is accomplished by intentionally overbalancing (first) and then underbalancing. In both cases the mercury would creep slowly upward and then downward, respectively. By timing the rate of movement, it is a relatively simple matter to interpolate for (or "trap") the balance point. Such a method is quite commonly used to determine ground water levels in bore holes in relatively impervious soils. The extension of the method to the pore pressure readings of this test is significant for any future testing, in that the sensitivity of measurement is greatly increased. Because of the low permeability of the clay, "haphazard" balancing of the null section, especially by an inexperienced operator, will (and undoubtedly did) produce less precise results. One operator reported on his data sheet that he estimated the sensitivity at about $\pm$0.2 inches. The operator who extended the trapping method (on System B2) was Dr. Tonis Raamot, then of the Department of Civil Engineering of Newark College of Engineering. Dr. Raamot had had considerable experience in pore pressure measurement in triaxial testing.

Settlement and Heave Measurement

The experience of this test indicated that the use of Ames Dials for settlement and heave determinations was not the best alternative. During the first two load increments, no problems were encountered, but midway through the third increment, it became apparent that the dial ranges would be insufficient due to impending large and rapid settlement and heave. Upon the application of Load Increment 4a, which was applied at about 10:35 A.M., the rate of settlement increased greatly, whereupon an engineer's level was quickly set up. A ruler was taped to the barrel and readings of settlement were resumed at 11 A.M. (Settlement estimate = 2.2 inches.) Because of the spinning of the Ames dials, no heave measurements of any validity were possible after Load 4a was applied. The heave data listed for Increment 4b were taken at the conclusion of the test as part of a determination of the final surface profile.

It is probable that the use of a battery of engineer's levels throughout the test would have been preferable to the use of Ames dials. Such a technique would also have eliminated the rather delicate nature of instrumentation with dials. Also, congestion around the soil model would have been avoided.

CHAPTER V

ANALYSIS OF THE MODEL TEST RESULTS

As has been demonstrated by the results of this investigation, and as has been reported by many investigators, pore pressures generally diminish with increasing loads for overconsolidated soils (cf. Fig. 4, Chapter II). It is postulated that the development of these excess pore pressures is governed by the following prediction equation.

$$\Delta u = \Delta\sigma_1 \, [K(1-A) + A]$$

State of Stress Analysis: A Comparison of Predicted and Measured Pore Pressures

In Chapter II, where the prediction equation is derived, it is suggested that the equation is applicable only to soils which have both a high overconsolidation ratio and a reasonably high consistency. It was further suggested that soft soils, such as the model tested in this study, be analyzed as if normally consolidated, irrespective of the OCR. The limitation was proposed largely on the basis of intuition, it being assumed that in such soft clays negative pore pressures would not develop.

The limited amount of data afforded by the single test associated with this thesis, however, tend to contradict the

assertion of a limitation, in that negative pore pressures were measured at failure at nearly all probe locations designated as "OK". (See Chapter IV for explanation of the designation.) In Table I, Chapter IV, there are listed two alternate predicted pore pressures at failure (Load Increment 4b). The values listed first in the column (eg., Probe B2, 1.5 in. Hg) are based upon an analysis of the soil as if it were normally consolidated, consistent with the suggested limitation described. Upon comparison of these values, all positive, with the generally negative values which were observed, it was decided to reconsider the validity of the limitation. The second set of values which are listed (underlined), all negative, are a result of the reevaluation described in the following section. It may be observed that, in general, these values are in fairly good agreement with observed pore pressures.

The details of the analyses are concerned with the specific choices of numerical values for the pore pressure parameters, A and K, for use in the prediction equation.

A and K for Normally Consolidated Clay

No data are available for the very low stress levels of the load test. However, representative A-values may be inferred by a study of the general variation of A with deviator stress levels. The graphs in Figures 21, 22, and 23 may be used for such a study. Figure 21 illustrates the results of consolidated-undrained triaxial tests (with pore pressure measurements) on the sodium kaolinite used in this study

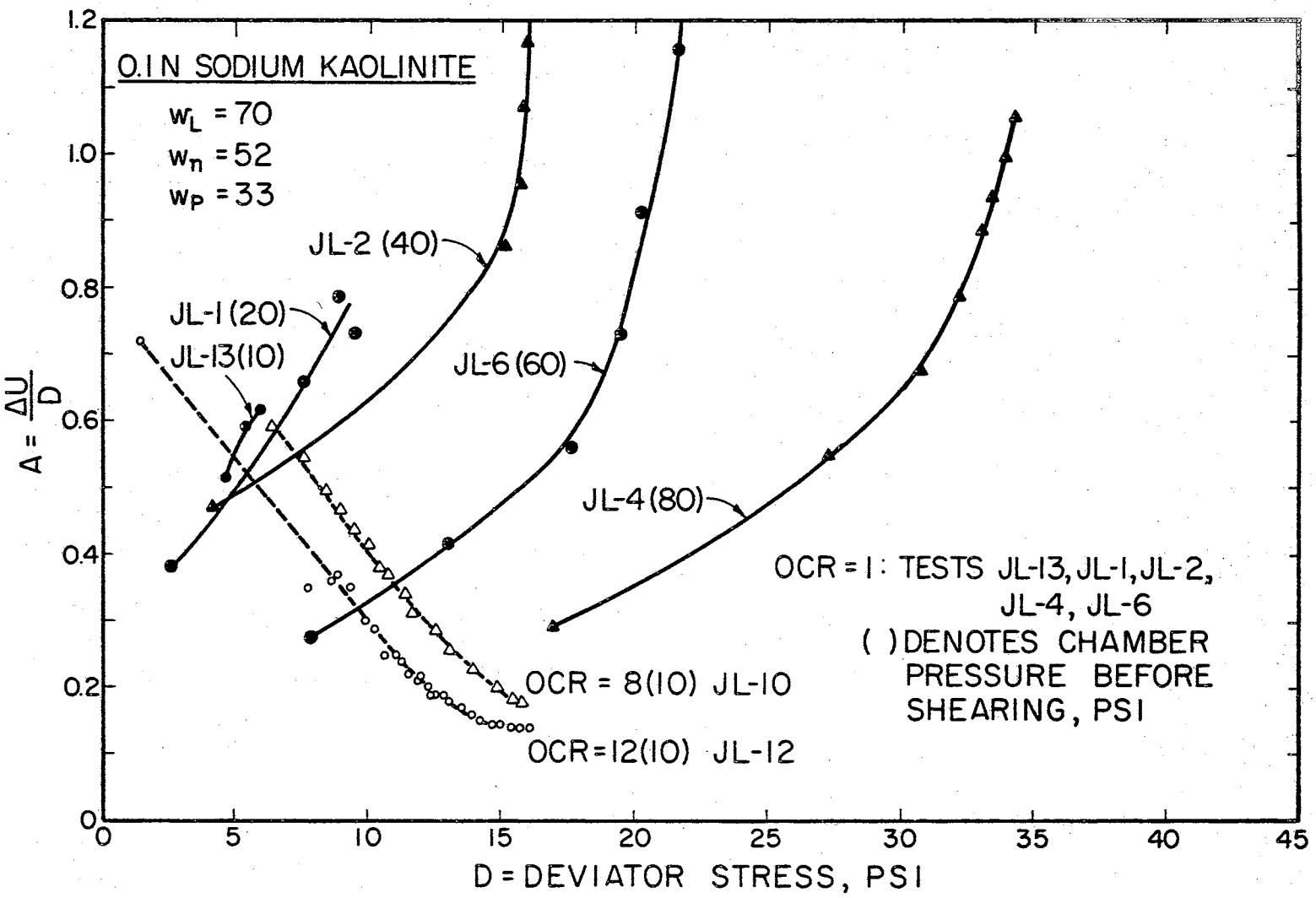

Figure 21. A-Value Variation for 0.1 N Sodium Kaolinite

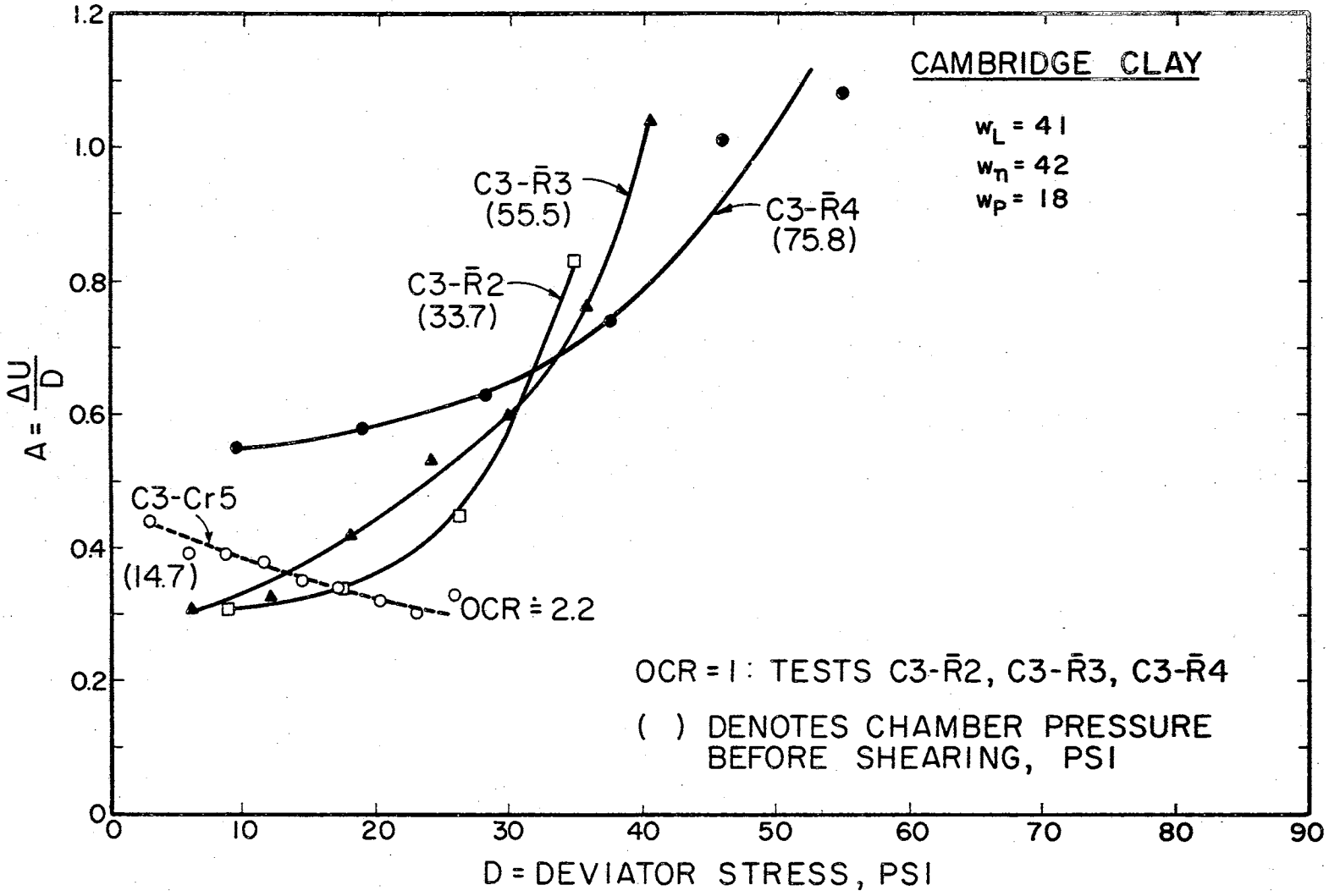

Figure 22. A-Value Variation for Boston Blue Clay

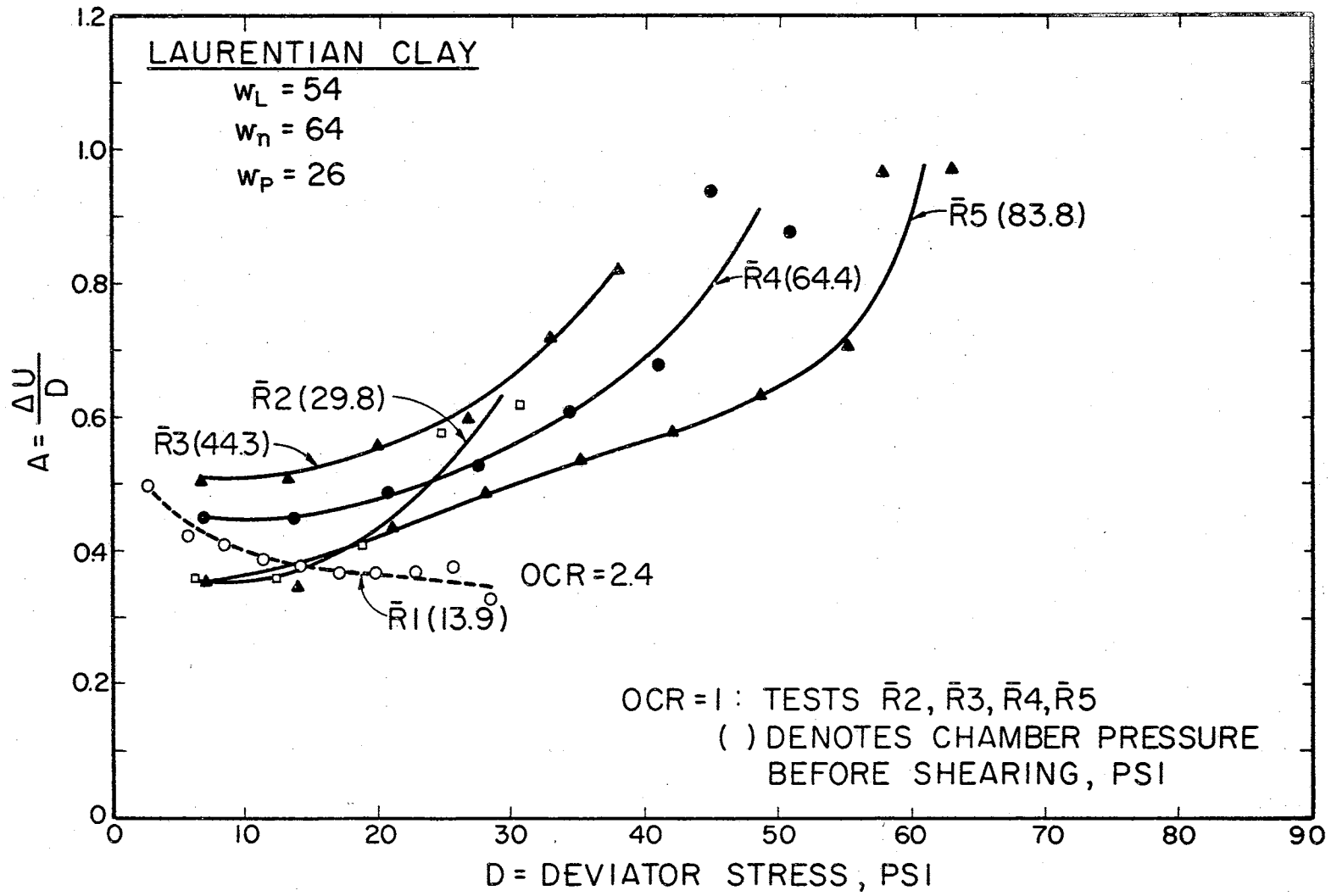

Figure 23. A-Value Variation for Laurentian Clay

(Leitch, 1964). Figures 22 and 23 are from tests performed by Parcher (1957) at Harvard University.

From these plots, some general observations may be made: First, for OCR values of 1, i.e. normally consolidated clays, all curves have positive slopes with increasing magnitudes. The initial flatness of these curves, particularly as shown by Parcher's data, indicate that A does not vary greatly with D, the deviator stress, at lower stress levels. Secondly, the initial values of A all lie within a rather small range of values, regardless of the magnitude of the overconsolidation ratio. For example, for 17 tests, eleven at OCR = 1, and six at OCR values between 1 and 12, the range of initial values of A was 0.28 and 0.55 (except for a single questionable value of 0.72 for test JL-12, Figure 21). The average of the initial values of A for 17 tests is 0.45. The average for the eleven tests at OCR = 1 is 0.41. For the six overconsolidated specimens, the average is 0.52. From this analysis, it can be seen that a representative A-value at low stress levels may be taken as 0.4.

The curves show that values of A at failure are generally lower at lower chamber consolidation pressures. The lowest failure value observed was for Test JL-13 (Figure 21) in which the chamber pressure, 10 psi, before shear was also lowest. The A_f-value recorded was 0.62. From these observations it is reasonable to surmise that the failure A-value for the very low stress levels for the soft clay of the model test will not differ considerably from the average value of

0.4 given above.

The choice of representative K-values for use in the prediction equation is based largely upon general considerations of strain and the relative consistency of the clay. As described in Chapter II, K is inversely related to both factors. Because of the relatively high strains that develop in the loading of a soft clay as in the model test, representative values of K would be about 0.3 for stress levels before failure, and 0.15 at failure. The choice of these values is somewhat arbitrary. It may be noted, however, that the range of possible K-values is rather small, as contrasted to the range of A-values. It is believed that K has a maximum value before loading of perhaps 0.6. Upon loading, rather high strains would develop, even at lower levels, for such a soft clay. Hence, the K-value would be reduced to, perhaps, 0.3. For the very high strains at failure, the proposed minimum value of 0.15 is chosen as representative. Bishop's data, cited previously (Table II, Chapter II), support these estimates.

The choice of these values as constants implies that at any given load level, the strain is independent of position. Since the induced total stress increments, $\Delta\sigma$, vary with position, and boundary restraints are also dependent upon position, it follows that strain and hence K-values also vary with position. It is for this reason that the values proposed for K are designated as "representative." The general effects of strain variation with position will be dis-

cussed further in a subsequent section describing the pore pressures observed at specific probe locations.

Consonant with the preceding analysis, the predicted pore pressures may be computed as follows:

At levels prior to failure (Load increments 1, 2, 3)

$$\Delta u = \Delta\sigma_1 [K (1-A) + A]$$

$$= \Delta\sigma_1 [0.3 (1-0.4) + 0.4]$$

$$= 0.58 \Delta\sigma_1 \text{ (say } 0.6 \Delta\sigma_1)$$

At failure

$$\Delta u_f = \Delta\sigma_1 [0.15 (1-0.4) + 0.4]$$

$$= 0.49 \Delta\sigma_1 \text{ (say } 0.5 \Delta\sigma_1)$$

These equations were used for the calculation of the predicted pore pressures in Table IX, Chapter IV. For example, for Probe B2, Load Level 3, $\Delta u = 0.6 \Delta\sigma_1 = 0.6$ (2.23) = 1.3 in Hg. For Load Level 4b, $\Delta u_f = 0.5 \Delta\sigma_1 = 0.5$ (2.92) = 1.5 in Hg.

It should be emphasized that these values are based upon the important initial assumption that the soil reacts as if it were normally consolidated. This assumption had been made on the basis of the soft consistency of the clay.

A and K for Overconsolidated Clay

According to the standard definition of overconsolidation ratio, OCR = $\bar{p}_c/\bar{p}_o$, the clay model tested may be said to have been highly overconsolidated, even though of soft consistency. The $\bar{p}_c$ value for the clay is 15 psi, and was applied by hydraulic jacks through a piston fitted in the 4-

ft. diameter tank. Since the entire piston load was removed subsequently, the only remaining vertical effective pressure was caused by the submerged unit weight of the clay. Thus, an average OCR value, based upon $\bar{p}_o$ at the mid-depth of the 27-in. thick model is calculated to be 43 ($\bar{p}_o$ = 0.35 psi, and $\bar{p}_c/\bar{p}_o$ = 15/0.35 = 43).

Figures 21, 22, and 23 may be studied once again to arrive at representative A-values for overconsolidated soils. It may be observed that the slopes of the curves for all overconsolidated clays are negative, and that the slopes increase at higher overconsolidation ratios. Failure values of A, as anticipated and reported by others, diminish with increasing OCR. The minimum value of A_f, from the available data, is for OCR = 12, and is +0.14 (Test JL-12, Figure 1). (Tests JL-10 and JL-12 are the same tests illustrated in Figure 4, Chapter II.)

If the very high OCR of the clay model test is considered, it can be inferred from the analysis in the preceding paragraph that the A-values will diminish with increasing load, and that the failure value of A will be negative. Consistent with failure values which have been reported (Skempton, 1954), a representative value would be -0.5. The K-value, as before, would be 0.15.

Thus, at failure, the predicted pore pressures are:

$$\Delta u_f = \Delta\sigma_1 [K_f(1-A_f) + A_f]$$

$$= \Delta\sigma_1 [0.15(1+0.5) - 0.5]$$

$$= -0.27\ \Delta\sigma_1 \ (\text{say} - \tfrac{1}{4}\ \Delta\sigma_1)$$

This equation was used for the calculation of the alternate entries of predicted pore pressures listed in Table IX, Chapter IV. For example, for Probe B2, Load Level 4b (failure), $\Delta u_f = -\frac{1}{4} \Delta\sigma_1 = -0.25(2.92) = -0.7$ in. Hg.

No alternate values are listed in Table IX for load levels prior to failure, but it follows from the analysis that the predicted pore pressures would be lower than those predicted on the basis of normal consolidation.

It may be noted that in the more typical case of natural soils, a more detailed and complete analysis could be made, since presumably a specific curve of A vs. D (the deviator stress) would have been obtained by conducting a consolidated-undrained triaxial test, with pore pressure measurements, for the soil in question. In such a case, specific values of A could be ascertained for any and all stress levels. Representative values could be used, as was necessary here, if warranted or desirable.

Distribution of Pore Pressures

The fact that negative pore pressures developed at five of the six probe locations where instrumentation systems were not suspect makes it relevant to consider the mechanism which might be associated with such behavior.

It is apparent from the form of Skempton's pore pressure equation

$$\Delta u = B\Delta\sigma_3 + A(\Delta\sigma_1 - \Delta\sigma_3)$$

that the induced shear stress, $(\Delta\sigma_1 - \Delta\sigma_3)$, has a marked influence on the development of pore pressure.

Thus, the manner in which shear strains developed during the loading of the model influenced the distribution of pore pressures. The value of K is also affected by strain, as previously explained.

Figure 24 is a plan view of the 4-ft. diameter soil model, in which the layout of probes, heave measurement locations, and the loaded area are shown. As suggested by the letter designations for the six probes on the A-circle, the probes on each of the four concentric circles (A, D, B, C-C representing the central circle beneath the loaded area) are installed in a spiral fashion, with the lower numbers representing the shallower depths within the soil, and conversely.

Figure 25 is a cross-section of the soil model, with probes represented as if in a radial plane. For clarity, only the ten functional probes are shown. (Ten probes had been eliminated prior to the test because of their remote locations with respect to the loading plate, of for system malfunction before the date of the load test, as explained previously.) The intent of the figure is to suggest in a general way the shear strain variation within the soil model, as caused by loading of the 10-in. diameter circular loading plate. The "R = 4a - circle", within which all stresses of significance occur, is shown in the figure. The arrows are meant to represent the direction of "flow" of the soft clay. Such a movement would be representative of what Terzaghi (1943) describes as a local shear failure; the shear strains would probably be different for a clay of substantial con-

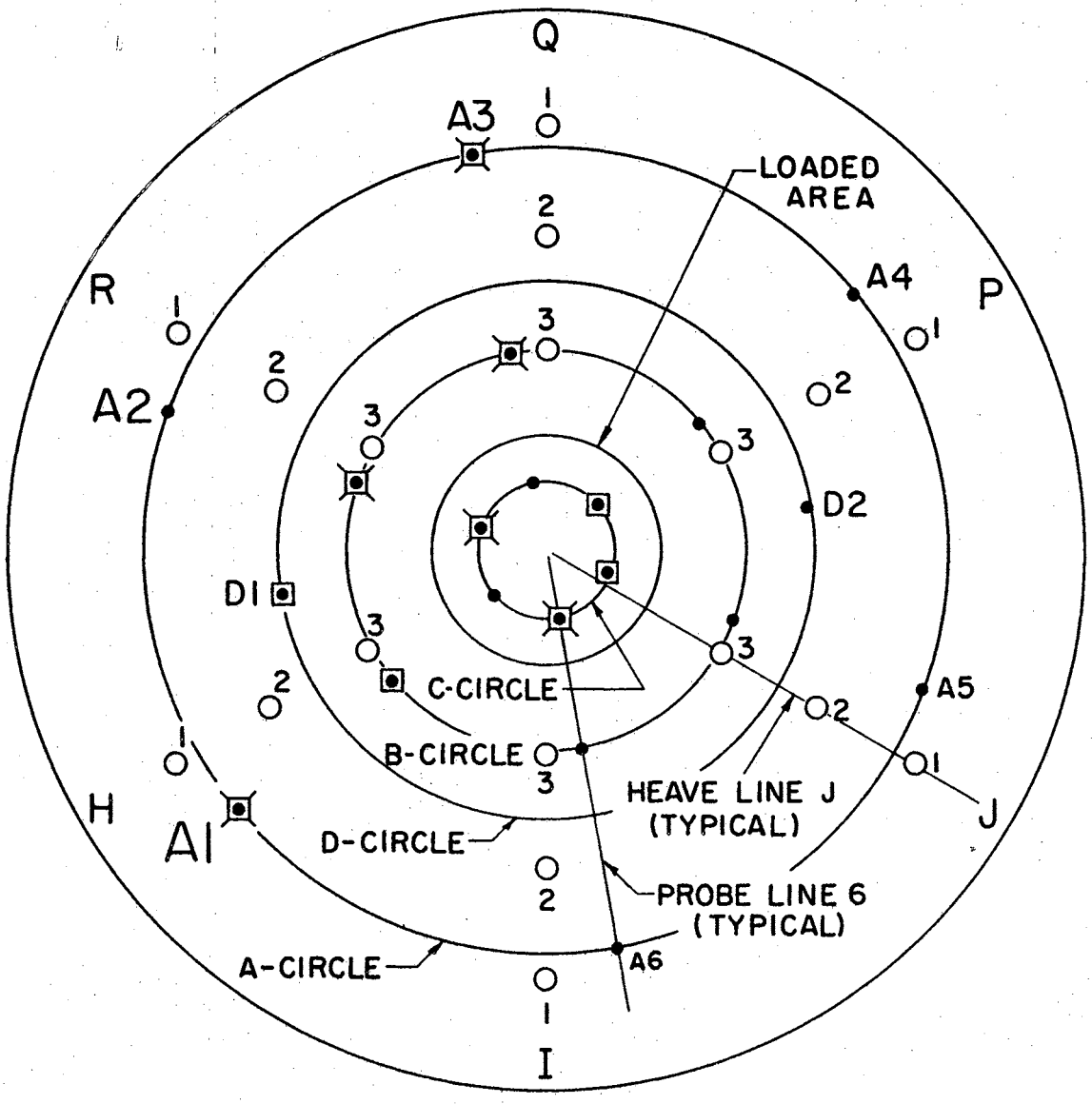

Figure 24. Summary of Functional Instrumentation

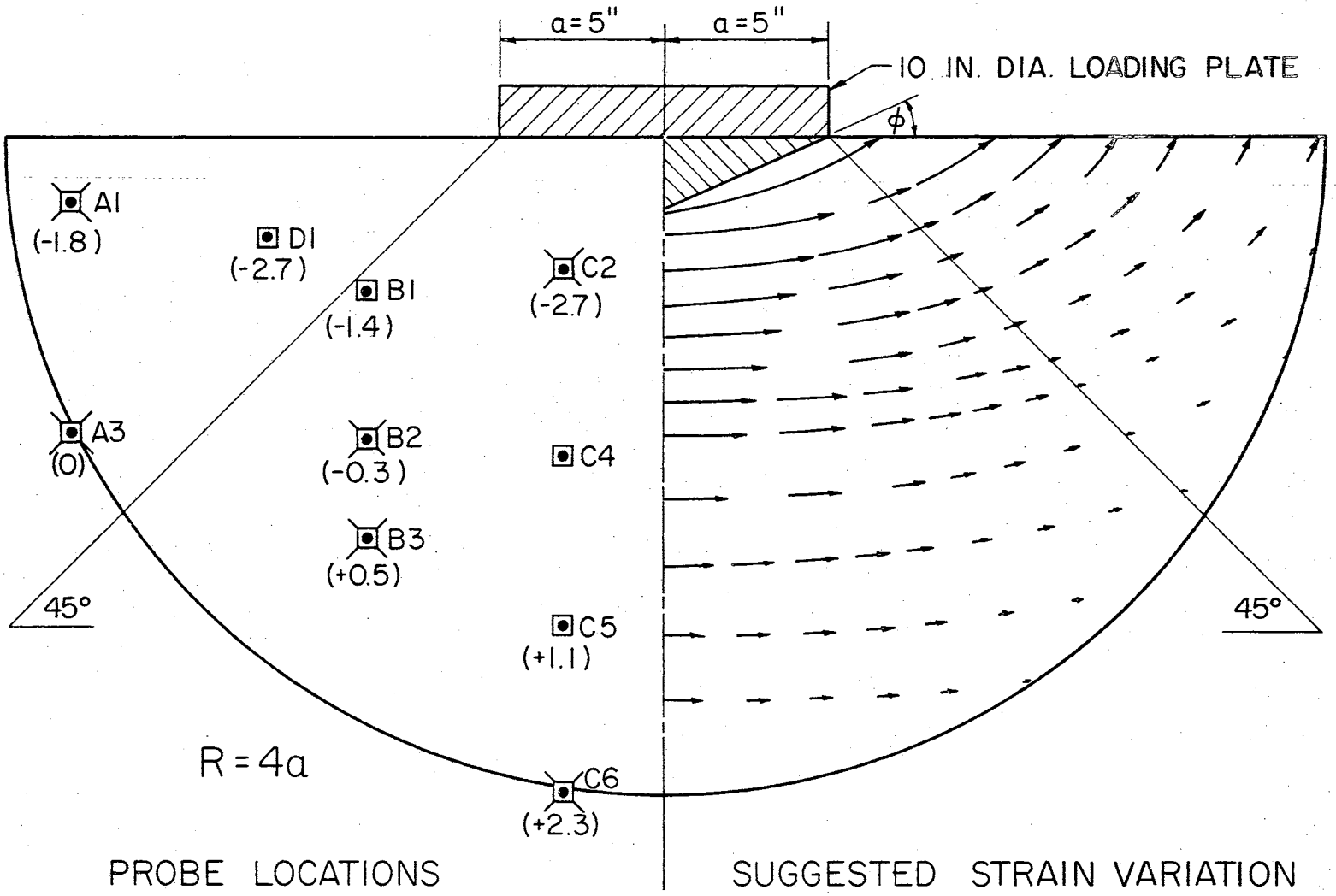

Figure 25. Strain Variation Within the Soil Model

sistency. The lengths of the arrows are intended to represent the magnitude of shear strain at the particular location. Forty-five degree lines, as shown in Fig. 25, were chosen somewhat arbitrarily as a locus of points along which the shear strain on a given "flow path" is a minimum. It may be noted that the use of 45° lines to approximate the average normal stress on a horizontal plane at some level beneath the loaded area is common (Wu, 1966), so the choice of these lines is not totally arbitrary. The increase in shear strain above these lines is explained on the basis of diminishing vertical restraint to dilation. Basically, this behavior is governed mathematically by the K-parameter. As noted previously, the principal stresses will have rotated nearly 90° in these areas, so that the minor principal stresses will be nearly vertical and the major principal stresses nearly horizontal. As a result of the low restraining effective pressure, i.e., the submerged weight of the soil, the K-value will approach a minimum. A typical soil element at a shallow depth outside the loaded area would tend to elongate in the vertical direction. Conversely, an element beneath the loaded area ($\Delta\sigma_1$ vertical, $\Delta\sigma_3$ horizontal) would tend to elongate horizontally. It follows that at some intermediate point, the strain tends to be isotropic, which is to say that the differences in principal stress increments are small (i.e., $K \doteq 1$), and hence shear stresses and strains are correspondingly low. The 45° lines are suggested as the locus of such points.

Figure 25 also shows the average of the recorded pore pressure readings for the failure load level (4b, Table IX). These values are shown in parentheses beneath each probe location. (No value is listed for Probe C4 because visible leaking was observed, see Table IX.) It may be noted that there is reasonably consistent correlation between the character (positive or negative) and magnitude of failure pore pressures and the suggested strain variation. Note, for example, that positive pore pressures were recorded only at probes remote from the load where shear strains are small (Probes A3, B3, C5, and C6). Conversely, the higher negative pore pressures are associated with areas of higher shear strain (Probes A1, D1, B1, and C2).

Bearing Capacity Analysis

In the most general sense, the allowable bearing pressure of a soil is taken as the lesser of two values: that pressure which results in an ultimate differential settlement no greater than a specified allowable value, or that pressure corresponding to a specified factor of safety, commonly 3.0, against shear failure.

For most foundations on cohesionless, free-draining soils, the settlement is immediate, since pore pressures cannot persist. As Skempton (1951) points out . . . "except for footings or piers with a breadth of only a few feet, the settlement criterion controls the allowable pressures on sands and gravels. Consequently, methods for estimating the

ultimate bearing capacity of cohesionless soils have a somewhat restricted value. In contrast, the possibility of a complete shear failure in clay is a very real one . . ."

Terzaghi (1943) presents an analysis of the bearing capacity for shallow continuous footings in which the ultimate bearing capacity consists of three parts whose values depend upon the cohesion c, the depth of foundation surcharge D_f, and the unit weight of the soil γ. The analysis is based upon the assumption of a general shear failure (Figure 26) in which the curved portion of the surface of sliding is approximated by either a log spiral or a circle. Terzaghi's analysis leads to the following expression for the ultimate bearing capacity:

$$q_f = \tfrac{1}{2}B\gamma N_\gamma + cN_c + \gamma D_f N_q \qquad \text{Eq. 5.1}$$

where q_f is the ultimate bearing capacity,

B is the width of the continuous footing,

and N_γ, N_c, N_q are Terzaghi's bearing capacity factors, which are dependent only on the value of ϕ, the friction angle of the soil.

For loose or compressible soils, Terzaghi recommends that the soil strength parameters, c and tan ϕ, be reduced to 2/3 c and 2/3 tan ϕ. These modifications would be applicable to the case of local shear failure. The failure mechanism in such a case differs from that of general shear failure (See Figure 26).

Yong, et al. (1963) present a bearing capacity analysis involving local shear failure, wherein a trapezoidal fail-

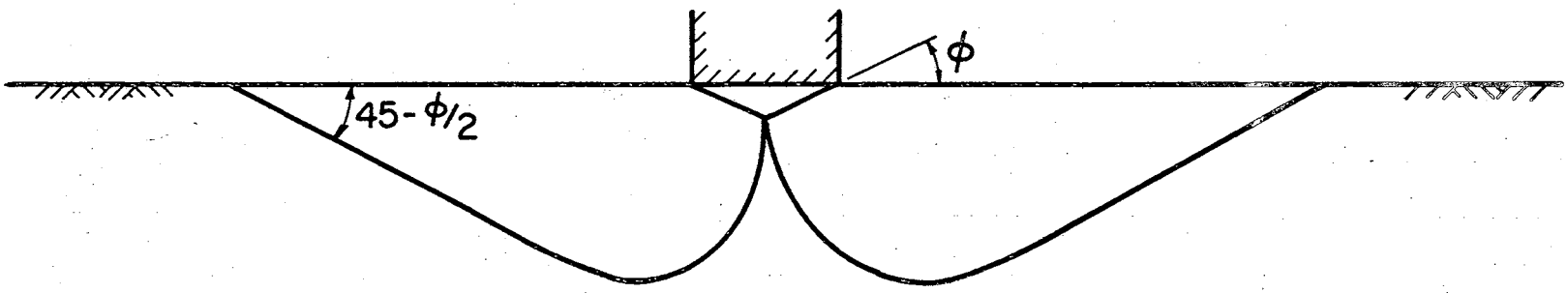

(a) GENERAL SHEAR (after Terzaghi)

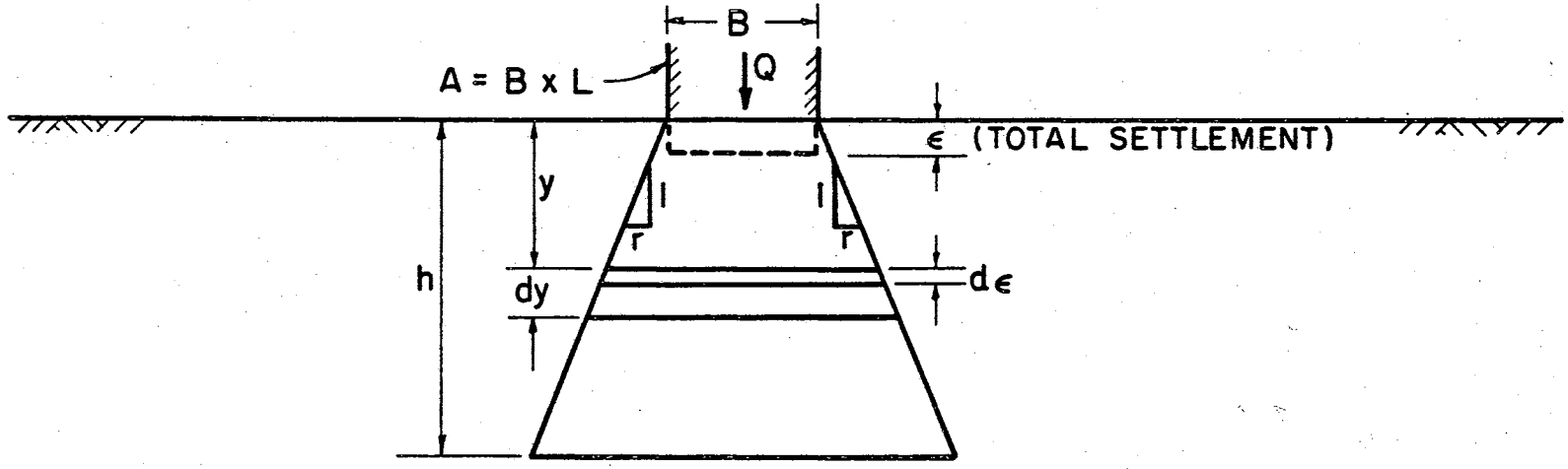

(b) LOCAL SHEAR (after Yong)

Figure 26. Failure Mechanisms for General and Local Shear Failure

ure mechanism is proposed. Figure 26 (b) shows the geometry of the soil which is postulated to be involved in the failure. The geometry upon which Terzaghi's analysis is based is shown on the same figure in order to illustrate the contrast between general shear failure and local shear failure. (See also Fig. 18, Chapter III, for contrasting load-settlement curves and surface heave.) In what Yong and his associates refer to as "quasi-elastic deformation theory", a representative modulus of deformation is defined as $E = (Q/A)/(d\epsilon/dy)$. The solution of the differential equation yields an expression for the ultimate load of

$$Q = \frac{2ErL\epsilon}{\ln\left(1+\frac{2rh}{B}\right)} \qquad \text{Eq. 5.2}$$

The nomenclature is designated in Figure 26 (b). The parameters which must be determined experimentally are E, r, and h. For E Yong used the secant modulus from unconfined compression tests. The values of r and h were determined by inspection of the deformed soil "immediately before failure".

In contrast to Yong's theoretical analysis, Terzaghi treated local shear failure by means of a simple empirical adjustment of his general equation, previously described. No specific geometry was proposed.

Terzaghi also gave the following approximate solution for a circular footing:

$$q_f = 0.6\gamma RN_\gamma + 1.3cN_c + \gamma D_f N_q \qquad \text{Eq. 5.3}$$

where R is the radius of the footing. Terzaghi describes this equation as an analog of his general

bearing capacity formula, Eq. 5.1. The values of the coefficients which are applicable to circular footings were based upon the results of model tests.

Equation 5.3 may be used to estimate the bearing capacity of the circular footing used in this study. For a surface footing, $D_f = 0$. For rapid loading, $\phi = 0$, so $N_\gamma = 0$ and $N_c = 5.7$. (The values of N are taken from a set of curves relating N_γ, N_c, and N_q to the friction angle ϕ. These curves, which were first presented by Terzaghi, are published in most books dealing with soil mechanics.) Substituting in the equation, and adopting the reduction factor for a soft clay (local shear failure) yields

$$q_f = 1.3(\tfrac{2}{3}c)(5.7)$$

$$q_f = 4.95\ c$$

It will be noted that the preceding analysis involves no consideration of pore pressures. The friction angle ϕ is assumed to be zero because the rapid loading does not permit the development of additional shear strength by consolidation. That is, $s = c$, and the failure envelope on a Mohr circle plot is a horizontal line (Figure 27). The plot is the common representation of the results of an unconfined compression test, where q_u is the unconfinued compression strength, and $c = q_u/2$ = the shear strength of the soil. The total principal stresses on an element of soil at failure are $\sigma_1 = q_u$ and $\sigma_3 = 0$.

As the pore pressures diminish during the consolidation

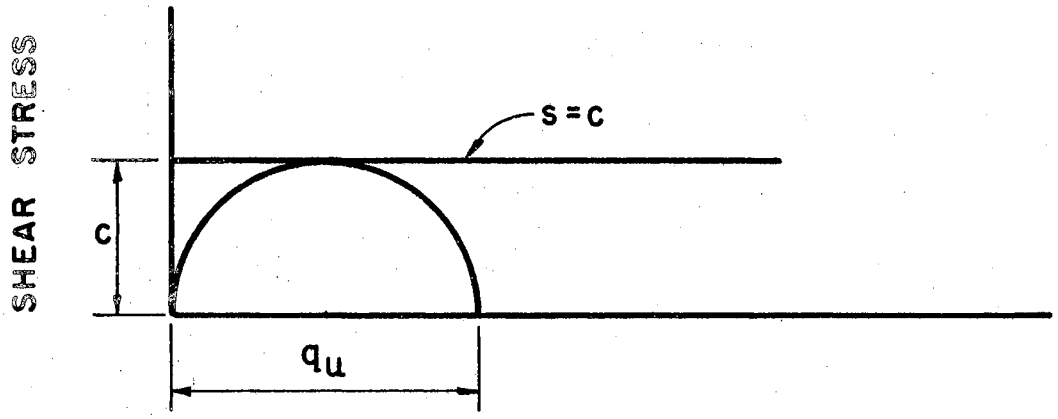

(a) UNCONFINED COMPRESSION TEST

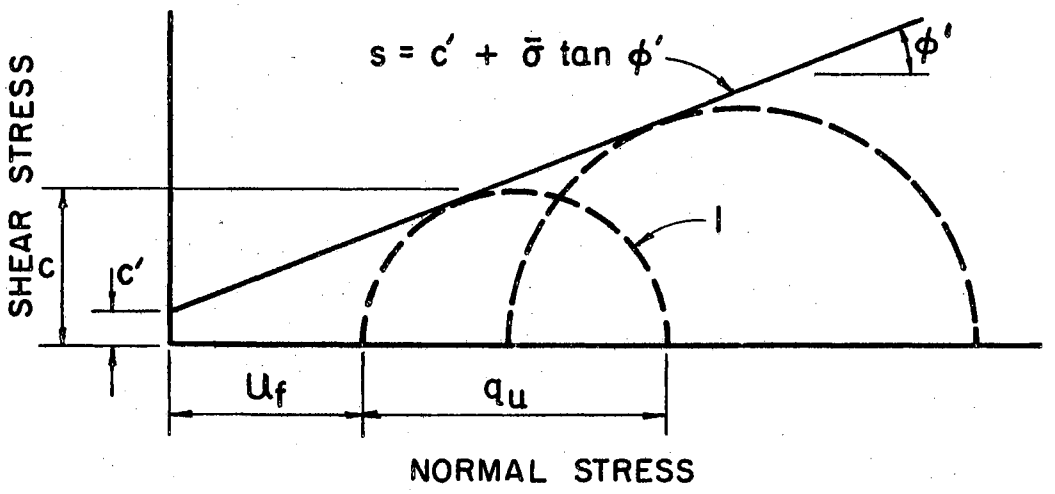

(b) CONSOLIDATED - UNDRAINED TEST

Figure 27. Mohr Circle Plots of Compression Tests

process, the effective normal pressures in the soil change. The frictional shear strength, as governed by the second component of Coulomb's equation, changes accordingly. After consolidation is complete, the shear strength of the soil is represented by the effective strength parameters in the Coulomb equation: $s = c' + \bar{\sigma} \tan \phi'$. As cited earlier, Leitch (1964) determined these parameters to be $c' = 1.3$ psi and $\phi' = 25.9^{\circ}$ for the Sodium Kaolinite. The plot is shown in Figure 27 (b). In this case, the circles shown are effective-stress plots. In the laboratory, the data can be obtained by performing two (or more) consolidated-undrained triaxial tests with pore pressure measurements. With the pore pressures at failure known, the major principal effective stresses may be readily determined by a shift of the total stress circles. The friction angle ϕ' may then be determined graphically by constructing a line which is tangent to both effective stress circles. For example, Circle no. 1 in Figure 27 (b) represents the effective stress equivalent of the Mohr Circle of Figure 27 (a). This comparison illustrates that negative pore pressures develop in the unconfined compression test.

The bearing capacity of the circular footing of the model test, based upon effective stress parameters, may be computed from Terzaghi's equation, as follows:

$$q_f = 0.6\ \gamma' R N'_{\gamma} + 1.3\left(\frac{2}{3}\ c'\right) N'_c$$

Using Terzaghi's reduction factor for soft clays, from published charts, $N'_{\gamma} \doteq 3$, $N'_c \doteq 15$. Also $\gamma' = .026$ lb/in^3 and

R = 5 in. Thus,

$$q_f = 0.6(.026)(5)(3) + 1.3(\tfrac{2}{3})(1.3)(15)$$

$$q_f = 0.234 + 16.9$$

$$q_f = \underline{17.1 \text{ psi}}$$

Effective stress analysis; fully consolidated

For comparison, the Ø-zero ultimate bearing capacity is

$$q_f = 4.95\ c$$

From shear vane tests (Fig. 19, Chapter III), c=1.91 psi

so, $q_f = 4.95(1.91)$

$$q_f = \underline{9.5 \text{ psi}}$$

Ø-zero analysis; no consolidation

Failure of the model was observed at about 8.6 psi. (See Table IX, Chapter IV, Load level 4a; Contact pressure - 17.3 in. Hg ≙ 8.6 psi.)

The two calculated values for the ultimate bearing capacity presumably represent the upper and lower limits of the strength of the soil. The Ø-zero analysis is usually conservative because any consolidation which occurs during the loading period will increase the strength of the soil. Since foundation design must be based upon the minimum strength that the soil is ever likely to have, the Ø-zero analysis is most commonly used in practice, usually with the employment of a safety factor of 3.0. In the case of the model of this study, the allowable soil pressure would have been about 3 psi, assuming that such a value would not cause unacceptable settlement.

The Ø-zero analysis is appropriate theoretically only when the period of loading is so short that there is no appreciable consolidation of the soil during that interval. The factor of safety is at a minimum immediately upon completion of loading, and tends generally to increase with time. It may be noted that the increase in strength during the longer construction periods of large projects is often considered in design (cf., Lumb, 1965). In some cases, construction procedures are altered in order to take advantage of the effects of the increase in strength caused by consolidation of the soil. An example of this procedure is the stage construction of highway fills. In very soft soils, sand drains are frequently used to reduce the time required for consolidation. Many sections of the New Jersey Turnpike which cross the pluvial lakes of the "Meadows Area" were prepared for construction in this manner.

As was mentioned with reference to Figure 27(a), the Ø-zero approach to design is based upon a total-stress analysis. No pore pressures are considered. Contrasted to this approach is the effective-stress analysis, in which, as the name indicates, effective stresses are considered. For such an analysis, the pore pressures must be known. Where possible, foundation engineers often employ a total-stress analysis and an effective-stress analysis. It is probable that a majority of such engineers have more confidence in the latter, since the analysis considers effective stresses explicitly. As has been reiterated throughout this work, the shear

strength is greatly dependent upon the development of effective stress. T. W. Lambe (1967) emphasized the importance of such analyses by the following comments:

> "There are a number of field cases involving bearing capacity failure (e.g., Szechy, 1960) described in the literature. For obvious reasons, these cases involving failure were seldom ones with good field instrumentation. There are practically no cases where undrained stability failure has occurred in clay in which pore pressures were measured on the failure zone during failure.
>
> "Critically needed are more thoroughly instrumented tests and actual cases in which the components of field performance are compared with the results of theoretical predictions based on carefully run laboratory tests on good samples."

Figure 28 illustrates the manner in which an effective-stress analysis can be made for the model of this study. Shown in the figure is the distribution of pore pressures along a hypothetical slip surface. The analysis would be based upon the effective strength parameters, $c' = 1.3$ psi and $\phi' = 25.9^{\circ}$ (Leitch, 1964). The shear strength would be given by Coulomb's equation, $s = c' + \bar{\sigma} \tan \phi'$, where $\bar{\sigma}$ represents the effective stresses which are developed along the failure zone (Meyerhof's Circle, ABC, Fig. 28). The effective normal stress at any point on this surface is the resultant of the pore pressure and the total pressure due to the weight of the soil. The pore pressure distribution shown in the figure is as suggested by the results of the model test: positive (neutral) pore pressures directly under the loaded area (A to B) and negative pore pressures generally outside of the loaded area (B to C).

Because of the local shear failure which occurred in the soft clay of the model test, the failure surface shown in Figure 28 most probably did not develop. Hence, a numerical analysis of the bearing capacity of the footing is not warranted. For similar tests on clays of firm to stiff consistency, the failure mechanism would be appropriate (Meyerhof, 1950-51). The analysis could then be completed by the Method of Slices (Taylor, 1948) or by the "Krey Ø-circle" method. The total-stress, or Ø-zero, analysis would be based on a soil strength of $c = q_u/2$, as previously described.

Finally, it should be noted that the change in soil strength with time would depend upon the net effect of pore pressure dissipation. As represented in Figure 28, the soil along the segment A to B would gain strength by consolidation and the soil from B to C would lose strength, in a transient fashion, as the negative pore pressures diminish.

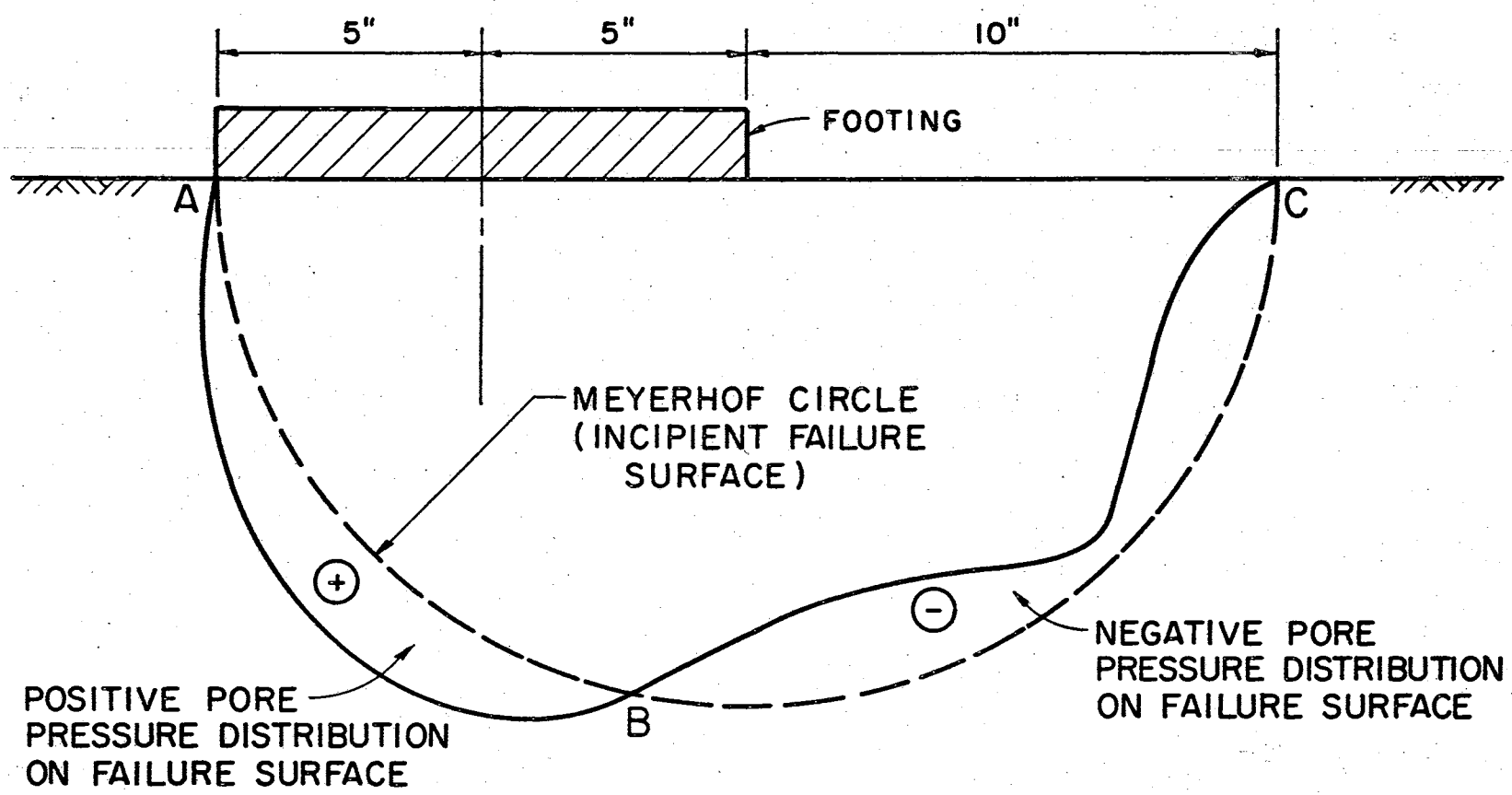

Figure 28. Pore Pressure Distribution for Effective Stress Bearing Capacity Analysis

CHAPTER VI

SUMMARY, CONCLUSIONS AND RECOMMENDATIONS

This study was concerned with, (a) the development of techniques and equipment for the preparation of large-scale clay models for the purpose of performing laboratory bearing capacity tests with pore pressure measurements, (b) the extension of Skempton's general pore pressure equation to the case of anisotropic overconsolidated clays, incorporating the theory of elasticity as an analytical tool for predicting pore pressures, and (c) the application of the theory which is developed in the study to an effective-stress analysis of bearing capacity for comparison to that of the more common total-stress, Ø-zero analysis.

Conclusions

1) The techniques which were used in this investigation for the preparation of a sedimented, preconsolidated clay are sound.

2) The pore pressure probe which was developed for the study is reliable. The technique of sedimenting the clay around the pre-installed probe is workable.

3) The method used for measuring pore pressures is adequate but quite awkward because of the large number of

people required for obtaining data.

4) The pore pressures induced by a footing load on an anisotropic clay are given by $\Delta u = \Delta\sigma_1[K(1-A) + A]$. Reasonably good agreement between predicted and measured pore pressures was observed. The limited amount of data available tends to support the contention that the prediction equation is generally applicable to clay soils on the basis of overconsolidation ratio, irrespective of consistency.

5) Shear deformations must be such as to produce a K-value of less than 1/3 in order that negative pore pressures develop. Because of this fact, indications are that the development of negative pore pressures is least likely in soils of intermediate consistency.

6) The theory, techniques, and equipment developed in this work contribute to the effective-stress approach to bearing capacity analysis.

Recommendations

1) Tests similar to that described in this study should be conducted using clay models of greater consistency so that:

   a) effective-stress analyses may be performed and compared to corresponding Ø-zero analyses, and
   b) a more definitive test of the validity of the prediction equation can be accomplished.

2) Separate testing techniques should be devised and employed to measure K directly.

3) Instrumentation for the measurement of pore pressures should be changed in order to eliminate the necessity for large numbers of people for the conduct of the test. Membrane-type pressure transducers are recommended for consideration.

4) With the instrumentation recommended above, some bearing capacity tests should be performed over an extended period in order to determine the rate and manner of pore pressure dissipation along a potential failure surface. This knowledge would be valuable in establishing the nature of the benefits to be derived from the use of controlled rates of loading in the field.

5) Sorely needed are more model tests designed for the purpose of determining the geometry of failure over a wide range of soil consistencies.

A SELECTED BIBLIOGRAPHY

Bishop, A. W., "The Use of Pore-Pressure Coefficients in Practice," Geotechnique, December, 1954, p. 148.

Brooke, E. W., "Earth Pressures at Rest Related to Stress History," Canadian Geotechnical Journal, February, 1965, p. 1.

French, L., "Shear Phenomena in One-dimensional Consolidation" (unpub. M. S. thesis, Newark College of Engineering, 1967).

Grim, R. E., Clay Mineralogy, New York: McGraw-Hill, 1953.

Jürgensen, L., "The Application of Theories of Elasticity and Plasticity to Foundation Problems," Journal BSCE, July, 1934.

Lambe, T. W., "Pore Pressures in a Foundation Clay," Proceedings, ASCE, Vol. 88, April, 1962, p. 19.

Lambe, T. W., "Shallow Foundations on Clay," Bearing Capacity and Settlement of Foundations, Duke University Symposium, 1967 Lecture 4, p. 35.

Leitch, J. (1964), "The Undrained Shear Strength Properties of Sedimented Samples of 0.1 N Sodium Kaolinite" (unpub. M. S. thesis, Newark College of Engineering, 1964).

Lumb, P., "Influence of Construction Time on Pore Pressure Dissipation Beneath Foundations," CE and Public Works Review, Vol. 60, No. 706, May, 1965, p. 675.

Meyerhof, G. G., "The Ultimate Bearing Capacity of Foundations," Geotechnique, Vol. II, 1950-51.

Parcher, J. V., Unpublished test results, 1957.

Ratzburg, H., "The Consolidation Characteristics of 0.1 N Sodium Kaolinite" (unpub. M. S. thesis, Newark College of Engineering, 1964).

Skempton, A. W., "The Bearing Capacity of Clays," Building Research Congress, Inst. of CE, 1951, p. 180.

Skempton, A. W., "The Pore Pressure Coefficients A and B," Geotechnique, December, 1954, p. 143.

Taylor, D. W., Fundamentals of Soil Mechanics, New York: Wiley, 1948.

Terzaghi, K. (1943), Theoretical Soil Mechanics, New York: Wiley.

Wu, T. H. (1966), Soil Mechanics, Boston: Allyn and Bacon.

Yong, R. et al. (1963), "Model Bearing Tests on a Remoulded Clay," Proceedings, 2nd Pan American Conference on SMF, Brazil, Vol. I, p. 337.

VITA

Edward James Monahan

Candidate for the Degree of

Doctor of Philosophy

Thesis: PORE PRESSURE DEVELOPMENT IN A BEARING CAPACITY TEST ON AN OVERCONSOLIDATED CLAY MODEL

Major Field: Engineering

Biographical:

Personal Data: Born September 18, 1931, in Bayonne, New Jersey, the son of John and Anna Monahan.

Education: Attended elementary school in Bayonne, New Jersey; graduated from Bayonne Technical and Vocational High School in 1949. Four years USAF (1950-1954). Received BSCE degree from Newark College of Engineering in June, 1958; MSCE degree, NCE, 1961. Completed course work and established residency as a National Science Foundation Fellow at Oklahoma State University during the period June, 1963 to September, 1964; admitted to Candidacy for the PhD in August, 1964. Pursued thesis research in absentia at Newark College of Engineering, 1964-1968; completed requirements for the Doctor of Philosophy degree at Oklahoma State University during July, 1968.

Professional Experience: Six summer's employment with five consulting engineering firms in the New York Metropolitan area, since 1956 (seven summers in that period devoted to academic pursuits); Assistant Instructor of Civil Engineering at Newark College of Engineering, 1958-1961; Instructor, CE, 1961-1963; Assistant Professor, CE. 1964-1968; Associate Professor, CE, 1968 (all NCE).

Professional Organizations: Member of American Society of Civil Engineers; Member of American Society for Engineering Education; Member of American Association of University Professors, Member of Undergraduate and Graduate Faculty of Newark College of

Engineering; Member of Chi Epsilon; Member of Tau Beta Pi. Registered Professional Engineer in New Jersey.